Cigarette Smoke-induced mitochondrial dysfunction and oxidative stress in epithelial cells

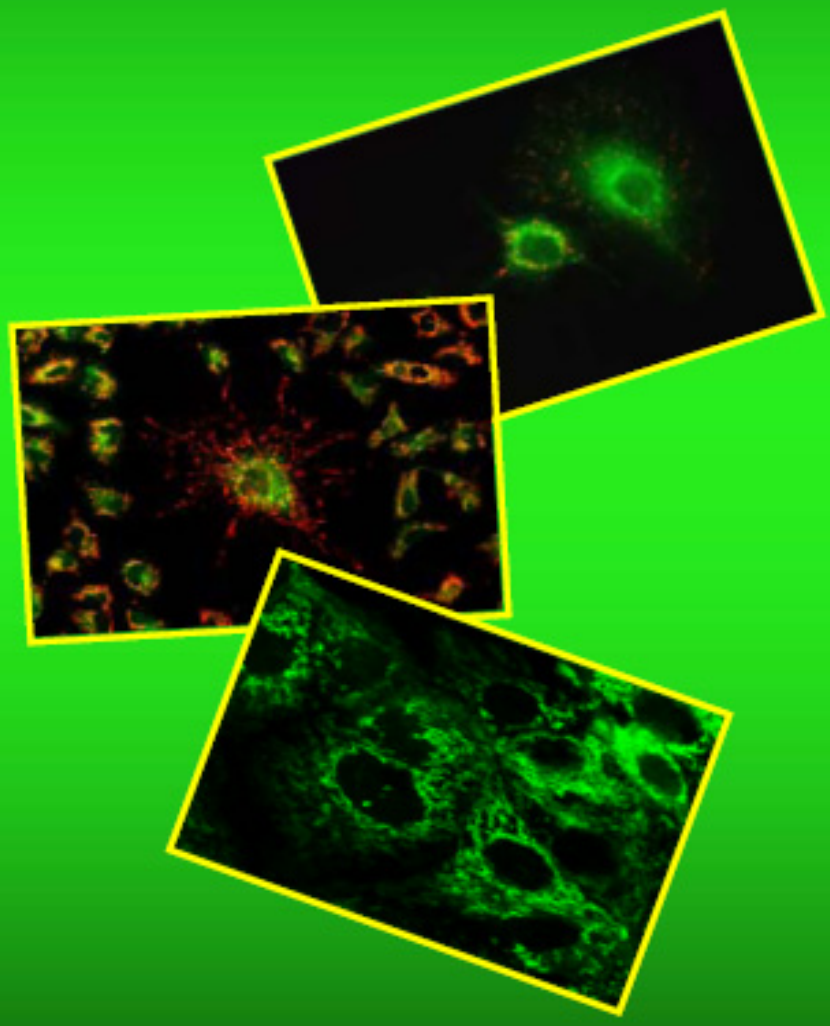

Marco van der Toorn

Paranimfen : H.G. de Bruin

R.K. Kooi

Van der Toorn, M.
Cigarette Smoke-induced mitochondrial dysfunction and oxidative stress in epithelial cells. Thesis University of Groningen with summary in Dutch.

The studies described in this thesis were financially supported by Nierstichting Nederland (Co1.1923), GlaxoSmithKline and Jan Kornelis de Cock stichting.

The printing of this thesis was financially supported by:
Dräger Medical, Nierstichting Nederland, Chiesi Pharmaceuticals, Novartis Pharma, Boehringer Ingelheim, J.E. Jurriaanse stichting, AstraZeneca, GlaxoSmithKline,

Stichting Astma Bestrijding, GUIDE, Nycomed, Phadia, Universitair Medisch Centrum Groningen, Rijksuniversiteit Groningen.
Their contribution is gratefully acknowledged!

Cover Design: C.H. Roelfsema & M. van der Toorn
Printed by: Drukkerij Doorn, Groningen

rijksuniversiteit
groningen

CIGARETTE SMOKE-INDUCED MITOCHONDRIAL DYSFUNCTION AND OXIDATIVE STRESS IN EPITHELIAL CELLS

Proefschrift

ter verkrijging van het doctoraat in de
Medische Wetenschappen
aan de Rijksuniversiteit Groningen
op gezag van de
Rector Magnificus, dr. F. Zwarts,
in het openbaar te verdedigen op
woensdag 11 februari 2009
om 16.15 uur

door

MARCO VAN DER TOORN

geboren op 27 maart 1972
te Hoogeveen

Promotores :	Prof. dr. H.F. Kauffman
	Prof. dr. R.O.B. Gans
	Prof. dr. G.H. Koëter
Copromotores :	Dr. D-J. Slebos
	Dr. S.J.L. Bakker
Beoordelingscommissie :	Prof. dr. A.M.W.J. Schols
	Prof. dr. R.P.H. Bischoff
	Prof. dr. H.A.M. Kerstjens

ISBN: 978-90-367-3695-4 (printed version)
ISBN: 978-90-367-3696-1 (digital version)

Lieve Lottie, Yaël, Lior en mijn kleine Jairo,
dit proefschrift draag ik op aan jullie.

CONTENTS

PREFACE

The research presented in this thesis started with studying the effects of oxidative stress in transplanted solid organs including kidneys. Immunosuppressive therapy with cyclosporin A (CsA) in order to prevent the rejection of transplanted organs is accompanied by undesired effects that promote a decline of the transplant function and accelerated atherogenesis. We hypothesized that CsA inhibits the mitochondrial permeability transition pore (MPTP). Inhibition of the MPTP will result in an increased mitochondrial membrane potential. Mitochondrial respiration was expected to proceed with an increased production of oxygen free radicals. In chapter 6 of this thesis we described that blocking of the MPTP did not play a role in CsA-induced oxidative stress. An important and unexpected result of this project stems from our use of cigarette smoke (CS) as a positive control for oxidative stress as shown in figure 1.

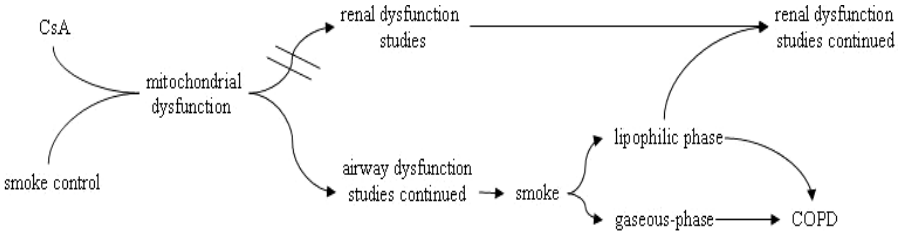

Figure 1. Incidence and significance of serendipity findings.

These serendipitous findings, described in chapter 1, showed that CS disturbs mitochondrial function, thereby decreasing the capacity of mitochondria for adenosine triphosphate synthesis, leading to increased susceptibility for cellular necrosis. We thought that it would be of interest to continue studying the effects of CS on airway epithelial cells. Finally, the results described in this thesis are of importance for both chronic obstructive pulmonary disease (COPD) and renal dysfunction after transplantation as described in the summary and future perspectives.

GENERAL INTRODUCTION

The consumption of tobacco has reached the proportion of a global epidemic. Although, smoking tobacco is an unhealthy habit, the number of smokers still increases. The world health organization has predicted that by the year 2030 there will be around 2 billion smokers (http://www.who.int). Tobacco companies often use the argument that smoking benefits the economy. These arguments cannot outweigh the fact that tobacco is the second major cause of death and the fourth most common risk factor for disease worldwide. Smoking has been documented to be a risk factor of multiple cancers, particularly lung cancer and of chronic obstructive pulmonary disease (COPD). Smokers are also at far greater risk of organ damage and cardio-vascular diseases (1-5). Smoking is associated with a more rapid decline of renal function in patients with different renal diseases (6-8). Prospective studies have shown that smokers are more susceptible for developing diabetes (9).

In this thesis we will focus especially on the effects of smoking on mitochondrial function and oxidative stress in airway epithelial cells and discuss the potential of these phenomena in the pathogenesis of COPD.

Pathogenesis of COPD

Many epidemiological studies have shown that smoking is the most important risk factor for COPD (10). COPD is a chronic lung disease that includes two main illnesses: chronic obstructive bronchitis and emphysema. Chronic obstructive bronchitis involves abnormal inflammation, swelling, and excessive mucus production. Emphysema is a lung disease involving damage to the alveoli. Progressive destruction of alveoli and the surrounding tissue that supports the alveoli reduces the elasticity of the lung. In both diseases, there is chronic obstruction of the flow of air through the airways and out of the lungs, and the obstruction generally is permanent and progressive over time.

COPD is not only a disease of the lungs, but also extends to systemic (disease) manifestations. A chronic inflammatory response, with loss of skeletal muscle mass (muscle wasting) and loss of body weight have both been observed in these patients (11; 12). Metabolic data shows that muscles undergo a shift from oxidative to glycolytic metabolism. Under glycolytic action, less adenosine triphosphate (ATP) per mole of glucose is produced when compared to an oxidative metabolism. The functional consequences of these changes are reflected in significant changes in skeletal muscle energy metabolism and accelerated acidification (possible by a mitochondrial dysfunction) of patients with COPD (13). These phenomena are already clear when using an acute cigarette smoke (CS) exposure mouse model, where after smoking for 5 days a significant reduction in body weight occurs when compared to control mice (Fig. 1A, B).

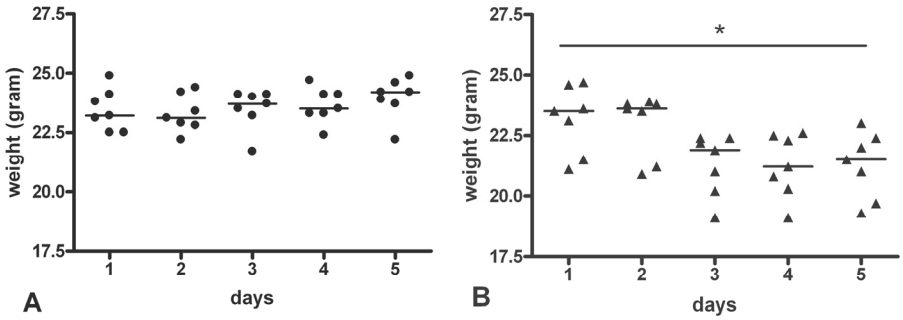

Figure 1. Effect of acute cigarette smoke on body weight in mice. BALB/C mice were exposed to air (A) or cigarette smoke (B) during 5 days. Results are expressed as mean±SEM of 7 mice in each group.
* $P < 0.05$ was considered significant.

Nowadays, it is recognized that COPD is multifactorial in origin, and that many (still unknown) factors play a role. Important factors in the pathogenesis of COPD are:

1) imbalance between reactive oxygen species (ROS) and antioxidants
2) chronic inflammation
3) imbalance between proteases and anti-proteases
4) increased tissue injury and cell death
5) new: disturbed mitochondrial function

CS-induced oxidative stress
Every day our airways are exposed to reactive environmental compounds, therefore the lung is always at risk of oxidative injury (13). To ensure an appropriate defense against this injury the lung is balanced with enzymatic and non-enzymatic antioxidant systems (Table 1).

Enzymatic antioxidant systems	***Non-enzymatic antioxidant systems***
family of superoxide dismutase	Glutathione
catalase	ascorbate (vitamin C)
glutathione peroxidase	α-tocopherol (vitamin E)
glutathione S-transferase	Bilirubin
thioredoxine	lipoic acid
	proteins that have oxidizable thiol groups
	transferring / ferritin
	urate

Table 1. Enzymatic and non-enzymatic antioxidants in normal subjects.

While the adverse effects of CS are well established, there is still an incomplete understanding of the mechanisms by which smoking leads to the development of COPD. CS contains >4000 compounds (14; 15). The smoke can be separated into a gas and particulate phase, whereas many substances are partitioned between these two phases. Both phases contain high levels of reactive components and radicals [1]. In the gas phase high levels of ROS and reactive nitrogen species (RNS) are found. In the particulate phase, highly reactive components like polycyclic aromatic hydrocarbons, aldehydes, phenols, heavy metals and amines are present. These components are candidates that either induce endogenous reactions that produce high levels of ROS or react directly with the antioxidant defenses (16). It is well established that smoking cigarettes contributes to an imbalance between ROS and antioxidant defenses (17). If ROS increase or if antioxidants decrease, oxidative stress will arise.

COPD patients show evidence of increased oxidative stress suggesting that antioxidants may be insufficient to prevent oxidative damage from CS (18). ROS species such as superoxide ($O_2^{\cdot-}$), hydrogen peroxide (H_2O_2), and hydroxyl radicals ($\cdot OH$) are associated with lung injury via several mechanisms as described in table 2. We believe that these species either directly inhaled via the gas phase of CS or endogenously produced in reaction to CS are a major cause of COPD.

Several mechanisms of ROS-mediated damage
damage to lipids, nucleic acids, proteins
depletion of antioxidants
initiation of redox-cycling reactions
enhancement of the respiratory burst in macrophages and neutrophils
inactivation of protease inhibitors
increased expression of inflammatory mediators

Table 2. Mechanisms by which ROS induce lung injury.

Inflammation and oxidative stress

Inflammation is a protective mechanism to remove the causative stimuli as well as initiate the healing process of the tissue. Prolonged inflammation, also called chronic inflammation, leads to a progressive shift in inflammatory cells to the tissue. Airway epithelial cells participate in this inflammatory response seen in COPD. When stimulated with pro-inflammatory mediators like ROS, redox-sensitive transcription factors like NFκB and AP-1 which lead to the expression of inflammatory genes are activated (19). The release of inflammatory mediators such as TNF-α, IL-8 and LTB4 by the activated epithelial cells stimulates the influx of inflammatory cells to the lung. Inflammatory cells release proteolytic enzymes like

[1] Free radicals are highly unstable species with unpaired electrons

neutrophil elastase (16) and also generate oxidants, which further enhance oxidative stress and tissue damage (Fig. 2).

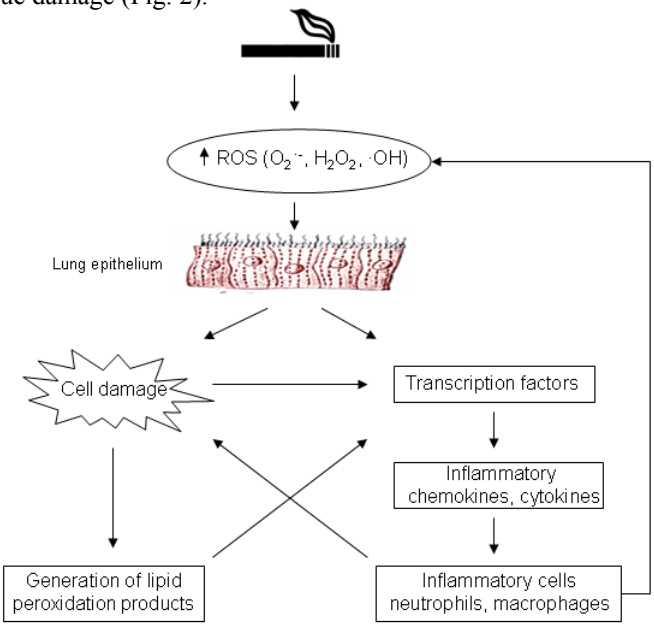

Figure 2. Mechanism of ROS mediated inflammation by cigarette smoke.

Many cells contribute to the inflammatory reaction in COPD and there seems to be a relationship between the severity of the disease and the content of inflammatory cells in the lung. For example the number of macrophages in the airways is increased in COPD. CS activates macrophages to produce and release TNF-α, IL-8, LTB4 and GROα, important chemoatractants for neutrophils. It is well established that in patients with COPD, recruitment of neutrophils and decline in lung function are related (20).

Cell death pathways in COPD

In the airways of smokers, accumulated phagocytic cells are seen at sites of inflammatory tissue injury. Apoptosis is considered to play an important role in effective repair of the injured airway, and in the resolution of inflammation. Apoptosis, or programmed cell death, is a highly regulated process that allows a cell to self-degrade in order to eliminate unwanted or dysfunctional cells. The apoptotic cell will be phagocytosed by macrophages before the cell's contents leak into the surrounding tissue (21). Apoptosis can be triggered in a cell through either the extrinsic pathway or the intrinsic pathway.

In the extrinsic pathway, signal molecules from the TNF family excreted by inflammatory cells, bind to transmembrane death receptors on epithelial and/or inflammatory cells and initiate a cascade of reactions leading to apoptosis. The

intrinsic pathway can be triggered by oxidative stress which results in mitochondrial dysfunction. This pathway is characterized by dissipation of the mitochondrial membrane potential ($\Delta\psi_m$) and transient opening of the mitochondrial permeability transition pore (MPTP) (22; 23). Transient opening of the MPTP causes swelling of mitochondria and release of apoptogenic factors like cytochrome c which initiate together with adenosine triphosphate (ATP) apoptosis. Caspases, belonging to the family of cysteine proteases, are of central importance in both pathways by activating DNases, inhibiting DNA repair enzymes and breaking down structural proteins in the nucleus (24). Finally the cell is fragmented into compact membrane-enclosed structures, called 'apoptotic bodies' which contain cytosol, the condensed chromatin, and organelles. The apoptotic bodies are phagocytosed by macrophages and removed from the tissue without causing an inflammatory response. Because of the tissue damage and airway inflammation present in COPD it can be hypothesized that in stead of the physiological apoptotic response to airway damage, cell death by necrosis occurs leading to secondary inflammation. This is in discrepancy with the severe inflammation seen in patients with COPD. Necrotic cell-death results in loss of membrane integrity, swelling and disrupture of cells. During necrosis, early $\Delta\psi_m$ depolarization, permanent opening of the MPTP and marked decline in ATP synthesis are seen (25). Consequential loss of membrane integrity and release of cellular content into the environment results in damage of surrounding cells and a strong inflammatory response (26). In vitro models of COPD have shown the induction of both apoptosis and necrosis in airway epithelial cells (27-29). Because mitochondria are involved in both cell death processes, it is to be assumed that an inefficient mitochondrial function plays a key role in the development of COPD.

Role of mitochondria in the pathogenesis of COPD

Mitochondria are the energy-producing organelles of our cells. Through oxidative phosphorylation, a series of four enzyme complexes (complex I-IV) transfer electrons and pump protons across the inner mitochondrial membrane. The proton motive force generated is used to drive the synthesis of chemical energy in the form of ATP. ATP is a multifunctional nucleotide that is used in energy-consuming processes like apoptosis. This molecule is the main source of energy in organisms and critical for life. It has been demonstrated that CS can disrupt $\Delta\psi_m$ in monocytes and macrophages in vitro and in vivo (30; 31).

Mitochondria consume approximately 85% of the oxygen during the production of ATP. During normal oxidative phosphorylation, ~4.0% of the oxygen is converted into ROS. Mitochondria are key players in the management of intracellular ROS-metabolism. This is best illustrated by the fact that all major antioxidants are functionally present within the mitochondria. Glutathione, catalase, thioredoxin, superoxide-dismutase and also, as described in chapter 3 heme oxygenase-1 (HO-1), are all linked to mitochondrial function. However when these enzymes cannot neutralize ROS or when exogenous and/or endogenous ROS production increase, oxidative damage occurs. Miro *et al.* showed that the function of complex IV of the electron transfer chain was inhibited in blood lymphocytes of smokers leading to increased production of endogenous ROS (32). Several *in vitro* studies demonstrated that treatment with specific blockers of the electron transfer

chain causes mitochondrial ROS production and alteration in mitochondrial morphology. These observations are similar to the increased levels of oxidative stress parameters and mitochondrial dysfunctions as documented in patients with COPD (12; 33; 34).

A third, very important function of mitochondria, is their crucial role in the regulation of apoptotic cell death through the release of apoptogenic factors (e.g. cytochrome-c, apoptosis inducing factor) in response to specific stimuli (35). In this thesis we show that CS is able to influence mitochondria and alter their role in the regulation of cell death.

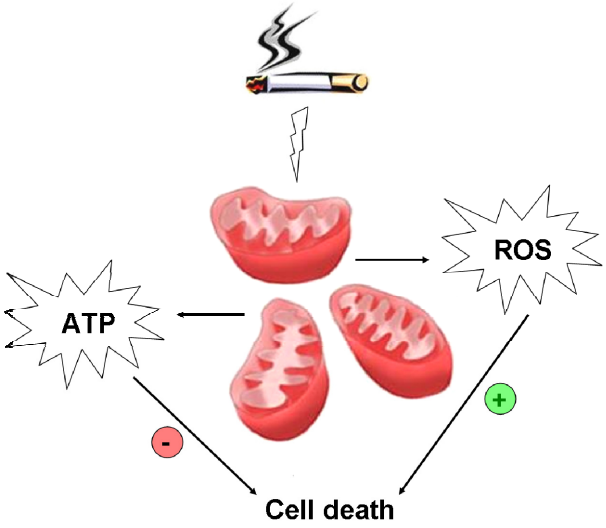

Figure 3. Influence of cigarette smoke on mitochondrial function.

These three -basic for life- features illustrated in figure 3: energy production, ROS management and regulation of cell death make the mitochondria potentially the "powerhouse" of disease (36-38).

SCOPE OF THE STUDIES

In the first three chapters we investigate a new pathophysiological paradigm, where mitochondrial dysfunction is crucial for disease development and progression. Mitochondria are crucial for cellular energy production, ROS management and regulation of cell death. In **chapter 1** we investigated whether cigarette smoke extract (CSE) disturbs the mitochondrial respiratory chain function leading to decreased production of intracellular energy (ATP). Furthermore, we investigated whether energy depletion by cigarette smoke (CS) is crucial in the routing of apoptotic-triggered cells towards necrosis.

CS can be separated into a gaseous and particulate phase. Reactive oxygen species (ROS) that are present in gaseous-phase of CS are thought to be the most important factor of the oxidative damage and stress present in chronic obstructive pulmonary disease (COPD). However these components are hardly able to enter the cell due to the presence of unpaired electrons and will therefore primarily react with the anti-oxidants present in the epithelial lining fluid. On the other hand, the particulate phase contains lipophilic components that can easily enter the cell and the systemic circulation. In **chapter 2** we investigated whether these lipophilic components have a direct interaction with mitochondria, leading to increased production of mitochondrial ROS. We also investigated whether increased production of mitochondrial ROS induces ROS-mediated cellular damage.

The airway epithelium provides an efficient barrier for the underlying tissue against toxic compounds present in CS. To maintain this barrier, two crucial protection systems are of importance:

1) cell replacement and regeneration of the epithelium
2) management of intracellular ROS-metabolism

Mitochondria are the key players in both systems. Normal cell removal and cell replacement in tissue remodeling is regulated by apoptosis (39). Mitochondria regulate apoptosis by the release of pro apoptotic mediators and supply of ATP. Although, mitochondria are the largest source of intracellular ROS, all major anti-oxidants are present within the mitochondria. In **chapter 3** we investigated whether heme oxygenase-1 was also an important antioxidant present in mitochondria. In the same chapter we studied the protective role of heme oxygenase-1 on mitochondrial function and CS-induced cell death.

A second important mechanism of the airway epithelium to ensure an appropriate defense against the highly reactive compounds present in CS is to keep a balance between ROS and antioxidants. Reduced glutathione plays a key role in the cellular redox balance. In **chapter 4** we investigated whether components of the gas phase of CS react irreversibly with the free thiol group of glutathione. A non-reducible glutathione derivates will reduce the pool of reduced glutathione. This may lead to a lack of protection against oxidative stress.

Epithelial injury and recovery are important in the pathogenesis of COPD. In **chapter 5**, oxidative stress and the damage that may result from it have been studied in quiescent and proliferating airway epithelial cells. It was hypothesized that resistance and recovery would be dependent on the concentration of the oxidative agent but also on the duration of exposure and on the quiescent and proliferating state of airway epithelial cells. This was studied in vitro by measuring morphology, viability and cell death pathways.

Oxidative stress has been implicated in many diseases. For example, accelerated atherosclerosis and fibrosis develop in prolonged smokers but also in transplanted patients which are treated with the immunosuppressive cyclosporine A. This contributes to the development of chronic transplant dysfunction. It has been suggested that mitochondrial ROS production play an important underlying role. Cyclosporine A is a well known inhibitor of the mitochondrial permeability transition pore. In **chapter 6** we investigated whether closure of the mitochondrial permeability transition pore by cyclosporine A results in a concomitant increase in mitochondrial membrane potential and production of ROS.

REFERENCE LIST

1. Critchley JA and Unal B. Health effects associated with smokeless tobacco: a systematic review. Thorax 58: 435-443, 2003.

2. Gandini S, Botteri E, Iodice S, Boniol M, Lowenfels AB, Maisonneuve P and Boyle P. Tobacco smoking and cancer: A meta-analysis. Int J Cancer 2007.

3. Gosker HR, Wouters EF, van der Vusse GJ and Schols AM. Skeletal muscle dysfunction in chronic obstructive pulmonary disease and chronic heart failure: underlying mechanisms and therapy perspectives. Am J Clin Nutr 71: 1033-1047, 2000.

4. Smith CJ, Perfetti TA and King JA. Perspectives on pulmonary inflammation and lung cancer risk in cigarette smokers. Inhal Toxicol 18: 667-677, 2006.

5. Yanbaeva DG, Dentener MA, Creutzberg EC, Wesseling G and Wouters EF. Systemic effects of smoking. Chest 131: 1557-1566, 2007.

6. Orth SR, Stockmann A, Conradt C, Ritz E, Ferro M, Kreusser W, Piccoli G, Rambausek M, Roccatello D, Schafer K, Sieberth HG, Wanner C, Watschinger B and Zucchelli P. Smoking as a risk factor for end-stage renal failure in men with primary renal disease. Kidney Int 54: 926-931, 1998.

7. Stengel B, Couchoud C, Cenee S and Hemon D. Age, blood pressure and smoking effects on chronic renal failure in primary glomerular nephropathies. Kidney Int 57: 2519-2526, 2000.

8. Ward MM and Studenski S. Clinical prognostic factors in lupus nephritis. The importance of hypertension and smoking. Arch Intern Med 152: 2082-2088, 1992.

9. Orth SR, Schroeder T, Ritz E and Ferrari P. Effects of smoking on renal function in patients with type 1 and type 2 diabetes mellitus. Nephrol Dial Transplant 20: 2414-2419, 2005.

10. Pauwels RA and Rabe KF. Burden and clinical features of chronic obstructive pulmonary disease (COPD). Lancet 364: 613-620, 2004.

11. Oudijk EJ, Lammers JW and Koenderman L. Systemic inflammation in chronic obstructive pulmonary disease. Eur Respir J Suppl 46: 5s-13s, 2003.
12. Rabinovich RA, Bastos R, Ardite E, Llinas L, Orozco-Levi M, Gea J, Vilaro J, Barbera JA, Rodriguez-Roisin R, Fernandez-Checa JC and Roca J. Mitochondrial dysfunction in COPD patients with low body mass index. Eur Respir J 29: 643-650, 2007.
13. Rahman I and MacNee W. Lung glutathione and oxidative stress: implications in cigarette smoke-induced airway disease. Am J Physiol 277: L1067-L1088, 1999.
14. Lu X, Cai J, Kong H, Wu M, Hua R, Zhao M, Liu J and Xu G. Analysis of cigarette smoke condensates by comprehensive two-dimensional gas chromatography/time-of-flight mass spectrometry I acidic fraction. Anal Chem 75: 4441-4451, 2003.
15. Rustemeier K, Stabbert R, Haussmann HJ, Roemer E and Carmines EL. Evaluation of the potential effects of ingredients added to cigarettes. Part 2: chemical composition of mainstream smoke. Food Chem Toxicol 40: 93-104, 2002.
16. Larsson K. Aspects on pathophysiological mechanisms in COPD. J Intern Med 262: 311-340, 2007.
17. Bowler RP, Barnes PJ and Crapo JD. The role of oxidative stress in chronic obstructive pulmonary disease. COPD 1: 255-277, 2004.
18. Rahman I. The role of oxidative stress in the pathogenesis of COPD: implications for therapy. Treat Respir Med 4: 175-200, 2005.
19. Rahman I and Adcock IM. Oxidative stress and redox regulation of lung inflammation in COPD. Eur Respir J 28: 219-242, 2006.
20. Stanescu D, Sanna A, Veriter C, Kostianev S, Calcagni PG, Fabbri LM and Maestrelli P. Airways obstruction, chronic expectoration, and rapid decline of FEV1 in smokers are associated with increased levels of sputum neutrophiles. Thorax 51: 267-271, 1996.
21. Raff M. Cell suicide for beginners. Nature 396: 119-122, 1998.
22. Halestrap AP, Kerr PM, Javadov S and Woodfield KY. Elucidating the molecular mechanism of the permeability transition pore and its role in reperfusion injury of the heart. Biochim Biophys Acta 1366: 79-94, 1998.
23. Halestrap AP, Doran E, Gillespie JP and O'Toole A. Mitochondria and cell death. Biochem Soc Trans 28: 170-177, 2000.
24. Bratton SB, MacFarlane M, Cain K and Cohen GM. Protein complexes activate distinct caspase cascades in death receptor and stress-induced apoptosis. Exp Cell Res 256: 27-33, 2000.
25. Lemasters JJ, Nieminen AL, Qian T, Trost LC, Elmore SP, Nishimura Y, Crowe RA, Cascio WE, Bradham CA, Brenner DA and Herman B. The mitochondrial permeability transition in cell death: a common mechanism in necrosis, apoptosis and autophagy. Biochim Biophys Acta 1366: 177-196, 1998.
26. Leist M and Jaattela M. Four deaths and a funeral: from caspases to alternative mechanisms. Nat Rev Mol Cell Biol 2: 589-598, 2001.
27. Hoshino Y, Mio T, Nagai S, Miki H, Ito I and Izumi T. Cytotoxic effects of cigarette smoke extract on an alveolar type II cell-derived cell line. Am J Physiol Lung Cell Mol Physiol 281: L509-L516, 2001.

28. Jung M, Davis WP, Taatjes DJ, Churg A and Mossman BT. Asbestos and cigarette smoke cause increased DNA strand breaks and necrosis in bronchiolar epithelial cells in vivo. Free Radic Biol Med 28: 1295-1299, 2000.
29. Wickenden JA, Clarke MC, Rossi AG, Rahman I, Faux SP, Donaldson K and MacNee W. Cigarette smoke prevents apoptosis through inhibition of caspase activation and induces necrosis. Am J Respir Cell Mol Biol 29: 562-570, 2003.
30. Aoshiba K, Tamaoki J and Nagai A. Acute cigarette smoke exposure induces apoptosis of alveolar macrophages. Am J Physiol Lung Cell Mol Physiol 281: L1392-L1401, 2001.
31. Banzet N, Francois D and Polla BS. Tobacco smoke induces mitochondrial depolarization along with cell death: effects of antioxidants. Redox Rep 4: 229-236, 1999.
32. Miro O, Alonso JR, Jarreta D, Casademont J, Urbano-Marquez A and Cardellach F. Smoking disturbs mitochondrial respiratory chain function and enhances lipid peroxidation on human circulating lymphocytes. Carcinogenesis 20: 1331-1336, 1999.
33. Dekhuijzen PN, Aben KK, Dekker I, Aarts LP, Wielders PL, van Herwaarden CL and Bast A. Increased exhalation of hydrogen peroxide in patients with stable and unstable chronic obstructive pulmonary disease. Am J Respir Crit Care Med 154: 813-816, 1996.
34. Biernacki WA, Kharitonov SA and Barnes PJ. Increased leukotriene B4 and 8-isoprostane in exhaled breath condensate of patients with exacerbations of COPD. Thorax 58: 294-298, 2003.
35. Green DR and Reed JC. Mitochondria and apoptosis. Science 281: 1309-1312, 1998.
36. Lane N. Mitochondrial disease: powerhouse of disease. Nature 440: 600-602, 2006.
37. Pieczenik SR and Neustadt J. Mitochondrial dysfunction and molecular pathways of disease. Exp Mol Pathol 83: 84-92, 2007.
38. Stevenson CS, Koch LG and Britton SL. Aerobic capacity, oxidant stress, and chronic obstructive pulmonary disease--a new take on an old hypothesis. Pharmacol Ther 110: 71-82, 2006.
39. Israels LG and Israels ED. Apoptosis. Oncologist 4: 332-339, 1999.

Chapter 1

CIGARETTE SMOKE-INDUCED BLOCKADE OF THE MITOCHONDRIAL RESPIRATORY CHAIN SWITCHES LUNG EPITHELIAL CELL APOPTOSIS INTO NECROSIS

Marco van der Toorn[1], Dirk-Jan Slebos[2], Harold G. de Bruin[1], Henri G. Leuvenink[3], Stephan J. L. Bakker[4], Rijk O. B. Gans[4], Gerard H. Koëter[2], Antoon J. M. van Oosterhout[1], Henk F. Kauffman[5].

[1]Laboratory of Allergology and Pulmonary diseases, [2]Department of Pulmonary diseases, [3]Department of Surgery, [4]Department of Internal Medicine, [5]Groningen University Institute for Drug Exploration, University Medical Center Groningen, University of Groningen, PO Box 30001, 9700 RB, Groningen, The Netherlands.

Am J Physiol Lung Cell Mol Physiol. 2007 May;292(5)

ABSTRACT

Increased lung cell apoptosis and necrosis occur in patients with chronic obstructive pulmonary disease (COPD). Mitochondria are crucially involved in the regulation of these cell death processes. Cigarette smoke is the main risk factor for development of COPD. We hypothesized that cigarette smoke disturbs mitochondrial function, thereby decreasing the capacity of mitochondria for ATP synthesis, leading to cellular necrosis. This hypothesis was tested in both human bronchial epithelial cells and isolated mitochondria. Cigarette smoke extract exposure resulted in a dose-dependent inhibition of complex I and II activities. This inhibition was accompanied by decreases in mitochondrial membrane potential, mitochondrial oxygen consumption and production of ATP. Cigarette smoke extract abolished the staurosporin-induced caspase-3 and -7 activities and induced a switch from epithelial cell apoptosis into necrosis. Cigarette smoke induced mitochondrial dysfunction, with compounds of cigarette smoke acting as blocking agents of the mitochondrial respiratory chain: loss of ATP generation leading to cellular necrosis instead of apoptosis is a new pathophysiological concept of COPD development.

INTRODUCTION

Oxidative stress caused by cigarette smoke resulting in airway inflammation is assumed to be directly involved in tissue injury and cell death in Chronic Obstructive Pulmonary Disease (COPD) (5, 30). In patients with COPD tissue injury and cell death have been related to the presence of both increased apoptosis and necrosis in lung and airway epithelial cells (16, 18, 21, 27, 43). The airway epithelium is the barrier between inhaled air, with the toxic compounds present like cigarette smoke, and the underlying lung tissue. To maintain this barrier, continuous cell replacement and repair of the epithelium are of crucial importance. Cell death through apoptosis is essential for eliminating damaged cells during development, tissue remodeling and inflammation (22, 41). Disturbance of this physiological process can, however, result in necrosis or excessive apoptosis with disruption of the barrier function of the epithelium, leading to lung disease (15, 19, 41). Cigarette smoke models have shown the induction of both apoptosis and necrosis in epithelial cells and fibroblasts in vitro. As recently demonstrated by our group (38), this death process depends on the amount and duration of cigarette smoke exposure and the type of cell line used. However, the regulatory mechanisms involved in these in vitro models, as well as in humans in vivo, remain speculative (10, 20, 27, 42).

Mitochondria play a crucial role in the regulation of apoptosis by the release of proapoptotic mediators (e.g., cytochrome c, apoptosis-inducing factor) in response to specific stimuli (14). Cytochrome c, released from mitochondria, together with apoptotic protease activating factor-1 and procaspase-9 combine to the apoptosome. This ATP-dependent apoptosome formation results in the activation of caspase-9, leading to caspase-3 activation and subsequent apoptotic cell death (14). Another crucial role for mitochondria in facilitating apoptosis is the production of ATP, a process linked to the action of the electron transfer chain (ETC) (34). Where apoptosis is a highly energy-consuming process, necrosis will occur even after an apoptotic stimulus when no energy is available (17). Therefore, alteration of cellular energy (ATP) levels is known to play a crucial role in the routing of cells to die by apoptosis or necrosis (11, 26, 31).

It has been known for decades that cigarette smoke contains many lipophilic compounds like phenolic structures, aldehydes, and aromatic compounds that are able to accumulate in mitochondria and may disturb the function of the mitochondrial respiratory chain, thereby affecting the cellular ATP production (13, 25, 29, 32, 39). These observations make mitochondria theoretically important players in cigarette smoke-induced cellular damage. Therefore, we hypothesized that cigarette smoke will disturb the mitochondrial respiratory chain function, leading to a decreased mitochondrial membrane potential ($\Delta\psi_m$) and a decreased ATP production. We furthermore hypothesized that this cigarette smoke induced ATP depletion is crucial in the routing of apoptotic-triggered cells and may switch them towards dying from necrosis.

Therefore we set out to identify the acute effect of cigarette smoke extract (CSE) on mitochondrial respiratory chain function in isolated mitochondria and mode of cell death in human bronchial epithelial cells. The consequences of the cigarette smoke-induced mitochondrial dysfunction might be of great importance in understanding the presence of an altered cell death process in COPD.

MATERIALS AND METHODS

Chemicals
2,4-Dinitrophenol (DNP) was obtained from Merck & Co., Inc. (Haarlem, The Netherlands), Nasuccinate, ATP, ADP, potassium cyanide (KCN), staurosporin (STS) and oligomycin from Sigma-Aldrich Chemie B.V. (Zwijndrecht, The Netherlands).

Preparation of CSE
Kentucky 2R4F research-reference filtered cigarettes (The Tobacco Research Institute, University of Kentucky, Lexington, KY) where smoked using a peristaltic pump. Just before the experiments, the filters were cut from the cigarettes. Each cigarette was smoked in 5 minutes with a 17 mm butt remaining. Four cigarettes were bubbled through 50 ml of cell growth medium or mitochondrial respiration buffer, and this solution was regarded as 100% strength CSE.

Cell cultures
Human primary bronchial epithelial cells were collected and cultured by the methods described by Borger *et al.* (8). For the experiments described, these cells were used at 80-90% confluency in passage 2. Beas-2b lung epithelial cells were purchased from American Type Culture Collection (ATCC, Manassas, VA). Cells were grown in RPMI 1640 with 25 mM HEPES, LGlutamine (BioWitthaker, Verviers, Belgium) supplemented with 10% heat-inactivated fetal calf serum (BioWitthaker, Verviers, Belgium) and 20 µg/ml gentamycin (Centafarm Services, Etten-Leur, The Netherlands). Before the experiments both the human primary bronchial epithelial cells and the Beas-2b cells were cultured for 16 h in serum- free RPMI media.

Isolation of mitochondria
Mitochondria were isolated from fresh pig's liver using a commercial mitochondria isolation kit (Sigma-Aldrich Chemie B.V., Zwijndrecht, The Netherlands). Briefly, fresh liver tissue (obtained within one hour of sacrifice) was washed twice with 2 volumes of extraction buffer (10 mM HEPES, 200 mM mannitol, 70 mM sucrose and 1 mM EGTA, pH7.5). The liver was cut into small portions and homogenized with 10 volumes extraction buffer containing 2 mg/ml delipidated Bovine Albumin (Sigma-Aldrich Chemie B.V., Zwijndrecht, The Netherlands), using a pestle and glass tube. The homogenate was centrifuged at 600 g for 5 minutes. The supernatant was collected and centrifuged at 11.000 g for 10 minutes. After this, the supernatant was removed and the pellet was resuspend in 10 volumes of extraction buffer and centrifuged at 600 g for 5 minutes. Finally, the supernatant was centrifuged at 11.000 g for 10 minutes, after which the supernatant was removed and the isolated mitochondria were resuspended in respiratory buffer (120 mM KCl, 5 mM K2PO4, 3 mM HEPES, 1 mM EGTA, brought to pH 7.2 with 5 mM KH2PO4). Mitochondrial protein was estimated by the Bradford method (Bio-Rad Laboratories, Veenendaal, The Netherlands) according to the manufacturer's instructions. To stabilize the mitochondria, respiration buffer was supplemented with 0.2% delipidated Bovine Albumin (w/v).

Detection of $\Delta\psi_m$

Primary bronchial epithelial cells were stained with 5 μg/ml JC-1 probe (Molecular Probes, Leiden, The Netherlands) according to the manufacturer's instruction. Loaded cells were stimulated for 1 h with different concentrations of CSE at 37°C. Isolated mitochondria were stained with 0.2 μg/ml JC-1 probe for 10 min at 37°C. State III respiration was reached after addition of 5 mM Na-succinate and 1 mM ADP. Mitochondria were stimulated for 15 min at 37°C with different concentrations of CSE. Epithelial cells and isolated mitochondria were monitored with an excitation wavelength of 485-nm through a 590-nm band-pass filter in a FL600 fluorescent plate reader (Bio-Tek instruments, The Netherlands).

Measurement of ATP

Intracellular ATP levels of epithelial cells were quantified after treatment with Triton X-100. For mitochondrial measurement of ATP, the isolated mitochondria (final concentration protein 100 μg/ml) were resuspended in respiration buffer. The experiments were performed in state III respiration. Different CSE concentrations were tested whereas DNP (final concentration of 20 μM) served as negative control. Mitochondria were incubated for 15 min at 37°C. At the end of the incubation period, ATP synthesis was stopped by freezing the samples in -196°C nitrogen. The ATP levels were measured using the Enliten® ATP assay from Promega (Leiden, The Netherlands) and a Berthold microplate Luminometer (Berthold Detection Systems GmbH, Pforzheim, Germany).

Mitochondrial respirometry

Mitochondrial respiration was measured according to the method of 't Hart *et al*. (39a). Briefly, mitochondria (final concentration 2 mg/ml) were resuspended in a 95% oxygen saturated respiration buffer supplemented with 0.2% (w/v) delipidated Bovine Albumin (Sigma-Aldrich Chemie B.V., Zwijndrecht, The Netherlands) in a 1-ml respiration chamber. Stimuli were preincubated for 1 min. State III respiration was started after addition of succinate (final concentration of 5 mM) and ADP (final concentration of 0.5 mM).

Complex I and II activity

The activity of NADH dehydrogenase (complex I) was assayed by the method of Minakami *et al.* (28). The enzyme activity was calculated by subtracting the residual activity remaining after the addition of the specific inhibitor (2 μM rotenone). Succinate dehydrogenase (complex II) was determined by enzymatic methods according to the method Slater and Bonner (37).

Mitochondrial swelling
We performed mitochondrial swelling, according to the method of Barzu *et al*. (7), as an index for mitochondrial viability. Briefly, mitochondria were resuspended in respiration buffer (without EGTA) containing 4 mg mitochondrial protein/ml. The mitochondria were 'energized' with succinate (final concentration 5 mM). The suspension was pipetted into the wells (100 µl/well) of a 96-well polystyrene microtiterplate (Greiner Bio-One B.V., Alphen aan den Rijn, The Netherlands). Different CSE concentrations were added and $CaCl_2$ (1 mM) was used as a positive control. Immediately after addition of the stimuli, the plate was measured in an EL808 spectrophotometer using a 550-nm filter (Bio-Tek instruments, Abcoude, The Netherlands). Measurements were repeated every 30 s for a period of 30 min.

Caspase-3 and -7 activities
Beas-2b cells were preincubated for 1 h with or without 2 µM STS. Thereafter, all cells were washed and incubated for 4 h with different concentrations of CSE. Caspase-3 and -7 activities were determined using the "caspase-glo 3/7" luminescent assay kit from Promega (Leiden, The Netherlands) and a Berthold microplate Luminometer. Caspase-3 and -7 activities of the Beas-2b cells were determined according to the manufacturer's instruction.

Flow cytometric analysis of cell death
Surface exposure of phosphatidylserine and plasma membrane disruption was stained by annexine-V-FITC and propidium iodide (PI) according to the manufacturer's instruction (IQ Products, Groningen, the Netherlands). Cells were analyzed by flow cytometry (Calibur, Becton Dickinson Medical Systems, Heidelberg, Germany).

Statistical analysis
Data were analyzed using SPSS/PC+ software (SPSS Benelux, Gorinchem, The Netherlands). Repeated-measures ANOVA was used for assessment of decline in dose-response CSE experiments. Comparisons between different experimental groups were performed with a one-sample t-test (see Figs. 1 and 2) and the non-parametrical Mann-Whitney U test (see Figs. 5, A and B, and 6C). $P < 0.05$ was considered significant. Results are presented as means ± SE unless otherwise mentioned.

RESULTS

CSE disturbs mitochondrial function in human primary bronchial epithelial cells
To investigate the acute effect of CSE on the mitochondrial respiratory chain function, we examined whether exposure of human primary bronchial epithelial cells to CSE would affect $\Delta\psi_m$. Exposure of increasing concentrations of CSE for 1 h caused a significant dose-dependent decrease of $\Delta\psi_m$ ($P < 0.0001$; Fig. 1A). Furthermore, intracellular ATP levels were measured to evaluate the consequences of the decreased mitochondrial depolarization. CSE caused a significant dose-dependent decrease of intracellular ATP ($P = 0.0021$; Fig. 1B). The protonophore DNP, used as a positive control showed, as expected, a depolarization of the

mitochondrial inner membrane and decreased intracellular levels of ATP in these epithelial cells (Fig. 1).

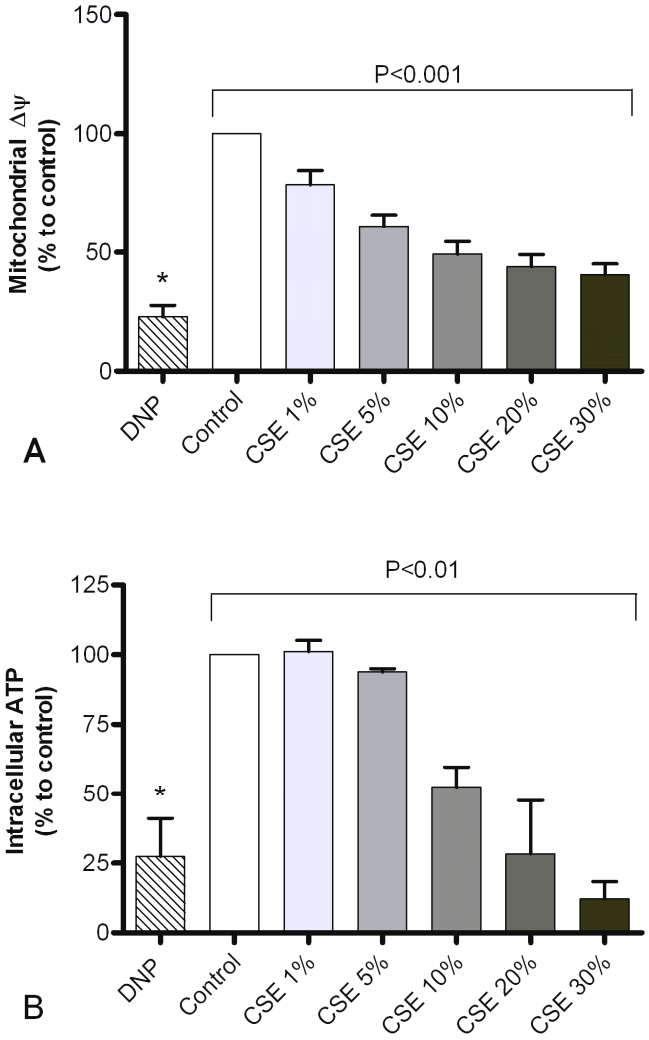

Figure 1. Cigarette smoke extract (CSE) induces a loss of mitochondrial function in human primary bronchial epithelial cells. Effects of increasing concentrations of CSE on mitochondrial inner membrane potential ($\Delta\psi_m$) (A) and intracellular ATP levels (B) in primary human bronchial epithelial cells exposed for 1 h (n = 3) are shown. *P < 0.05 for 2,4-dinitrophenol (DNP; 20 μM) vs. control. P values given above the horizontal lines represent the significance for the total decline of all CSE concentrations used (repeated-measures ANOVA).

The mitochondrial respiratory chain is the target of CSE-mediated ATP depletion
In intact epithelial cells we demonstrated that CSE disrupts mitochondrial function. To study whether CSE also directly affects mitochondria, we isolated fresh pig liver mitochondria. Exposure of isolated mitochondria to CSE caused no mitochondrial swelling under the experimental conditions, thus indicating mitochondrial viability (Fig. 2). However, we were able to demonstrate that CSE significantly depolarizes the mitochondrial inner membrane in a state III respiration (in the presence of ADP, change of -61.4% ± 2.4%; $P < 0.0001$; Fig. 3A). A similar effect was observed for state IV respiration (absence of ADP, data not shown). Because the ETC facilitates the transfer of hydrogen ions across the mitochondrial inner membrane, a decreasing $\Delta\psi_m$ in a state III respiration by CSE should negatively affect the proton gradient. To demonstrate this, we exposed isolated mitochondria to different concentrations of CSE for 15 min and showed a significant dose-dependent decrease of the synthesis of ATP (change of -80.6% ± 4.3%; $P < 0.0001$; Fig. 3B).

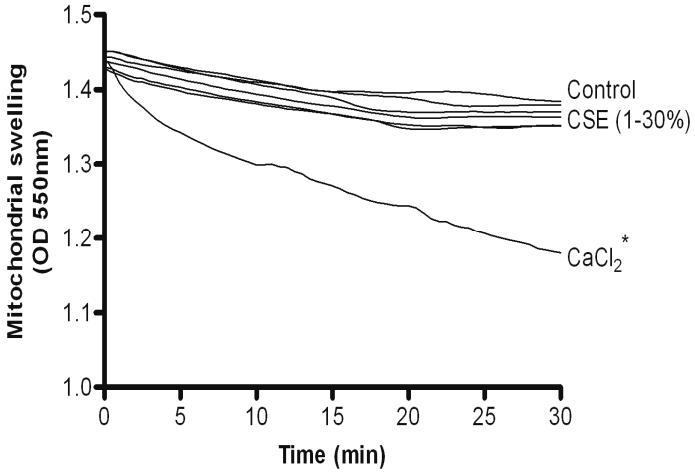

Figure 2. CSE induces no mitochondrial swelling. Mitochondrial swelling assay was used to test the viability of mitochondria ($n = 4$). Mitochondria were incubated for 15 min with increasing concentrations of CSE. $CaC1_2$ was used as a positive control. OD, optical density. $*P < 0.05$.

CSE inhibits complex I and II of the ETC
We hypothesized that CSE is able to produce an ETC failure through inhibition of the respiratory chain, especially at the sites of input of energy (complex I and II). We therefore tested the activity of both complex I (NADH dehydrogenase) and complex II (succinate dehydrogenase) in response to CSE. Low concentrations of CSE (0.05% – 10%) resulted in a dose dependent inhibition of complex I activity (change of -79.7% ± 4.6%; $P < 0.0001$; Fig. 4A), whereas 1–30% of CSE caused a dose-dependent inhibition of complex II activity (change of -50.4% ± 3.4%; $P < 0.0001$; Fig. 4B).

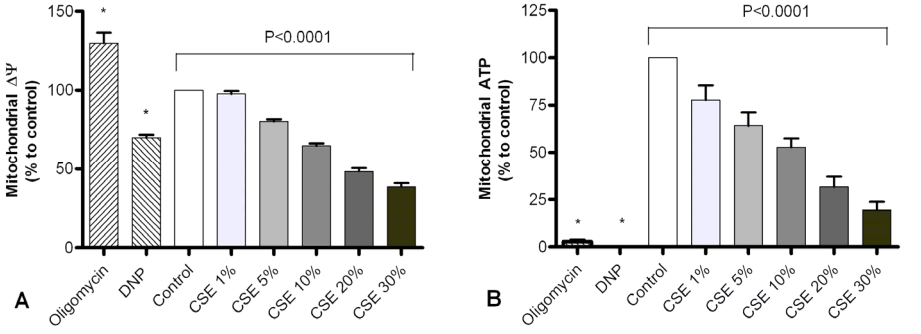

Figure 3. CSE induces a decreased $\Delta\psi_m$ and depletes ATP in isolated mitochondria. Effects of increasing concentrations of CSE on $\Delta\psi_m$ (A) and ATP levels (B) in isolated mitochondria exposed for 15 min (n = 6) are shown.. *P < 0.05 for 20 μM DNP or 5 μM oligomycin vs. control. All experiments were performed in a state III mitochondrial respiration. P values given above the horizontal lines represent the significance for the total decline of all CSE concentrations used (repeated-measures ANOVA).

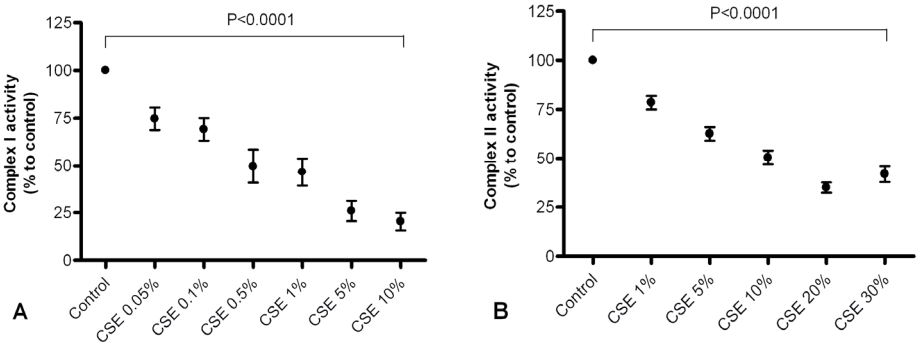

Figure 4. Complexes I and II of the electron transfer chain are blocked by CSE. Effects of increasing concentrations of CSE on activities of NADH dehydrogenase (complex I; A) and succinate dehydrogenase (complex II; B) in isolated mitochondria (n = 9) are shown. P values given above the horizontal lines represent the significance for the total decline of all CSE concentrations used (repeated-measures ANOVA).

CSE affects mitochondrial respiration

Blocking complex I and II by CSE contributes to a decreased flow of electrons along the mitochondrial ETC, resulting in a decreased $\Delta\psi_m$ and decreased ATP production. This sequence of "ETC events" that occurs in response to CSE may result in a decreased mitochondrial respiration. To prove that CSE actually acts as a blocking agent, we incubated isolated mitochondria in an oxygraph sample chamber with a 95% oxygen saturated respiration buffer (Fig. 5A). After addition of succinate as metabolic substrate mitochondria started to respirate in a state IV respiration (154.2 ± 15.4 ng $O_2 \cdot min^{-1} \cdot mg^{-1}$). Addition of ADP directly induces increased oxygen uptake (state III respiration; 494.6 ± 56.5 ng $O_2 \cdot min^{-1} \cdot mg^{-1}$) because ADP is rapidly converted into ATP. The respiratory control index (indicating the coupling between

respiration and phosphorylation) was 3.2 ± 0.3 for these experiments (Fig. 5A). Thereafter, we investigated the effects on the mitochondrial respiration of additional exposure of the isolated mitochondria to CSE (Fig. 5, B and C). In Fig. 5B, an example of such a single experiment is shown. For this experiment, isolated mitochondria were preincubated with 30% CSE in respiration buffer. By using this approach we demonstrated that CSE induced a blockade of the ETC dose dependently in state III respiration (change of 318.2 ± 29.9 ng $O_2 \cdot min^{-1} \cdot mg^{-1}$; $P < 0.05$). Even the addition of the protonophore DNP was not able to induce an increased oxygen uptake, which indicates a strong blockade of electrons along the ETC (Fig. 5B).

CSE-induced ATP depletion is crucial in the routing of apoptotic-triggered cells to die by necrosis

We examined the mode of cell death in Beas-2b cells induced by the protein kinase inhibitor STS under conditions of intracellular ATP depletion caused by CSE. STS triggers apoptosis in lung epithelial cells without disturbing the function of the respiratory chain (4; 26). Therefore, Beas-2b cells were preincubated for 1 h with 2 μM STS, followed by incubation for 4 h with different concentrations of CSE. In this model, CSE concentrations ≥ 10% caused an intracellular ATP depletion of >50% within 1 h in primary epithelial cells (Fig. 1) and within 2 h in Beas-2b cells (Fig. 6, A and B). Caspase activation and apoptosis induction by STS were significantly prevented by CSE in a dose-dependent manner (Fig. 6, C and D). CSE concentrations ≥ 10% completely abolish the STS-induced caspase -3 and -7 activities (STS alone: 477.4% ± 69.88% of control; STS + CSE 10%: 118.3% ± 35.73%). Furthermore, the early apoptotic cells exposed to CSE switched their mode of cell death into necrosis using annexin-V and propidium iodide flow cytometry. Addition of CSE to STS-treated cells resulted in decreased numbers of apoptotic cells (60.25 ± 15.2%; $P < 0.05$) and an increase of the cells going into necrosis for the highest concentrations of CSE used (29.83 ± 6.6%; $P < 0.05$). These results suggest that intracellular ATP levels decide the mode of cell death after giving the epithelial cells an apoptotic cell death signal.

DISCUSSION

In the present study, we investigated the effects of CSE on the function of the mitochondrial respiratory chain in human bronchial epithelial cells and isolated mitochondria. We were able to demonstrate that CSE acts as a blocking agent of complex I and II of the ETC. The inhibition of the two entry points of the ETC caused a decrease in $\Delta\psi_m$ and proton motive force. As a consequence of that, the consumption of oxygen and production of ATP was diminished.

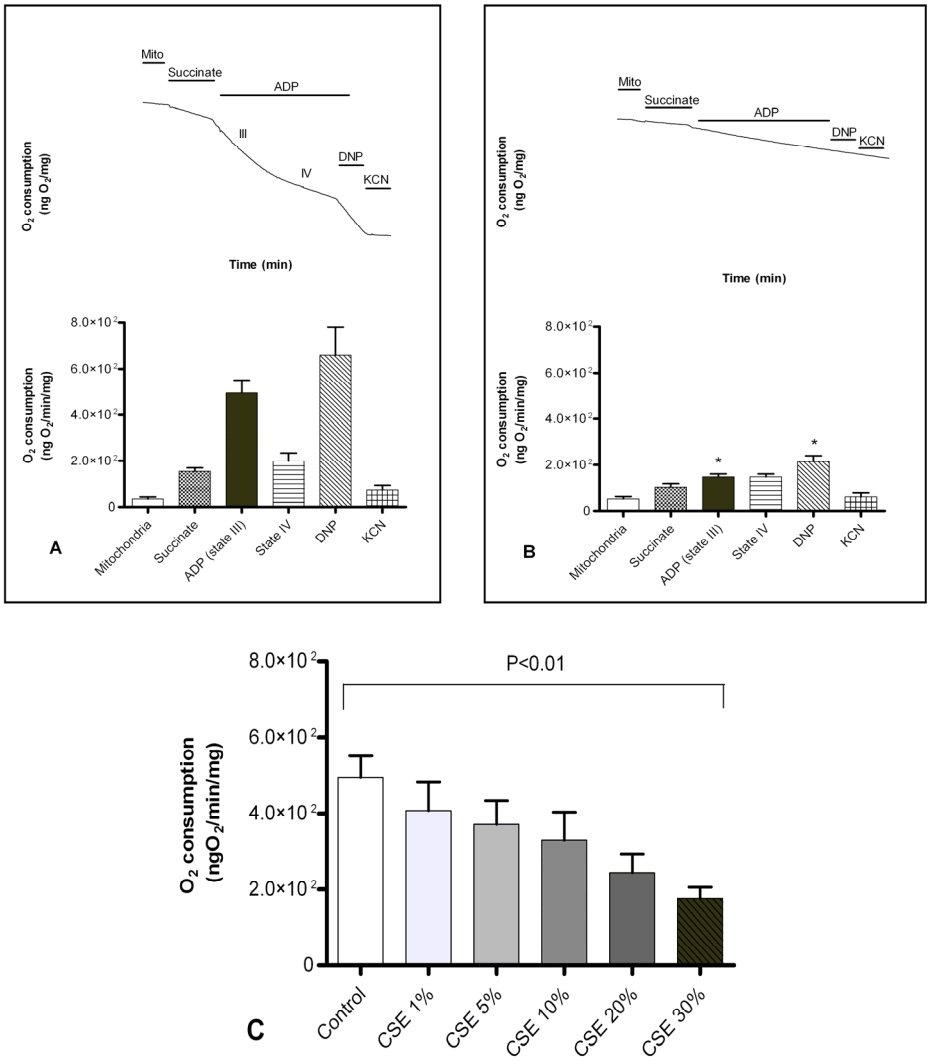

Figure 5. Mitochondrial respiration is decreased by exposure to CSE. Mitochondrial respiration rate was measured with the oxygraph chamber method (n = 4). A: control experiment. B: CSE-pretreated mitochondria (1 min with 30% CSE before the respiration experiment was started). C: dose response of CSE-induced inhibition of the mitochondrial state III respiration rate (n = 4). Oxygen consumption plots are representative for 1 experiment of 4. Mito, mitochondria without addition of substrates; III, state III mitochondrial respiration; IV, state IV mitochondrial respiration; ADP, 5 mM ADP; DNP, 20 µM DNP; KCN, 20 µM potassium cyanide. *P < 0.05, comparison between the CSE and control experiment. P value given above the horizontal line in C represents the significance for the total decline of all CSE concentrations used (repeated-measures ANOVA).

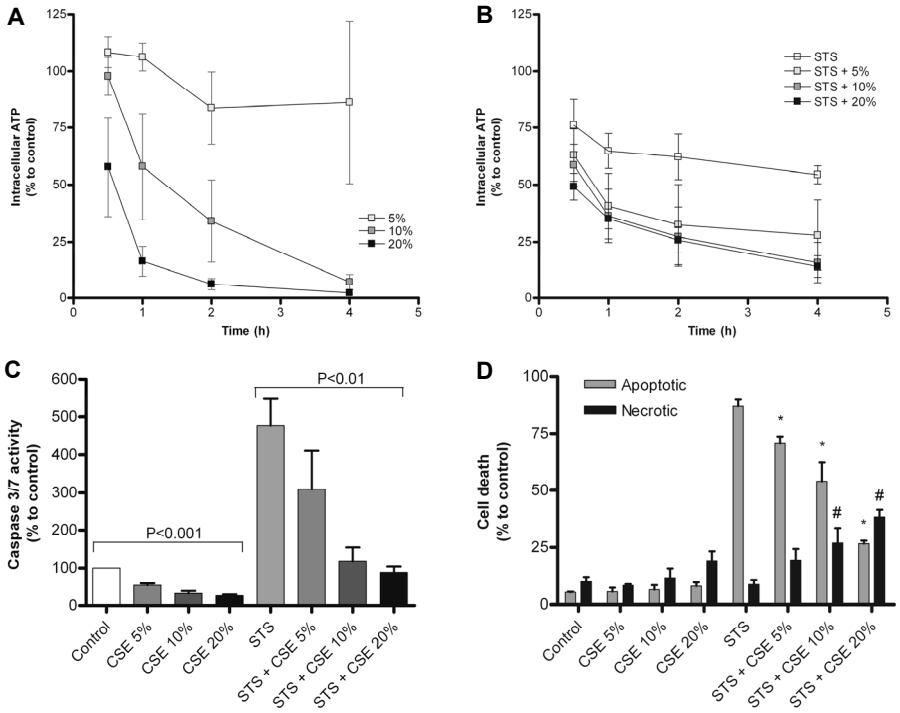

Figure 6. CSE-induced depletion of ATP switches apoptosis to necrosis. A and B: effects of the experimental conditions [increasing length of the exposure to and concentrations of CSE (A) and staurosporin (STS; B)] on intracellular ATP levels in Beas-2b bronchial epithelial cells. Changes in mode of cell death occur after CSE treatment of Beas-2b cells preincubated for 1 h with 2 STS. C and D: cells were washed and incubated for 4 h with different concentrations of CSE. Caspase-3 and -7 activation (C) and apoptosis induction (D; assessed with annexin-V and propidium iodide FITC on flow cytometry) by STS was prevented by CSE in a dose-dependent mimer ($n = 4$). *$P < 0.05$ for comparison between the STS + CSE and STS apoptosis control experiment. #$P < 0.05$ for comparison between the STS + CSE and STS necrosis control experiment.

Mitochondria play a major role in the generation of ATP, which is required for the cell to die by apoptosis (17). Our data demonstrate that early apoptotic epithelial cells that become ATP deficient switch their mode of cell death from apoptosis into necrosis.

Until now, only a few studies have investigated the effects of cigarette smoke on mitochondrial function; however, these studies have not been able to elucidate its mechanism of inhibition. So far no studies have been performed in epithelial cells. However, the inhibition of complex I and II by cigarette smoke has been observed in two previous studies using different models (3, 39). Anbarasi *et al*. (3) demonstrated a decrease in complex I and II activity in brain cells from rats inhaling cigarette smoke and suggested that the alteration in the phospholipids environment of the membrane could be responsible for the inhibition of the electron flow. Similarly, Smith *et al*. (39) demonstrated a decrease in complex I activity in platelets of a human smoking group compared with that of a nonsmoking control group. Besides the action of cigarette smoke on the activity of complex I and II, it has also been

shown that CSE exposure for 3 h induces a dose-dependent mitochondrial membrane depolarization in human isolated monocytes (5). Together, these limited results suggest that cigarette smoke can affect mitochondrial function in different cells and disease models.

Our results now clearly show that CSE inhibits mitochondrial function in primary human bronchial epithelial cells. Additionally, by using direct incubation of isolated mitochondria with CSE, we were able to show for the first time that CSE acts directly as a blocking agent of complex I and II on the ETC without interference of other cellular metabolic activities. To confirm actual blockade, we tested the respiratory activity of isolated mitochondria and showed that the CSE-induced decrease in mitochondrial respiration could not be overruled with the protonophore (uncoupler) DNP.

The components that are actually responsible for the inhibition of Complex I and II respiratory activity are not known. It is known that several compounds of cigarette smoke, like carbon monoxide and cyanides, can inhibit cytochrome-c oxidase at the level of complex IV activity (2, 12). However, CSE stored for a few weeks and therefore devoid of carbon monoxide still showed the same blocking effects (data not shown). Cigarette smoke contains over 4,000 components, and many of those might hypothetically affect the ETC function at many different sites, e.g., phenolic compounds, heavy metals (cadmium, arsenic, lead), gaseous molecules (nitric oxide, $ONOO^-$, carbon monoxide), nicotine, aromates (ubiquinones, acrolein), etc (32).

The final consequence of the CSE-induced ETC blockade is a loss of the capacity of the mitochondria to generate ATP. Because mitochondria play a crucial role in delivering energy for the apoptotic process, alteration of ATP levels may play a crucial role in the routing of cells to die by apoptosis or necrosis (26, 31). The large amount of free radicals present in inhaled cigarette smoke will initially be able to induce an apoptotic signal in the exposed cells (9). In the presence of an intact energy system the cells will be able to generate apoptotic death. In case of apoptotic death, the loss of cells will result in a repair response with limited inflammatory consequences (15). Our results show a decrease in caspase-3 and caspase-7 activity in STS-treated Beas-2b bronchial epithelial cells. These results are conflicting with the observation of Jiao *et al*. (23), who showed a clear induction of caspase-3 activity in A549 lung epithelial cells, but is in agreement with the report of Wickenden *et al*. (42), who showed that CSE inhibits caspase-3 activity after apoptosome formation but before actual caspase-3 cleavage. This difference might be explained by our recently published results, which showed that bronchial epithelial cells indeed can behave differently with respect to the initiation of apoptosis or necrosis (38). Apoptosis tends to occur when lower amounts of CSE are given or CSE is given for a shorter period, whereas cells go into necrosis when the CSE is applied for a longer time or at higher concentrations. We now show that, when early triggered apoptotic cells become deficient in ATP, they will switch from apoptosis to necrosis.

It is now increasingly recognized that cell death, and in particular apoptosis, may play an important role in the pathophysiology of COPD (24, 36). When apoptotic cells die, they are cleared by monocyte phagocytic activity without the release of proinflammatory substances, whereas necrotic cells release their cellular

contents, resulting in an inflammatory response in the environment of these dying cells (44). One link between necrosis acting as a proinflammatory stimulus is through the passive release of the high-mobility group box-1 (HMGB1) protein by necrotic cells but not by apoptotic cells (35). HMGB1 is a nuclear factor and is a secreted protein. The secreted form is a potent inducer of inflammatory mediators like TNF-α (44). The role of necrosis-induced HMGB1 secretion in COPD is not established yet, but recently it has been shown that HMGB1 release may play a key role in the pathogenesis of acute lung injury (40). It can thus be hypothesized that the release of HMGB1 by cigarette smoke-induced necrotic cell death is of great importance in the pathophysiology of COPD and that modulation of this pathway might reveal new treatment modalities (33).

In conclusion, our study demonstrates that CSE induces a blockade of the mitochondrial ETC. This results in a loss of $\Delta\psi_m$, causing a decrease in ATP production. By this depletion of cellular energy, early apoptotic cells exposed to CSE showed a switch to a necrotic cell death. This cigarette smoke-induced mitochondrial dysfunction may become a new pathophysiological concept in the development of COPD and other cigarette smoke-induced diseases and may open new pathways for treatment modalities. Future studies can elucidate the role of cigarette smoke-induced mitochondrial dysfunction and mode of cell death in COPD.

GRANTS

This work was supported by research grants of the Netherlands Kidney Foundation (M. van der Toorn; project C01.1923) and from GlaxoSmithKline (H. G. de Bruin).

REFERENCE LIST

1. Alonso JR, Cardellach F, Lopez S, Casademont J and Miro O. Carbon monoxide specifically inhibits cytochrome c oxidase of human mitochondrial respiratory chain. Pharmacol Toxicol 93: 142-146, 2003.
2. Anbarasi K, Vani G and Devi CS. Protective effect of bacoside a on cigarette smoking induced brain mitochondrial dysfunction in rats. J Environ Pathol Toxicol Oncol 24: 225-234, 2005.
3. Anel A, Gamen S, Alava MA, Schmitt-Verhulst AM, Pineiro A and Naval J. Role of oxidative damage and IL-1 beta-converting enzyme-like proteases in Fas-based cytotoxicity exerted by effector T cells. Int Immunol 8: 1173-1183, 1996.
4. Banzet N, Francois D and Polla BS. Tobacco smoke induces mitochondrial depolarization along with cell death: effects of antioxidants. Redox Rep 4: 229-236, 1999.
5. Barnes PJ, Shapiro SD and Pauwels RA. Chronic obstructive pulmonary disease: molecular and cellular mechanisms. Eur Respir J 22: 672-688, 2003.
6. Barzu O, Muresan L and Tarmure C. Spectrophotometric method for assay of mitochondrial oxygen uptake. II. Simultaneous determination of mitochondrial swelling, respiration, and phosphate esterification. Anal Biochem 24: 249-258, 1968.

8. Borger P, Kauffman HF, Scholma J, Timmerman JA and Koeter GH. Human allogeneic CD2+ lymphocytes activate airway-derived epithelial cells to produce interleukin-6 and interleukin-8. Possible role for the epithelium in chronic allograft rejection. J Heart Lung Transplant 21: 567-575, 2002.
9. Bowler RP, Barnes PJ and Crapo JD. The role of oxidative stress in COPD. J COPD 1:255-277, 2004.
10. Carnevali S, Petruzzelli S, Longoni B, Vanacore R, Barale R, Cipollini M, Scatena F, Paggiaro P, Celi A and Giuntini C. Cigarette smoke extract induces oxidative stress and apoptosis in human lung fibroblasts. Am J Physiol Lung Cell Mol Physiol 284: L955-L963, 2003.
11. Duke RC, Ojcius DM and Young JD. Cell suicide in health and disease. Sci Am 275: 80-87, 1996.
12. Fosslien E. Mitochondrial medicine--molecular pathology of defective oxidative phosphorylation. Ann Clin Lab Sci 31: 25-67, 2001.
13. Gairola C and Aleem MI. Cigarette smoke: effect of aqueous and nonaqueous fractions on mitochondrial function. Nature 241: 287-288, 1973.
14. Green DR and Reed JC. Mitochondria and apoptosis. Science 281: 1309-1312, 1998.
15. Gulbins E, Jekle A, Ferlinz K, Grassme H and Lang F. Physiology of apoptosis. Am J Physiol Renal Physiol 279: F605-F615, 2000.
16. Hageman GJ, Larik I, Pennings HJ, Haenen GR, Wouters EF and Bast A. Systemic poly(ADP-ribose) polymerase-1 activation, chronic inflammation, and oxidative stress in COPD patients. Free Radic Biol Med 35: 140-148, 2003.
17. Halestrap A. Biochemistry: a pore way to die. Nature 434: 578-579, 2005.
18. Hodge S, Hodge G, Holmes M and Reynolds PN. Increased airway epithelial and T-cell apoptosis in COPD remains despite smoking cessation. Eur Respir J 25: 447-454, 2005.
19. Hogg JC. Pathophysiology of airflow limitation in chronic obstructive pulmonary disease. Lancet 364: 709-721, 2004.
20. Hoshino Y, Mio T, Nagai S, Miki H, Ito I and Izumi T. Cytotoxic effects of cigarette smoke extract on an alveolar type II cell-derived cell line. Am J Physiol Lung Cell MolPhysiol 281: L509-L516, 2001.
21. Imai K, Mercer BA, Schulman LL, Sonett JR and D'Armiento JM. Correlation of lung surface area to apoptosis and proliferation in human emphysema. Eur Respir J 25: 250-258, 2005.
22. Israels LG and Israels ED. Apoptosis. Stem Cells 17: 306-313, 1999.
23. Jiao ZX, Ao QL and Xiong M. Cigarette smoke extract inhibits the proliferation of alveolar epithelial cells and induces apoptosis. Sheng Li Xue Bao 58: 244-254, 2006.
24. Kasahara Y, Tuder RM, Taraseviciene-Stewart L, Le Cras TD, Abman S, Hirth PK, Waltenberger J and Voelkel NF. Inhibition of VEGF receptors causes lung cell apoptosis and emphysema. J Clin Invest 106: 1311-1319, 2000.
25. Kennedy JR and Elliott AM. Cigarette smoke: the effect of residue on mitochondrial structure. Science 168: 1097-1098, 1970.
26. Leist M, Single B, Castoldi AF, Kuhnle S and Nicotera P. Intracellular adenosine triphosphate (ATP) concentration: a switch in the decision between apoptosis and necrosis. J Exp Med 185: 1481-1486, 1997.

27. Liu X, Conner H, Kobayashi T, Kim H, Wen F, Abe S, Fang Q, Wang X, Hashimoto M, Bitterman P and Rennard SI. Cigarette smoke extract induces DNA damage but not apoptosis in human bronchial epithelial cells. Am J Respir Cell Mol Biol 33: 121-129, 2005.
28. Minakami S, Ringeler RL and Singer TP. Studies on the respiratory chain-linked dihydrodiphosphopyridine nucleotide dehydrogenase. I. Assay of the enzyme in particulate and in soluble preparations. J Biol Chem 237: 569-576, 1962.
29. Miro O, Alonso JR, Jarreta D, Casademont J, Urbano-Marquez A and Cardellach F. Smoking disturbs mitochondrial respiratory chain function and enhances lipid peroxidation on human circulating lymphocytes. Carcinogenesis 20: 1331-1336, 1999.
30. Rahman I and MacNee W. Role of oxidants/antioxidants in smoking-induced lung diseases. Free Radic Biol Med 21: 669-681, 1996.
31. Richter C, Schweizer M, Cossarizza A and Franceschi C. Control of apoptosis by the cellular ATP level. FEBS Lett 378: 107-110, 1996.
32. Rustemeier K, Stabbert R, Haussmann HJ, Roemer E and Carmines EL. Evaluation of the potential effects of ingredients added to cigarettes. Part 2: chemical composition of mainstream smoke. Food Chem Toxicol 40: 93-104, 2002.
33. Sadikot RT, Christman JW and Blackwell TS. Molecular targets for modulating lung inflammation and injury. Curr Drug Targets 5: 581-588, 2004.
34. Saraste M. Oxidative phosphorylation at the fin de siecle. Science 283: 1488-1493, 1999.
35. Scaffidi P, Misteli T and Bianchi ME. Release of chromatin protein HMGB1 by necrotic cells triggers inflammation. Nature 418: 191-195, 2002.
36. Shapiro SD and Ingenito EP. The pathogenesis of chronic obstructive pulmonary disease: advances in the past 100 years. Am J Respir Cell Mol Biol 32: 367-372, 2005.
37. Slater EC and Bonnner WD. Inhibition of the succinic oxidase system by fluoride. Biochem J 49: l-li, 1951.
38. Slebos DJ, Ryter SW, van der Toorn M, Liu F, Guo F, Baty CJ, Karlsson JM, Watkins SC, Kim HP, Wang X, Lee JS, Postma DS, Kauffman HF and Choi AM. Mitochondrial Localization and Function of Heme Oxygenase-1 in Cigarette Smoke-Induced Cell Death. Am J Respir Cell Mol Biol 2006.
39. Smith PR, Cooper JM, Govan GG, Harding AE and Schapira AH. Smoking and mitochondrial function: a model for environmental toxins. Q J Med 86: 657-660, 1993.
39a.'t Hart NA, van der Plaats A, Leuvenink HG, Wiersema-Buist J, Olinga P, van Luyn MJ, Verkerke GJ, Rakhorst G and Ploeg RJ. Initial blood washout during organprocurement determines liver injury and function after preservation and reperfusion. Am J Transplant 4: 1836-1844, 2004.
40. Ueno H, Matsuda T, Hashimoto S, Amaya F, Kitamura Y, Tanaka M, Kobayashi A, Maruyama I, Yamada S, Hasegawa N, Soejima J, Koh H and Ishizaka A. Contributions of high mobility group box protein in experimental and clinical acute lung injury. Am J Respir Crit Care Med 170: 1310-1316, 2004.

41. Vandivier RW, Henson PM and Douglas IS. Burying the dead: the impact of failed apoptotic cell removal (efferocytosis) on chronic inflammatory lung disease. Chest 129: 1673-1682, 2006.
42. Wickenden JA, Clarke MC, Rossi AG, Rahman I, Faux SP, Donaldson K and MacNee W. Cigarette smoke prevents apoptosis through inhibition of caspase activation and induces necrosis. Am J Respir Cell Mol Biol 29: 562-570, 2003.
43. Yokohori N, Aoshiba K and Nagai A. Increased levels of cell death and proliferation in alveolar wall cells in patients with pulmonary emphysema. Chest 125: 626-632, 2004.
44. Zong WX, Ditsworth D, Bauer DE, Wang ZQ and Thompson CB. Alkylating DNA damage stimulates a regulated form of necrotic cell death. Genes Dev 18: 1272-1282, 2004.

Chapter 2

MITOCHONDRIA ARE ESSENTIAL IN CIGARETTE SMOKE

INDUCED ROS GENERATION

Marco van der Toorn[1], Delaram Rezayat[1], Henk F. Kauffman[2],
Stephan J.L. Bakker[3], Rijk O.B.Gans[3], Gerard H. Koëter[4],
Augustine M. K. Choi[5], Antoon J.M. van Oosterhout[1], Dirk-Jan Slebos[4].

[1]Laboratory of Allergology and Pulmonary Diseases, Department of Pathology and Medical Biology, [2]Department of Pathology, [3]Department of Internal Medicine, [4]Department of Pulmonary Diseases, University Medical Center Groningen, University of Groningen, The Netherlands, [5]Division of Pulmonary and Critical Care Medicine, Brigham and Women's Hospital, Harvard Medical School, Boston, Massachusetts, USA.

Submitted

ABSTRACT

Reactive oxygen species (ROS) present in cigarette smoke (CS) are thought to contribute to the development of COPD. Although CS-ROS can hardly enter airway epithelial cells, and certainly not the circulation, systemic levels of ROS have been found to be elevated in COPD patients. We hypothesize that lipophilic components present in CS can enter airway epithelial cells and increase intracellular ROS production by disturbing mitochondrial function. Airway epithelial cell-lines Beas-2b, A549 and A549-ρ0 cells, which lack functional mitochondria were used. Beas-2b cells were used for assessment of the influence of CS on mitochondrial membrane potential ($\Delta\psi_m$) and ATP levels. A549 and A549-ρ0 cells were used to investigate the role of mitochondria in intracellular ROS generation (by DCF fluorescence). ROS-mediated damage was assessed by measuring free thiol groups (-SH). Removal of lipophilic components from CS-extract (CSE) was performed using hexane extraction. ROS were removed from the gaseous-phase of CS using a water filter. In Beas-2b cells, CSE (4h) caused a dose-dependent decrease $\Delta\psi_m$ and ATP levels, whereas hexane treated CSE did not. DCF fluorescence in A549 cells increased in response to CSE, whereas this was not the case in A549-ρ0 cells. Exposure of A549 cells to CS resulted in a rapid decrease in free –SH, whereas exposure to ROS-depleted CS only resulted in a delayed decrease. This delayed decrease was less pronounced in A549-ρ0 cells. Lipophilic components in CS disturb mitochondrial function, which contribute to increased intracellular generation of ROS. Our results are of importance in understanding the systemic effects of smoking observed in patients with COPD.

INTRODUCTION

Smoking cigarettes is a major risk factor for the development of Chronic Obstructive Pulmonary Disease (COPD)(2; 21). Cigarette smoke (CS) contains more than 4000 chemicals (5), including reactive oxygen species (ROS), such as superoxide ($O_2^{\cdot-}$) and hydroxyl radicals ($\cdot OH$), which are present in high concentrations in the gaseous-phase. ROS in CS will primarily react with the anti-oxidants in the epithelial lining fluid covering airway epithelial cells and their plasma cell membranes, causing direct damage (11). However, these ROS are not capable of diffusing through the plasma membranes of these cells, and therefore are not capable of entering the circulation (1; 6; 16). Despite this, there is considerable evidence for induction of systemic oxidative stress by CS, as certified by high circulating levels of malondialdehyde (MDA) and low plasma levels of vitamin C and reduced glutathione (GSH) in smokers and patients with COPD (7; 31; 32). Such systemic oxidative stress may result in tissue injury with apoptotic and necrotic cell death, muscle dysfunction, organ failure and maintenance of systemic inflammation, all potentially of importance in the development and progression of COPD (26; 27; 33).

Whereas the gaseous-phase ROS in CS are hardly able to enter the cells, and thus are unlikely to pass the airway epithelial barrier, lipophilic components in CS, including phenolic compounds, aldehydes and polycyclic aromatic hydrocarbons, can easily pass the cell and enter the systemic circulation (23; 34). We hypothesize that once inside cells, lipophilic components disturb mitochondrial function, leading to increased mitochondrial ROS formation.

The potential importance of mitochondrial ROS metabolism in COPD may be best illustrated by the fact that all major anti-oxidants that are supposed to be important in the pathophysiology of COPD are linked to mitochondria. These include GSH, catalase, thioredoxin, superoxide-dismutase and also, as we recently demonstrated, heme-oxygenase-1 (HO-1) (29). The primary function of mitochondria is production of ATP, a process linked to the action of the electron transfer chain (ETC). Disturbance of the ETC by lipophilic components may enhance leakage of single electrons from complex I and complex II of the ETC. These electrons that leak from the ETC can be accepted by oxygen, converting it into $O_2^{\cdot-}$, a very potent free radical (12; 18).

In this study we aimed to investigate whether lipophilic components present in CS result in (I) disturbance of mitochondrial function and (II) increased mitochondrial ROS formation. To assess potential disturbance of mitochondrial function we used the bronchial epithelial cell line Beas-2b, and to investigate whether mitochondria are involved in increased ROS production upon exposure to CS, we made use of alveolar epithelial cells devoid of functional mitochondria (A549-ρ0), with normal A549 cells serving as controls.

MATERIALS AND METHODS

Chemicals

Bovine serum albumin (BSA), 5,5'-dithiobis-(2)-nitrobenzoic acid (DTNB), hexane, L-cystein, Phorbol 12-Myristate 13-Acetate (PMA), sodium pyruvate, Triton X-100, uridine and vitamin C were obtained from Sigma-Aldrich Chemie B.V.

(Zwijndrecht, The Netherlands). 5,5′,6,6′-tetrachloro-1,1′,3,3′-tetraethyl-benzimidazolyl-carbocyanine iodide (JC-1), 5-(and-6)-chloromethyl-2',7'-dichlorodihydrofluorescein diacetate, acetyl ester (DCF) and ethidium bromide were purchased from Invitrogen (Breda, the Netherlands).

Cell culture and preparation of ρ0 cells
The human bronchial epithelial cell line (Beas-2b) and the human alveolar type II epithelium-like adherent cell line (A549) were purchased from American Type Culture Collection (ATCC, Manassas, VA). Cells were grown in RPMI 1640 with 25 mM HEPES, L-Glutamine (BioWitthaker, Verviers, Belgium) supplemented with 10% heat-inactivated fetal calf serum (BioWitthaker, Verviers, Belgium) and 20 μg/ml gentamycin (Centafarm Services, Etten-Leur, The Netherlands). Cells were grown in 25 cm^2 plastic culture flasks (Costar, Cambridge, MA) and 6-well tissue cell culture plates (Costar, Cambridge, MA) at 37°C in an atmosphere of 5% CO_2 until 80-90% confluency was reached. Before the experiments cells were incubated for 16 h in serum free RPMI 1640 media. A549-ρ0 cells generated by chemical elimination of mitochondrial DNA were kindly provided provided by Navdeep Chandel (Department of Medicine, University of Chicago, USA). Briefly, A549-ρ0 cells were prepared by long-term growth in medium supplemented with ethidium bromide (50 ng/ml), sodium pyruvate (110 μg/ml), and uridine (100 μg/ml). The lack of a functional ETC in these cells was examined with the potentiometric fluorescent dye JC-1.

Preparation of CS-extract
Kentucky 2R4F research-reference filtered cigarettes (The Tobacco Research Institute, University of Kentucky, Lexington, KY) where smoked using a peristaltic pump. Just before the experiments, the filters were cut from the cigarettes. Each cigarette was smoked in 5 min with a 17 mm but remaining. Two cigarettes were bubbled through 25 ml of cell growth medium, and this solution was regarded as 100% strength CS-extract **(**CSE).

Hexane extraction of CSE
Extraction of lipophilic compounds from CSE was performed using a two-step hexane extraction procedure. Briefly, one volume of CSE was added to 2 volumes of hexane. The vial was tightly closed and fastened on a rocking platform for 5 minutes. Thereafter, the mixture was centrifuged at low speed (2000 rpm) for 2 min to separate the aqueous and organic phase. The hexane phase, containing the lipophilic compounds, was removed by careful suction with needle and pump or syringe. The previous step was then repeated.

Fluorescent monitoring of the mitochondrial membrane potential
Beas-2b cells were incubated for 4 h with different concentration of CSE or hexane treated CSE (Hx-CSE). At the end of the incubation period, cells were loaded with the potentiometric fluorescent dye JC-1 (4 μM) for 10 minutes in an incubator. At the end of the incubation period, cells were washed with PBS and measured on a Perkin Elmer Victor^3 V fluorescent plate reader (Perkin Elmer, Groningen, The Netherlands).

Luminescence monitoring of intracellular ATP levels
Beas-2b cells were incubated for 4 h with different concentration of CSE or Hx-CSE. At the end of the incubation period, intracellular ATP levels were quantified by treating the cells with 0.1% (v/v) Triton X-100. ATP levels were measured using the Enliten® ATP assay from Promega (Leiden, The Netherlands) and a Berthold microplate Luminometer (Berthold Detection Systems GmbH, Pforzheim, Germany).

DCF-fluorescence microscopy analyses of intracellular ROS
ROS generation was determined using the fluorescent probe DCF. A549 cells and A549-ρ0 cells were grown in 6-well tissue culture plates and treated with CSE (20%) or PMA (10 ng/ml) for 4 h. Cells were washed twice with PBS and then loaded for 30 min with DCF (2.5 μg/ml) at 37°C in the dark. At the end of the incubation period, cells were washed twice with PBS and images were acquired with a Leica DM IL inverted fluorescence microscope (Leica Microsystems B.V., Rijswijk, The Netherlands).

Exposure of L-cystein to different oxidizing agents
A solution of L-cystein (150 μM) was exposed to air, different concentration of H_2O_2, the gaseous-phase of CS (with and without vitamin C (1 mM)) and the gaseous-phase of water-filtered CS (WF-CS). Briefly, 25 ml solution was placed in a 50 ml Falcon tube (BD Biosciences, Alphen aan den Rijn, The Netherlands) at 37°C. Kentucky 2R4F research-reference cigarettes (The Tobacco Research Institute, University of Kentucky, Lexington, KY) were smoked using a peristaltic pump. Just before the experiments, filters were cut from the cigarettes. Each cigarette was smoked in exactly 5 min at a flow rate of 8 L/h and bubbled through the L-cystein solution. This solution was used immediately for the experimental procedures as described below. WF-CS was produced with the same peristaltic pump, but the smoke was first passed through a receptacle of water (1 L) before it was bubbled through the L-cystein solution. Air, produced with the same peristaltic pump, but without a cigarette, was used as a negative control under the same conditions.

Exposure of airway epithelial cells to CS and water-filtered CS
Epithelial cells were exposed to air, the gaseous-phase of CS or the gaseous-phase of WF-CS as described previously (36). Briefly, A549 cells were grown in 25 cm^2 plastic culture flasks as described above. Just before the experiments, medium was removed and the culture flask was positioned up-side down, allowing a direct contact of smoke with epithelial cells. Kentucky 2R4F research-reference cigarettes were smoked using a peristaltic pump. Just before the experiments, filters were cut from the cigarettes. Each cigarette was smoked in exactly 5 minutes at a rate of 8 L/h. Gaseous-phase CS or WF-CS was directly distributed inside the culture flasks, by blowing the smoke inside through a small plastic tube. After the exposure, cells were washed with PBS, lysed by one freeze-thaw cycle in 2.5 ml pure H_2O and analyzed. Air was used as negative control under the same conditions as CS.

Quantitative determination of free thiol groups
Total protein concentration in cell culture was determined by the Bradford method, using BSA as standard (Bio-rad Laboratories, The Netherlands). Ellman's reagent was used for the determination of free thiol groups in cell culture and a cell-free solution of L-cystein. Ellman's reagent (12 mM DTNB) was added to the lysed cells or L-cystein solution to a final concentration of 6 mM DTNB followed by 10 min incubation. Thereafter, samples were centrifuged at 1000 g for 5 min. The supernatant was used in the assay and measured at 405 nm in a Biotek EL808 microplate reader (Bio-Tek Instruments, Abcoude, The Netherlands). The amount of free thiol groups was calibrated against a standard curve of L-cystein.

Statistical analysis
Calculations were performed using Prism 4 for windows (GraphPad Software, inc., San Diego, USA). Statistical analysis was performed using repeated measures ANOVA. Comparisons between different experimental groups were performed with Dunnet's multiple comparison test. $P < 0.05$ was considered significant. Results are presented as mean (± SEM) unless otherwise mentioned.

RESULTS

Lipophilic compounds in CSE disturb mitochondrial function
To investigate the acute effects of lipophilic components on mitochondrial function, we examined whether exposure of Beas-2b cells to CSE or Hx-CSE affects the mitochondrial membrane potential ($\Delta\psi_m$) and intracellular ATP levels. Exposure of Beas-2b cells to increasing concentrations of CSE for 4 h caused a significant dose-dependent decrease of $\Delta\psi_m$ (Δ = -76.9 ± 3.4 % , P < 0.0001; Fig. 1 A) and ATP levels (Δ = -88.0 ± 10.2 %, P < 0.01; Fig. 1 B). Compared to CSE, Hx-CSE exposed Beas-2b cells displayed a significantly attenuated decrease in $\Delta\psi_m$ and ATP levels.

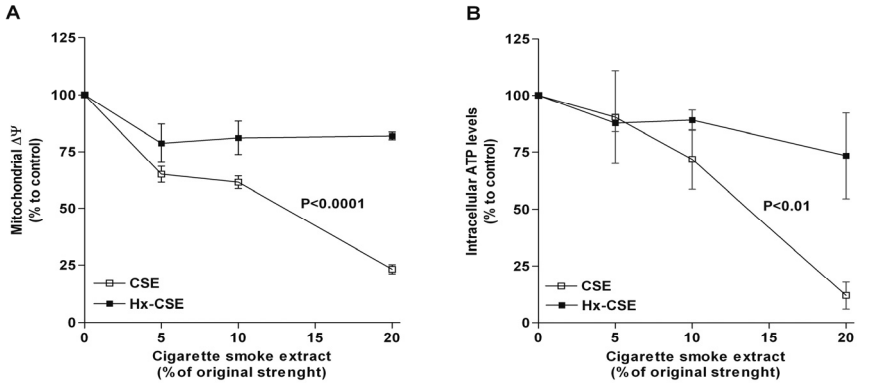

Figure 1. Cigarette smoke extract (CSE) induces a loss of mitochondrial function in human bronchial epithelial cell line (Beas-2b). Effects of increasing concentrations of CSE and hexane treated CSE (Hx-CSE) on (A) mitochondrial membrane potential ($\Delta\psi$) and (B) intracellular ATP levels in Beas-2b exposed for 4 h (n = 3) are shown. P values given above the CSE lines represent the significance for the decline of $\Delta\psi$ and ATP levels (repeated-measures ANOVA).

Functional mitochondria are essential in CSE induced ROS generation

After the observation made in Beas-2b cells above, we set out to further investigate mitochondrial function. Therefore, we made use alveolar epithelial cells devoid of functional mitochondria by treatment with ethidium bromide (A549-ρ0 cells), with normal A549 cells serving as controls. A549-ρ0 cells are characterized by lacking a $\Delta\psi_m$. This was confirmed with the potentiometric probe JC-1 (data not shown). The fluorescent dye DCF was used to detect the levels of intracellular ROS. Both cell lines (A549 and A549-ρ0 cells) were exposed to CSE or PMA for 4 h. A549 cells stimulated with CSE showed an increase in DCF fluorescence whereas A549-ρ0 cells did not. PMA was used as a positive control. Addition of PMA resulted in A549 cells as well as A549-ρ0 cells in an increase in DCF fluorescence when compared to control (Fig. 2). These results suggest that a functional mitochondrial ETC is necessary to produce ROS in response to CSE.

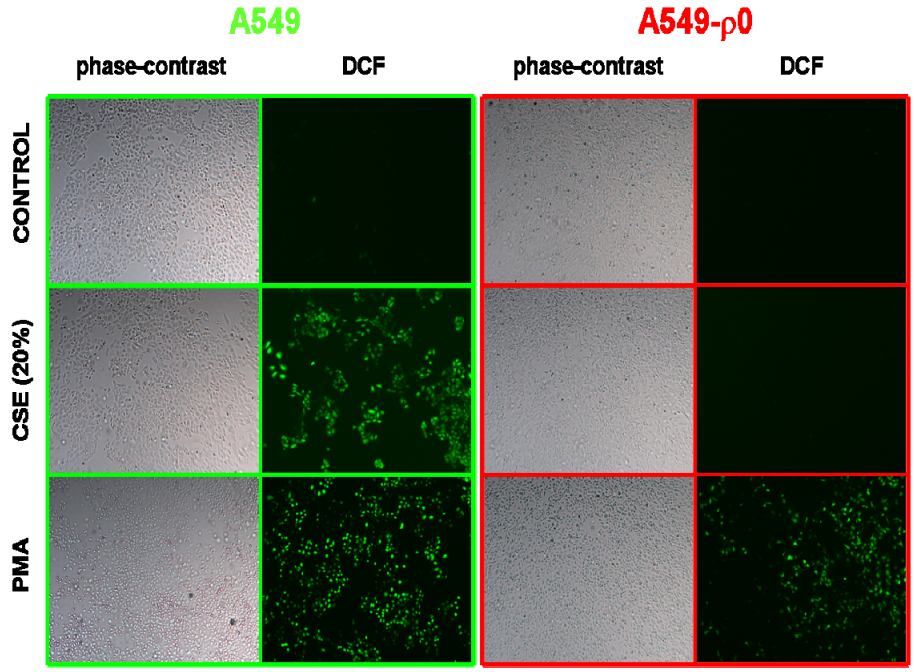

Figure 2. Cigarette smoke extract (CSE) induces reactive oxygen species (ROS) generation in human alveolar epithelial cells (A549). Effects of CSE (20%) or PMA (10 ng/ml) on ROS generation in A549 and alveolar epithelial cells lacking a mitochondrial membrane potential (A549-ρO) are shown. Live cells were loaded with 2',7'-dichlorodihydrofluorescein diacetate (DCF) before being imaged on an inverted light and fluorescence microscope. Representative images selected from randomly chosen fields are shown.

Gaseous-phase CS can be depleted of its ROS

The thiol-specific interaction between L-cystein and free radicals induced by gaseous-phase CS was studied by the DTNB assay that measures the free thiol content. L-cystein is easily oxidized by ROS. The results showed that the free thiol groups of L-cystein were fully oxidized within minutes after incubation with H_2O_2

(Fig. 3 A). In figure 3 B we showed that CS significantly decreases the free thiol groups of L-cystein in solution, thereby indirectly showing that CS contains ROS. Treatment with the antioxidant vitamin C caused a significant attenuation of the effects of CS. Interestingly, WF-CS did not alter the free thiol groups of L-cystein, indicating that ROS is easily removed from CS by a single passage through water.

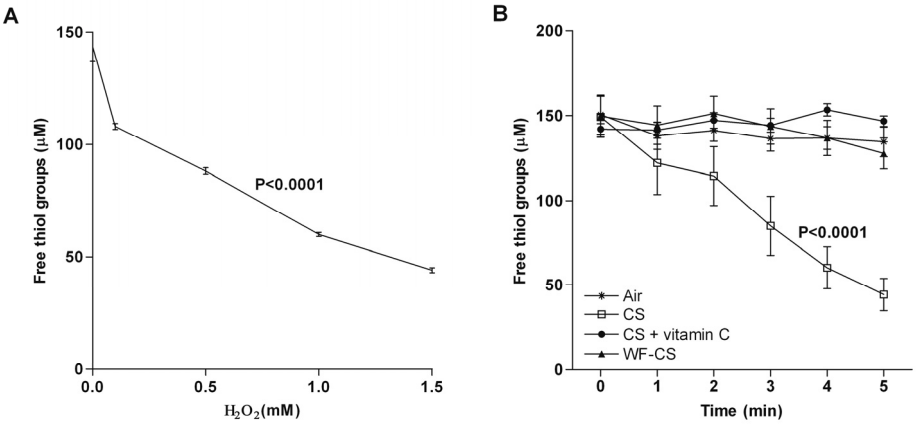

Figure 3. Effects of different oxidizing agents on the level of free thiol groups of L-cystein in solution. Incubation of 150 µM of L-cystein with increasing concentrations of (A) H_2O_2, (B) control air (Air), cigarette smoke (CS), CS + vitamin C and water-filtered CS (WF-CS) in the absence of light (*n = 4*) are shown. Free thiol groups studied using Ellman's reagent. *P* values given above the lines represents the significance for the total decline of free thiol groups (repeated-measures ANOVA).

Mitochondrial ROS generation oxidizes free thiol groups in epithelial cells

To investigate the effect of CS on intracellular ROS generation, A549 cells were exposed for 5 minutes to gaseous-phase CS and WF-CS. CS significantly decreases free thiol content in airway epithelial cells compared to air control, proving that gaseous-phase CS contains ROS (CS Δ = -68.3 ± 5.5 %, $P < 0.01$; Fig. 4 A) . WF-CS initially showed no effect on free thiol content, showing that this smoke does not contain ROS. However, eight hours after incubation of the cells with WF-CS, a significant decline of free thiol groups was observed, indicating an intracellular generation of ROS (WF-CS Δ = -41.1 ± 2.5 %, $P < 0.01$; Fig. 4 A). To test the involvement of mitochondria in this 'indirect' ROS generation, A549 and A549-ρ0 cells were exposed to CS. Air exposure used as a negative control did not affect free thiol groups in both cell types. A strong decline of free thiol groups was seen in the A549 cells treated with CS (Δ = - 119.5 ± 12.6 µM / mg, $P < 0.01$; Fig. 4 B). A549-ρ0 cells lacking a functional ETC, were significantly less responsive to CS when compared to the A549 cells ($P < 0.01$) (Fig. 4 B). These results suggest that mitochondria play a role in CS-induced intracellular oxidative stress.

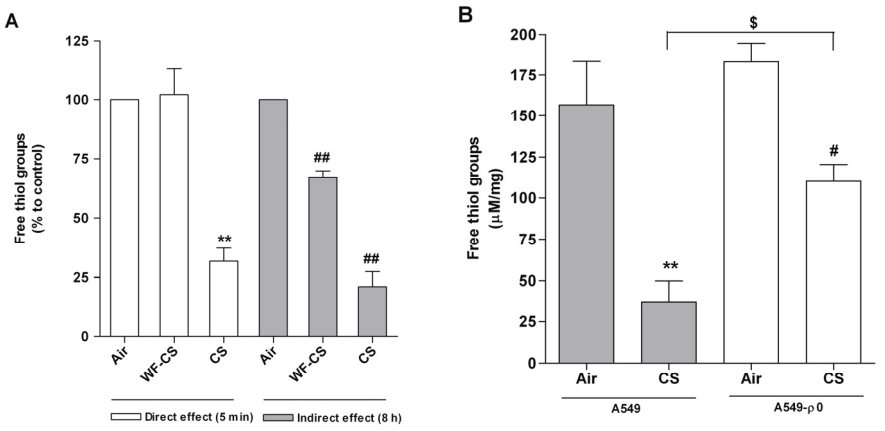

Figure 4. Effects of gaseous-phase cigarette smoke (CS) on free thiol groups in human alveolar epithelial cells (A549) and human alveolar epithelial cells lacking a mitochondrial membrane potential (A549-ρ0). Free thiol groups in A549 cells were measured after 5 min and 8 h using Ellman's reagent (A). Free thiol groups in both, A549 and A549-ρ0 cells were measured after 8 h using Ellman's reagent (B). Data are expressed as mean values ± SEM and are referred to 4 experiments. WF-CS = exposure to 1 cigarette (first passed through a receptacle of water), CS = exposure to 1 cigarette (directly distributed inside the culture flasks). **, $P < 0.01$ vs control (A549); ##, $P < 0.01$ vs control; #, $P < 0.05$ vs control (A549-ρ0); $, $P < 0.05$ vs CS (A549) by Dunnet's multiple comparison test.

DISCUSSION

ROS present in gaseous-phase CS are thought to be important factors for the development of COPD (25). In patients with COPD increased systemic markers of oxidative stress have been shown, this despite the fact that the ROS that are present in the CS hardly enter the circulation nor passes cellular membranes. In the current study we investigated the effects of CS on mitochondrial ROS generation and demonstrated that next to a 'direct' ROS effect, from the gaseous-phase of CS, an 'indirect' intracellular ROS generation was observed which depends on disturbance of functional mitochondria by lipophilic components in CS.

There is a very strong physiological link between mitochondria, which are located in the cytoplasm of all eukaryotic cells, and the human respiration. The lungs extract oxygen which is essential for mitochondria to generate ATP, necessary for life, by oxidative phosphorylation. Under physiological conditions, oxygen-based radicals such as $O_2^{\cdot -}$ and $\cdot OH$ are by-products of the oxidative phosphorylation. To ensure an appropriate defense against these by-products, mitochondria are balanced with enzymatic and non-enzymatic antioxidant systems. If the amount of ROS increases or if antioxidant defense decreases, oxidative stress will be enhanced. Direct damage to mitochondria can result in a feed-forward process, whereby mitochondrial injury causes additional damage (14; 22). It is well established that smoking cigarettes contributes to an imbalance between ROS and antioxidant defenses (4).

CS is a complex aerosol which can be separated into a gas and particulate-phase, whereas many substances are partitioned between these two phases. Both phases contain high levels of reactive components and radicals. In the gaseous-phase high levels of ROS are found. ROS are highly reactive due to the presence of unpaired valence shell electrons, which make them incapable to diffuse through the respiratory membranes (1; 6; 16). Therefore gaseous-phase ROS only cause local damage in the lung, especially at the lipid bilayer of the epithelial cells and decreases the anti-oxidant content in the ELF (25; 35).

In the particulate-phase of CS, lipophilic components are present. Lipophilic components are able to pass the lipid bilayer. Recent reports have shown that components present in CSE, which does not contain ROS, are able to pass through the membranes of cells and subsequently disturb mitochondria (17; 33). Highly reactive components like polycyclic aromatic hydrocarbons, aldehydes, phenols, heavy metals and amines are lipophilic candidates that easily enter the cell and disturb mitochondria (15; 28). We recently showed that two examples of these highly reactive lipophilic components, acrolein and crotonaldehyde, indeed easily enter the cell and react very fast with antioxidant proteins like glutathione (34). Our data now demonstrates that the lipophilic fraction present in CSE is responsible for a decrease in $\Delta\psi_{m,}$ ATP and concomitant generation of mitochondrial ROS. By using A549 cells and A549-ρ0 cells, which lack a functional ETC, we prove that mitochondria are essential in CS-induced ROS generation. Different studies show that disturbing mitochondria is accompanied by enhanced generation of ROS and decreases $\Delta\psi_m$, mitochondrial oxygen consumption, and production of ATP (8; 12; 33). Not only pulmonary cells, but also circulating cells can be affected in this way (17).

Gaseous-phase CS contains a higher percentage of lipophilic components than CSE. To investigate these lipophilic components in gaseous-phase CS without the influence of ROS, a water filter or so called ‘waterpipe’ was used to remove ROS from the gaseous-phase of CS. The effects of the lipophilic components, still present in the gaseous-phase of WF-CS, did not immediately oxidize free thiol groups in airway epithelial cells. This may indicate that these components firstly disturb mitochondrial function and secondly induce an ‘indirect’ burst of intracellular ROS resulting in oxidation of free thiol groups. This is in agreement with the findings of the group of Nel and colleagues (13). They showed that quinones and aromatic compounds in air pollution induce mitochondrial dysfunction and intracellular ROS generation. In this regard, Bonvallot et al. (3) showed that different organic compounds from diesel exhaust induce generation of ROS in airway epithelial cells after 4h incubation. The authors described two other mechanisms which could explain the intracellular burst of ROS. The main generation of ROS may proceed from the metabolization of the organic compounds and secondly from the increased catalytic activities of cytochrome P450 system, which is responsible for the breakdown of the organic compounds. In this study, it was not investigated whether there was increased ROS generation as a consequence of a dysfunction of mitochondria.

A new paradigm wherein lipophilic components easily pass the membrane of cells, disturb mitochondrial function and enhance ROS generation is shown in figure 5. ROS in the gaseous-phase of CS and generated by the mitochondria themselves

may both be of importance in the pathogenesis of COPD. This concept is strengthened by the fact that smokers not only develop respiratory diseases, but disease manifestations are also observed systemically. A chronic inflammatory response, loss of skeletal muscle mass (muscle wasting) and loss of body weight have all been observed in smoking COPD patients (10; 20). Interestingly, the group of Schols and colleagues showed that muscles undergo a shift from oxidative to glycolytic metabolism (10). The glycolytic metabolism produces less ATP per mole of glucose than oxidative metabolism. The functional consequences are reflected in significant changes in skeletal muscle energy metabolism and accelerated acidification, indicating that mitochondrial function is disturbed (24).

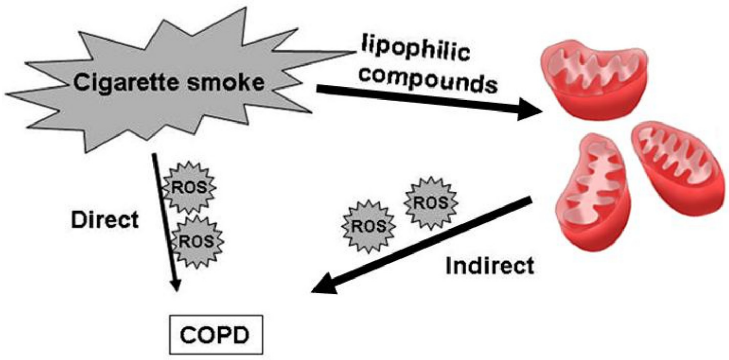

Figure 5. Hypothetical model of the role of mitochondria in intracellular ROS generation in response to cigarette smoke. Lipophilic compounds inside the gaseous-phase of cigarette smoke easily pass the membrane of cells, disturb mitochondrial function and enhance intracellular ROS generation. ROS inside the gaseous-phase of CS 'Direct' and generated by the mitochondria themselves 'Indirect' are both of importance for the pathogenesis of COPD.

In addition; lipophilic components inside the gaseous-phase of cigarette smoke easily enter the blood stream facilitating systemic effects, by influencing organs distal from the lungs e.g. heart, liver, kidney, pancreas etc. (9; 19; 23; 30).

In conclusion, in this study we showed that mitochondria are essential in the generation of intracellular ROS in response to CS. The current data strengthen the idea that ROS in the gaseous-phase of CS and generated by the mitochondria themselves, can attenuate both local and systemic injury in smokers leading to the development of COPD.

GRANTS

This study was financially supported by the Dutch Kidney foundation (MvdT, Co1.1923), the Jan Kornelis de Cock foundation (MvdT, DS) and NIH R01-HL6234, NIH R01-HL079904, and NIH R01-HL55330 (AC).

REFERENCES

1. Afri M, Gottlieb HE and Frimer AA. Superoxide organic chemistry within the liposomal bilayer, part II: a correlation between location and chemistry. Free Radic Biol Med 32: 605-618, 2002.
2. Barnes PJ, Shapiro SD and Pauwels RA. Chronic obstructive pulmonary disease: molecular and cellular mechanisms. Eur Respir J 22: 672-688, 2003.
3. Bonvallot V, Baeza-Squiban A, Baulig A, Brulant S, Boland S, Muzeau F, Barouki R and Marano F. Organic compounds from diesel exhaust particles elicit a proinflammatory response in human airway epithelial cells and induce cytochrome p450 1A1 expression. Am J Respir Cell Mol Biol 25: 515-521, 2001.
4. Bowler RP, Barnes PJ and Crapo JD. The role of oxidative stress in chronic obstructive pulmonary disease. COPD 1: 255-277, 2004.
5. Brunnemann KD and Hoffmann D. Analytical studies on tobacco-specific N-nitrosamines in tobacco and tobacco smoke. Crit Rev Toxicol 21: 235-240, 1991.
6. Brzezinska AK, Lohr N and Chilian WM. Electrophysiological effects of O2*- on the plasma membrane in vascular endothelial cells. Am J Physiol Heart Circ Physiol 289: H2379-H2386, 2005.
7. Calikoglu M, Unlu A, Tamer L, Ercan B, Bugdayci R and Atik U. The levels of serum vitamin C, malonyldialdehyde and erythrocyte reduced glutathione in chronic obstructive pulmonary disease and in healthy smokers. Clin Chem Lab Med 40: 1028-1031, 2002.
8. Chen Y, Millan-Ward E, Kong J, Israels SJ and Gibson SB. Mitochondrial electron-transport-chain inhibitors of complexes I and II induce autophagic cell death mediated by reactive oxygen species. J Cell Sci 120: 4155-4166, 2007.
9. Chen Z and Boreham J. Smoking and cardiovascular disease. Semin Vasc Med 2: 243-252, 2002.
10. Gosker HR, Wouters EF, van d, V and Schols AM. Skeletal muscle dysfunction in chronic obstructive pulmonary disease and chronic heart failure: underlying mechanisms and therapy perspectives. Am J Clin Nutr 71: 1033-1047, 2000.
11. Hoshino Y, Mio T, Nagai S, Miki H, Ito I and Izumi T. Cytotoxic effects of cigarette smoke extract on an alveolar type II cell-derived cell line. Am J Physiol Lung Cell Mol Physiol 281: L509-L516, 2001.
12. Koopman WJ, Verkaart S, Visch HJ, van der Westhuizen FH, Murphy MP, van den Heuvel LW, Smeitink JA and Willems PH. Inhibition of complex I of the electron transport chain causes O2-. -mediated mitochondrial outgrowth. Am J Physiol Cell Physiol 288: C1440-C1450, 2005.
13. Li N, Sioutas C, Cho A, Schmitz D, Misra C, Sempf J, Wang M, Oberley T, Froines J and Nel A. Ultrafine particulate pollutants induce oxidative stress and mitochondrial damage. Environ Health Perspect 111: 455-460, 2003.
14. Liu J, Killilea DW and Ames BN. Age-associated mitochondrial oxidative decay: improvement of carnitine acetyltransferase substrate-binding affinity and activity in brain by feeding old rats acetyl-L- carnitine and/or R-alpha -lipoic acid. Proc Natl Acad Sci U S A 99: 1876-1881, 2002.

15. Lu X, Cai J, Kong H, Wu M, Hua R, Zhao M, Liu J and Xu G. Analysis of cigarette smoke condensates by comprehensive two-dimensional gas chromatography/time-of-flight mass spectrometry I acidic fraction. Anal Chem 75: 4441-4451, 2003.
16. Mao GD and Poznansky MJ. Electron spin resonance study on the permeability of superoxide radicals in lipid bilayers and biological membranes. FEBS Lett 305: 233-236, 1992.
17. Miro O, Alonso JR, Jarreta D, Casademont J, Urbano-Marquez A and Cardellach F. Smoking disturbs mitochondrial respiratory chain function and enhances lipid peroxidation on human circulating lymphocytes. Carcinogenesis 20: 1331-1336, 1999.
18. Nohl H, Gille L, Kozlov A and Staniek K. Are mitochondria a spontaneous and permanent source of reactive oxygen species? Redox Rep 8: 135-141, 2003.
19. Orth SR, Ritz E and Schrier RW. The renal risks of smoking. Kidney Int 51: 1669-1677, 1997.
20. Oudijk EJ, Lammers JW and Koenderman L. Systemic inflammation in chronic obstructive pulmonary disease. Eur Respir J Suppl 46: 5s-13s, 2003.
21. Pauwels RA, Buist AS, Calverley PM, Jenkins CR and Hurd SS. Global strategy for the diagnosis, management, and prevention of chronic obstructive pulmonary disease. NHLBI/WHO Global Initiative for Chronic Obstructive Lung Disease (GOLD) Workshop summary. Am J Respir Crit Care Med 163: 1256-1276, 2001.
22. Pieczenik SR and Neustadt J. Mitochondrial dysfunction and molecular pathways of disease. Exp Mol Pathol 2007.
23. Prokopczyk B, Hoffmann D, Bologna M, Cunningham AJ, Trushin N, Akerkar S, Boyiri T, Amin S, Desai D, Colosimo S, Pittman B, Leder G, Ramadani M, Henne-Bruns D, Beger HG and El-Bayoumy K. Identification of tobacco-derived compounds in human pancreatic juice. Chem Res Toxicol 15: 677-685, 2002.
24. Rabinovich RA, Bastos R, Ardite E, Llinas L, Orozco-Levi M, Gea J, Vilaro J, Barbera JA, Rodriguez-Roisin R, Fernandez-Checa JC and Roca J. Mitochondrial dysfunction in COPD patients with low body mass index. Eur Respir J 29: 643-650, 2007.
25. Rahman I. The role of oxidative stress in the pathogenesis of COPD: implications for therapy. Treat Respir Med 4: 175-200, 2005.
26. Rahman I and MacNee W. Role of oxidants/antioxidants in smoking-induced lung diseases. Free Radic Biol Med 21: 669-681, 1996.
27. Remels AH, Gosker HR, van d, V, Langen RC and Schols AM. Systemic inflammation and skeletal muscle dysfunction in chronic obstructive pulmonary disease: state of the art and novel insights in regulation of muscle plasticity. Clin Chest Med 28: 537-52, vi, 2007.
28. Rustemeier K, Stabbert R, Haussmann HJ, Roemer E and Carmines EL. Evaluation of the potential effects of ingredients added to cigarettes. Part 2: chemical composition of mainstream smoke. Food Chem Toxicol 40: 93-104, 2002.
29. Slebos DJ, Ryter SW, van der Toorn M, Liu F, Guo F, Baty CJ, Karlsson JM, Watkins SC, Kim HP, Wang X, Lee JS, Postma DS, Kauffman HF and Choi

AM. Mitochondrial Localization and Function of Heme Oxygenase-1 in Cigarette Smoke-Induced Cell Death. Am J Respir Cell Mol Biol 2006.

30. Smith CJ and Fischer TH. Particulate and vapor phase constituents of cigarette mainstream smoke and risk of myocardial infarction. Atherosclerosis 158: 257-267, 2001.

31. Tkacova R, Kluchova Z, Joppa P, Petrasova D and Molcanyiova A. Systemic inflammation and systemic oxidative stress in patients with acute exacerbations of COPD. Respir Med 101: 1670-1676, 2007.

32. Tsuchiya M, Asada A, Kasahara E, Sato EF, Shindo M and Inoue M. Smoking a single cigarette rapidly reduces combined concentrations of nitrate and nitrite and concentrations of antioxidants in plasma. Circulation 105: 1155-1157, 2002.

33. van der Toorn M, Slebos DJ, de Bruin HG, Leuvenink HG, Bakker SJ, Gans RO, Koeter GH, van Oosterhout AJ and Kauffman HF. Cigarette smoke induced blockade of the mitochondrial respiratory chain switches lung epithelial cell apoptosis into necrosis. Am J Physiol Lung Cell Mol Physiol 2007.

34. van der Toorn M, Smit-de Vries MP, Slebos DJ, de Bruin HG, Abello N, van Oosterhout AJ, Bischoff R and Kauffman HF. Cigarette smoke irreversibly modifies glutathione in airway epithelial cells. Am J Physiol Lung Cell Mol Physiol 293: L1156-L1162, 2007.

Chapter 3

MITOCHONDRIAL LOCALIZATION AND FUNCTION OF HEME OXYGENASE-1 IN CIGARETTE SMOKE-INDUCED CELL DEATH

Dirk-Jan Slebos[1], Stefan W. Ryter[2], Marco van der Toorn[1], Fang Liu[2], Fengli Guo[2], Catherine J. Baty[2], Jenny M. Karlsson[2], Simon C. Watkins[2], Hong Pyo Kim[2], Xue Wang[2], Janet S. Lee[2], Dirkje S. Postma[1], Henk F. Kauffman[1] Augustine M. K. Choi[2]

[1]Departments of Pulmonary diseases and Allergology, University Medical Center Groningen, Groningen, The Netherlands; and [2]Division of Pulmonary, Allergology and Critical Care Medicine, Department of Medicine, and Center for Biologic Imaging, Department of Cell Biology and Physiology, School of Medicine, University of Pittsburgh, Pittsburgh, Pennsylvania

Am J Physiol Lung Cell Mol Physiol. 2007 May;292(5)

ABSTRACT

Cigarette smoke–induced apoptosis and necrosis contribute to the pathogenesis of chronic obstructive pulmonary disease. The induction of heme oxygenase-1 provides cytoprotection against oxidative stress, and may protect in smoking-related disease. Since mitochondria regulate cellular death, we examined the functional expression and mitochondrial localization of heme oxygenase-1 in pulmonary epithelial cells exposed to cigarette smoke extract (CSE), and its role in modulating cell death. Heme oxygenase-1 expression increased dramatically in cytosolic and mitochondrial fractions of human alveolar (A549), or bronchial epithelial cells (Beas-2b) exposed to either hemin, lipopolysaccharide, or CSE. Mitochondrial localization of heme oxygenase-1 was also observed in a primary culture of human small airway epithelial cells. Furthermore, heme oxygenase activity increased dramatically in mitochondrial fractions, and in whole cell extracts of Beas-2b after exposure to hemin and CSE. The mitochondrial localization of heme oxygenase-1 in Beas-2b was confirmed using immunogold-electron microscopy and immunofluorescence labeling on confocal laser microscopy. CSE caused loss of cellular ATP and rapid depolarization of mitochondrial membrane potential. Apoptosis occurred in Beas-2b at low concentrations of cigarette smoke extract, whereas necrosis occurred at high concentrations. Overexpression of heme oxygenase-1 inhibited CSE-induced Beas-2b cell death and preserved cellular ATP levels. Finally, heme oxygenase-1 mRNA expression was elevated in the lungs of mice chronically exposed to cigarette smoke. We demonstrate the functional compartmentalization of heme oxygenase-1 in the mitochondria of lung epithelial cells, and its potential role in defense against mitochondria-mediated cell death during CSE exposure.

INTRODUCTION

Chronic obstructive pulmonary disease (COPD) ranks among the top five leading causes of death worldwide, with mortality rates still increasing (1). Cigarette smoke (CS), a complex mixture of over 4,000 components including reactive oxygen species (ROS), heavy metals, aldehydes, aromatic hydrocarbons and phenolics, represents the main causative factor in the development of COPD (1–5). To date, the exact pathophysiology of COPD remains unknown, thus very few effective treatment modalities exist (5, 6). In susceptible smokers, CS exposure potentially results in chronic inflammation of the airways, leading to airways obstruction and an alveolar wall inflammatory response associated with lung cell death, lung tissue destruction, and emphysema (2, 5, 7).

ROS may directly participate in specific tissue injury and cell death (both apoptosis and necrosis) in COPD (3, 8, 9). A significant portion of cellular ROS arises in mitochondria, associated with the leakage of partially reduced oxygen from the electron transport chain under normal and pathologic conditions. In addition, mitochondria regulate apoptosis induced by extracellular signals through the release of pro-apoptotic mediators (e.g., cytochrome c, apoptosis-inducing factor) (10). Furthermore, mitochondria serve as the principal energy source of the cell through the production of ATP. Cellular ATP levels play an essential role in the determination of apoptotic or necrotic cell fate (11). Many constituents of CS can accumulate in the mitochondria and perturb mitochondrial respiratory chain function, thereby affecting cellular ATP production (12–14).

Heme oxygenase-1 (HO-1; E.C. 1:14:99:3), which catalyses the rate-limiting step in the oxidative degradation of heme (15, 16), confers protection against exogenous stresses and inhibits apoptotic cell death in a variety of disease states (17–19). The mechanisms by which HO-1 provides protection likely involve its enzymatic reaction products: carbon monoxide (CO), biliverdin-IXα, and ferrous iron (17–19). The transcriptional induction of HO-1 responds to a wide variety of cellular stress, including oxidants and altered states of oxygen tension, identifying this response as a major inducible cellular defense mechanism (19). We have recently shown a lower expression of HO-1 in ex-smoking patients with COPD compared with ex-smoking healthy control subjects (20). A $(GT)_n$ dinucleotide length polymorphism that is linked to the development of COPD has been described in the promoter region of HO-1, resulting in a lower expression of HO-1 in people who have the polymorphism (21). Thus, a genetically dependent down-regulation of HO-1 expression may arise in subpopulations, possibly linked to increased susceptibility to the pathologic consequences of ROS (22).

Together, these observations led to the hypothesis that HO-1 exerts a potential regulatory and/or protective function in COPD by preserving mitochondrial function, and by inhibiting cell death associated with CS exposure. Therefore, we sought to characterize the potential localization of HO-1 in the mitochondria and its function with respect to cell survival.

Given the historical characterization of HO-1 as a resident of the endoplasmic reticulum (ER), we have recently observed the redistribution of HO-1, after stress induction, to various subcellular fractions, including caveolae and cytochrome c–containing fractions (23). This work was the first to suggest the potential localization

of HO-1 to the mitochondria and provided the rationale for the current study. We demonstrate the mitochondrial compartmentalization of active HO-1 protein, and its accumulation in this organelle in response to discrete forms of cellular stress. Furthermore, these observations have been made in the context of pulmonary epithelial cells treated with aqueous cigarette smoke extract (CSE) as a specific *in vitro* model of CS exposure. We also demonstrate that HO-1 protects epithelial cells against CSE-induced cell death, in part by preserving cellular ATP production. These studies expand our knowledge of the subcellular distribution and functional significance of HO-1, as it relates to CS-induced cellular injury.

MATERIALS AND METHODS

Materials

All reagents were from Sigma (St. Louis, MO) unless otherwise indicated. Bovine hemin (ferriprotoporphyrin-IX chloride), and tin protoporphyrin-IX (SnPPIX) (Frontier Scientific, Logan, UT) were dissolved in dimethyl sulfoxide as 10 mM stock solutions, and stored at –20°C. The hemin was dissolved in cell culture media to a working concentration of 10 μM. Lipopolysaccharide (LPS) was freshly prepared and used for experiments at a concentration of 100 ng/ml. JC-1 (5,5',6,6'-tetrachloro-1,1',3,3' tetraethylbenzimidazolylcarbocyanine iodide/chloride) was from Invitrogen (Carlsbad, CA).

Preparation of CSE

Kentucky 1R3F research-reference filtered cigarettes (The Tobacco Research Institute, University of Kentucky, Lexington, KY) were smoked using a peristaltic pump (VWR International, West Chester, PA). Before the experiments, the filters were cut from the cigarettes. The smoke was bubbled through cell growth medium. Each cigarette was smoked in 6 min with a 17-mm butt remaining. Four cigarettes were bubbled through 20 ml of medium, and this solution was regarded as 100% strength CSE. The 100% CSE was adjusted to a pH of 7.45 and was used within 15 min after preparation.

Cell Culture

A549 and Beas-2b lung epithelial cells were purchased from American Type Culture Collection (ATCC, Manassas, VA). A549 cells were cultured in Ham's F-12 medium supplemented with 10% FBS and 0.1% gentamycin (Gibco-Invitrogen, Carlsbad, CA) in a humidified atmosphere of 5% CO_2/balanced air at 37°C. Beas-2b cells were cultured according to the ATCC prescription in the serum-free medium BEGM (Cambrex, East Rutherford, NJ). Before the experiments the A549 or Beas-2b cells were cultured for 16 h in serum-free F-12 media or growth factor-free media (BEBM; Cambrex), respectively. Small airway human bronchial epithelial cells were purchased as frozen primary cultures from Clonetics Ltd (Walkersville, MD). They were cultured in the manufacturer's basal medium (SAGM) and supplements.

Western Blot Analysis
The following antibodies were used for immunoblotting: anti-heme oxygenase-1 (1:2,000), anti-NADPH cytochrome p450 reductase (NPR), anti-biliverdin reductase (BVR) (Stressgen, Victoria, BC, Canada), anti–cytochrome c, anti–β-actin (Santa Cruz, Santa Cruz, CA), or anti-p110 (Calbiochem, San Diego, CA). Western immunoblot analyses were performed as previously described (23).

Mitochondrial Isolation
A549 and Beas-2b cells were harvested in 0.05% digitonin in an extraction buffer containing 10 mM Hepes, pH 7.5, 150 mM NaCl, 1 mM EGTA, and 1.5 mM $MgCl_2$. The cell extracts were spun at 700 x *g* for 10 min. The supernatants were transferred to new tubes and centrifuged again at 30,000 x *g* at 4°C for 30 min. The resulting supernatants were removed, and the pellets were either retained for Western blotting, or for assessment of HO-enzyme activity. Alternatively, mitochondria were isolated using a commercial mitochondria isolation kit (Sigma-Aldrich Chemie B.V., Zwijndrecht, The Netherlands) and suspended in respiratory buffer (120 mM KCl, 5 mM K_2PO_4, 3 mM HEPES, 1 mM EGTA, pH 7.2). Mitochondrial protein content was determined by the Bradford method (Bio-Rad Laboratories, Veenendaal, The Netherlands) according to the manufacturer's instructions. Both extraction methods gave comparable results in Western immunoblot analyses.

Heme Oxygenase Activity
Heme oxygenase activity was measured in both whole cell and mitochondrial fractions by the spectrophotometric determination of bilirubin production as previously described (24). HO activity was reported as pmol bilirubin/mg protein/h assuming an extinction coefficient of 40 mM^{-1} cm^{-1} for bilirubin in chloroform.

Immunofluorescence Labeling and Confocal Laser Microscopy
Beas-2b cells were grown on 35 mm/10 mm glass-bottom culture dishes (MatTek Corp., Ashland, MA). After experimental treatments, cells cultured under standard growth conditions at 37°C were stained for mitochondria using the Mitotracker Red dye (M-7513; Molecular Probes, Eugene, OR), at 1 μM for 45 min. Cells were then washed with PBS, fixed, and permeabilized in 2% paraformaldehyde with 0.1% Triton-X100. Cells were then washed with PBS and wash buffer (0.5% bovine serum albumin, 0.15% glycine in PBS), and blocked with 10% goat serum in wash buffer. Immunostaining was performed using a polyclonal HO-1 antibody (1:1,000; Stressgen), and goat anti-rabbit Alexa 488–conjugated secondary antibodies (1:1,000; Jackson ImmunoResearch Laboratories, West Grove, PA). Cells were viewed with an Olympus Fluoview BX 61 confocal microscope (Olympus, Center Valley, PA) and images were collected using a DC-330S cooled CCD camera (DAGE-MTI, Michigan City, IN).

Transition Electron Microscopy
After experimental manipulations, Beas-2b cells were washed with PBS and fixed in 2.5% glutaraldehyde in PBS. The cells were photographed using a JEOL JEM 1210 transmission electron microscope (JEOL, Peabody, MA) at 80 or 60 kV onto electron microscope film (ESTAR thick base; Kodak, Rochester, NY) and printed

onto photographic paper. Rabbit anti–HO-1 polyclonal antibody (Stressgen) suitable for IHC was used for gold-immunostaining.

Annexin V–Fluorescein Isothiocyanate Propidium Iodide Staining
Annexin V–fluorescein isothiocyanate (FITC)/propidium iodide (PI) staining was performed using the FITC-labeled annexin V kit (BD Pharmingen, San Diego, CA), according to the manufacturers protocol. Labeled cells were analyzed using a FACS-Calibur (BD Biosciences, San Jose, CA).

Transfections
Adenovirus–ho-1 (Ad-HO-1) and adenovirus-LacZ (Ad-LacZ) were supplied by the Center for Biotechnology and Bioengineering, University of Pittsburgh, Pittsburgh, PA (www.vectorcore.pitt.edu). Beas-2b cells were grown to subconfluence and starved overnight. Ad-HO-1 and Ad-LacZ were added to culture media at 50 plaque-forming units per cell. After 6 h the medium containing the virus was changed to regular growth medium and the experiment were performed 24 h from the initiation of transfection.

Adenosine Triphosphate Assay
ATP was measured using an ATP-luciferase assay kit (Calbiochem) using the manufacturer's instructions and standards. Beas-2b cells were seeded at 5 x 10^3 cells/well in opaque 96-well microplates (BD Falcon, Bedford, MA) and grown under standard cell culture conditions for 48 h before the experiments. Luciferase activity was measured within 1 min of reagent addition using a luminometer (Lmax; Molecular Devices, Sunnyvale, CA).

Determination of Mitochondrial Membrane Potential
JC-1 is a cationic dye that is accumulated into mitochondria in a membrane potential–dependent manner. Upon accumulation within the mitochondria, the dye forms aggregates (J-aggregates) that emit a red fluorescence imaged with standard rhodamine optical filters. In the presence of depolarized mitochondria the dye remains dispersed within the cytoplasm as a monomer, emitting a green fluorescence detected with FITC filters. Therefore, depolarization of mitochondria can be detected as an increase in the green/red fluorescence intensity ratio. The excitation, dichroic, and emission wavelengths are 485 ± 11 nm, 505 nm, and 530 ± 15 nm for the monomer, and 535 ± 17.5 nm, 570 nm, and 590 ± 17.5 nm for the J-aggregate, respectively.

Normal Beas-2b were grown to 50% confluence on Lab-Tek four-well chambered coverglass (Nalge Nunc, Rochester, NY) overnight and then were incubated for 30 min at 37°C in the presence of 1 μg/ml JC-1 (Invitrogen, Carlsbad, CA), and then washed. Cells were maintained at 37°C in a heated microincubator (Harvard Apparatus, Inc., Hamden, CT) in HEPES-buffered media during imaging. Images were acquired at five different positions in a given chamber, using an Olympus IX81 with x20 objective (0.70 NA) and Retiga EXi CCD camera (Q-Imaging, Burnaby, BC, Canada), every 30 s for a 5 min baseline; then media or CSE was added and imaging was continued for an additional 20 min. Hydrogen peroxide was added to the media at 1 mM for a positive control. MetaMorph 6.3 (Molecular

Devices) was used for image acquisition and subsequent analysis. In calculating the green/red fluorescence ratio, background correction was used for each image and time point. Data are reported as the average change in the green/red ratio for each cell over a 20-min exposure interval, normalized to corresponding average baseline. Data represent mean average change for three to five independent positions, in which 20 cells were analyzed for each position.

In Vivo Cigarette Smoke Exposure

Animals were housed according to guidelines from the American Association for Laboratory Animal Care and Research Protocols and were approved by the Animal Care and Use Committee (University of Pittsburgh School of Medicine). Male, age-matched AKR/J strain mice (Jackson Laboratories, Bar Harbor, ME) were exposed to CS or filtered air under identical conditions beginning at 8 wk of age. Total body CS exposure was performed in a stainless steel chamber (71 cm x 61 cm x 61 cm) using a smoking machine (Model TE-10; Teague Enterprises, Woodland, CA), similar to that reported by others (25, 26). The smoking machine puffs each 1R3F cigarette for 2 s, for a total of 9 puffs before ejection, at a flow rate of 1.05 liters/min, providing a standard puff of 35 cm^3. The smoke machine was adjusted to deliver five cigarettes at one time. Mice were exposed 5 d/wk for up to 24 wk. The chamber atmosphere was periodically measured for total particulate matter concentrations of ~120 mg/m^3. Carboxyhemoglobin levels in the AKR/J strains of mice after 2 wk of cigarette exposure were < 8% immediately after exposure.

Real-Time PCR

At 2, 12, and 24 wk, control or CS-exposed mice were killed by an overdose of pentobarbital, injected intraperitoneally. The left lung was removed during necropsy, snap-frozen immediately in liquid nitrogen, and stored at –80°C till use. Lung tissue was homogenized and RNA extracted using the TRIZOL method (Invitrogen, Carlsbad, CA). The RNA samples were reverse transcribed into cDNA, which served as template for quantitative RT-PCR. Probes and primers for the HO-1 gene as well as the TaqMan Master Mix containing the necessary reagents for gene expression studies were obtained from Applied Biosystems (Foster City, CA). Gene expression was analyzed by the delta delta Ct method, with 18 s rRNA as the endogenous control. The average dCT of age-matched air-exposed AKR/J male mice served as the calibrator. Three to eight animals in each group were used for each time point measured.

Statistical Analysis

All values were expressed as the mean ± S.D. from at least three independent experiments. Differences in measured variables between experimental and control group were assessed using the Student's *t* test (Statview II Statistical Package; Abacus Concepts, Berkeley, CA). Statistically significant difference was accepted at $P < 0.05$. *In vivo* gene expression data were analyzed using the rank-sum Mann Whitney U test for non-normally distributed data.

RESULTS

HO-1 Is Expressed in Mitochondria in Response to Stimuli

To examine the inducible stress response in lung epithelial cells, A549 and Beas-2b cells were treated with hemin (10 μM), a potent inducer and substrate of HO-1, for 18 h. As expected, HO-1 protein expression increased in response to hemin treatment in both cell lines (Fig. 1A). Surprisingly, inducible HO-1 expression appeared in the mitochondrial fractions of both cell lines after heme treatment (Fig. 1A). To examine whether this phenomenon also occurred in response to other known inducers of the HO-1 response, independently of substrate loading (hemin), Beas-2b cells were exposed to either bacterial LPS (0.1 μg/ml) or CSE (15%) for 18 h. While both stimuli also induced HO-1 protein expression in whole cell and mitochondrial fractions, the CSE treatment produced the most dramatic mitochondrial accumulation of HO-1 (Fig. 1B). Furthermore, CSE induced HO-1 in Beas-2b cells in a dose-responsive and time-dependent manner (Fig. 1C). In addition to the epithelial cell lines, the response was also observed in human primary small airway epithelial cells (SAEC) (Fig. 1D). HO-1 accumulated in whole cells, and in mitochondrial fractions of SAEC in a dose-dependent fashion after 24 h continuous CSE exposure.

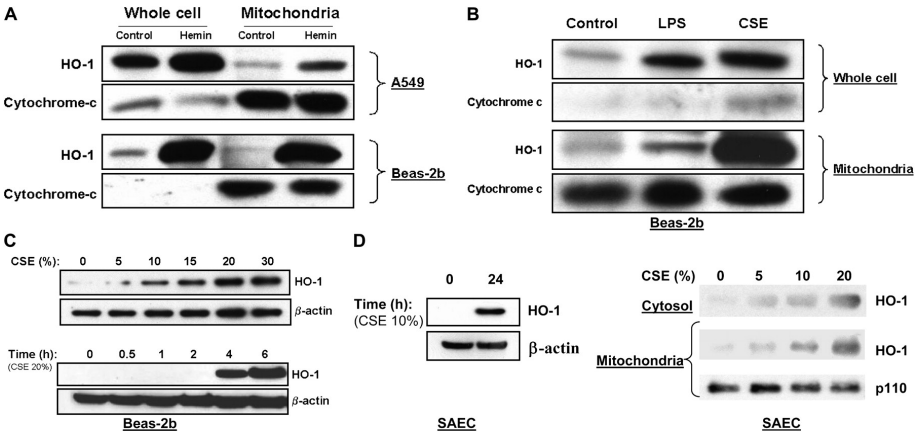

Figure 1. CSE and stress treatments result in mitochondrial accumulation of HO-1 protein in epithelial cells. (*A*) A549 cells or Beas-2b cells were treated in the absence (control) or presence of hemin (10 μM) for 18 h. (*B*) Beas-2b cells were treated with LPS (0.1 μg/ml) or CSE (15%) for 18 h. (*C*) Beas-2b cells were starved overnight in growth factor–free media and then treated with varying concentrations of CSE (0–30%) for 4 h, or with a fixed dose (20%) for 0–6 h. (*D*) Primary small airway epithelial cells (SAEC) were cultured as described in Materials and Methods, and treated with varying concentrations of CSE (10% for 0–24 h, *left panel*) or (0–20% for 24 h, *right panel*). Cells were harvested and fractionated into either whole cell or mitochondrial fractions as described in Materials and Methods. Samples containing equivalent amounts of protein were subjected to SDS-PAGE and Western immunoblot analysis for expression of HO-1 (*A–D*). Cytochrome-c (*A*, *B*) or mitochondrial p110 (*D*) served as a marker of the relative content of mitochondrial protein. β-Actin served as a standard for protein loading in whole cell experiments (*C*, *D*).

Mitochondrial HO-1 Is Highly Inducible and Functionally Active

The functional activity of HO-1 in whole cell and mitochondrial extracts after stress treatments was verified by spectrophotometric determination of bilirubin production. Beas-2b cells were subjected to hemin (10 μM) or CSE (15–20%) for 18-h exposures, followed by the isolation of mitochondrial protein and whole cell lysates. As expected, both hemin and CSE (20%) induced HO activity in whole cell extracts from a basal activity of 175 ± 28 pmol bilirubin/mg protein/h, approximately 4- to 5-fold (hemin: 849 ± 114; CSE: 675 ± 35 pmol bilirubin/mg protein/h) (Fig. 2A), which correlated with HO-1 protein expression at this time point. HO activity in the mitochondrial fractions increased from 13-fold (for hemin), up to 19 fold after CSE treatment relative to the basal mitochondrial HO activity (308 ± 58 pmol bilirubin/mg mitochondrial protein/h) (Fig. 2B). In addition, we examined the mitochondrial localization of enzymes associated with HO activity. NADPH cytochrome p-450 reductase was detected in the mitochondrial fractions of Beas-2b cells, but did not vary significantly in response to CSE treatment. NADPH biliverdin reductase (BVR), in contrast, was not detected in the mitochondria of Beas-2b cells (Fig. 2C).

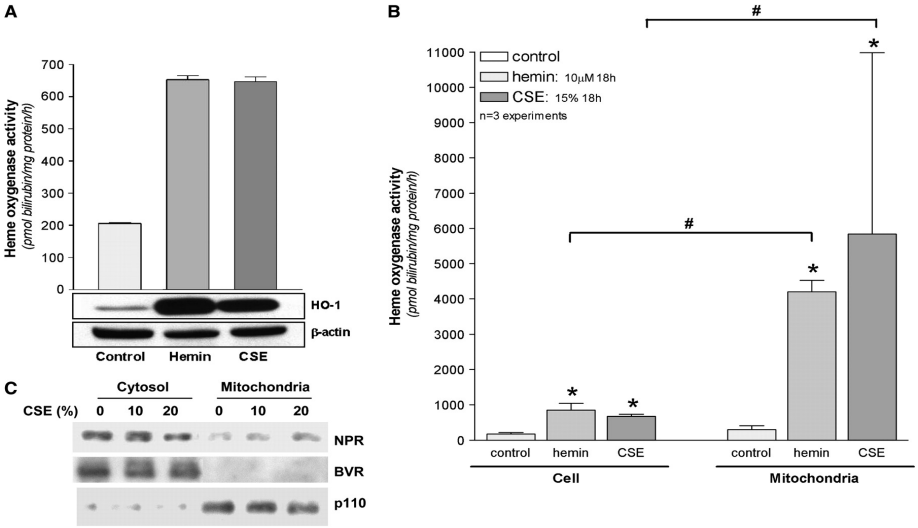

Figure 2. Cellular or mitochondrial HO-1 induced by CSE and heme is functionally active. (*A*) Beas-2b cells were subjected to heme (10 μM) or CSE (20%) for 18 h. Corresponding whole cell extracts were analyzed for HO activity and HO-1 protein by Western immunoblot analysis. β-Actin served as a standard for protein loading. Western blots are representative of three independent experiments. (*B*) Beas-2b were subjected to heme (10 μM) or CSE (15%) for 18 h. Corresponding whole cell and mitochondrial extracts were analyzed for relative HO activity. Activity data represent mean ± SD of three independent experiments ($n = 3$), each with triplicate determinations $^{*}P < 0.05$, $^{\#}$relative to corresponding whole cell extract. Units represent pmol bilirubin/mg protein (cellular or mitochondrial)/h (*A*, *B*). (*C*) Beas-2b treated with CSE (10–20%) or media were harvested and fractionated into either whole cell or mitochondrial fractions as described in Materials and Methods. Samples containing equivalent amounts of protein were subjected to SDS-PAGE and Western immunoblot analysis for expression of NADPH cytochrome p450 reductase (NPR) or NAD(P)H biliverdin reductase (BVR). Mitochondrial p110 served as a marker of the relative content of mitochondrial protein.

Immunofluorescence staining for confocal laser microscopy revealed a colocalization of HO-1 expression and mitochondrial staining in Beas-2b cells after hemin treatment (Fig. 3A). We further confirmed the mitochondrial localization of HO-1 using immunogold labeling on electron microscopy (Fig. 3B).

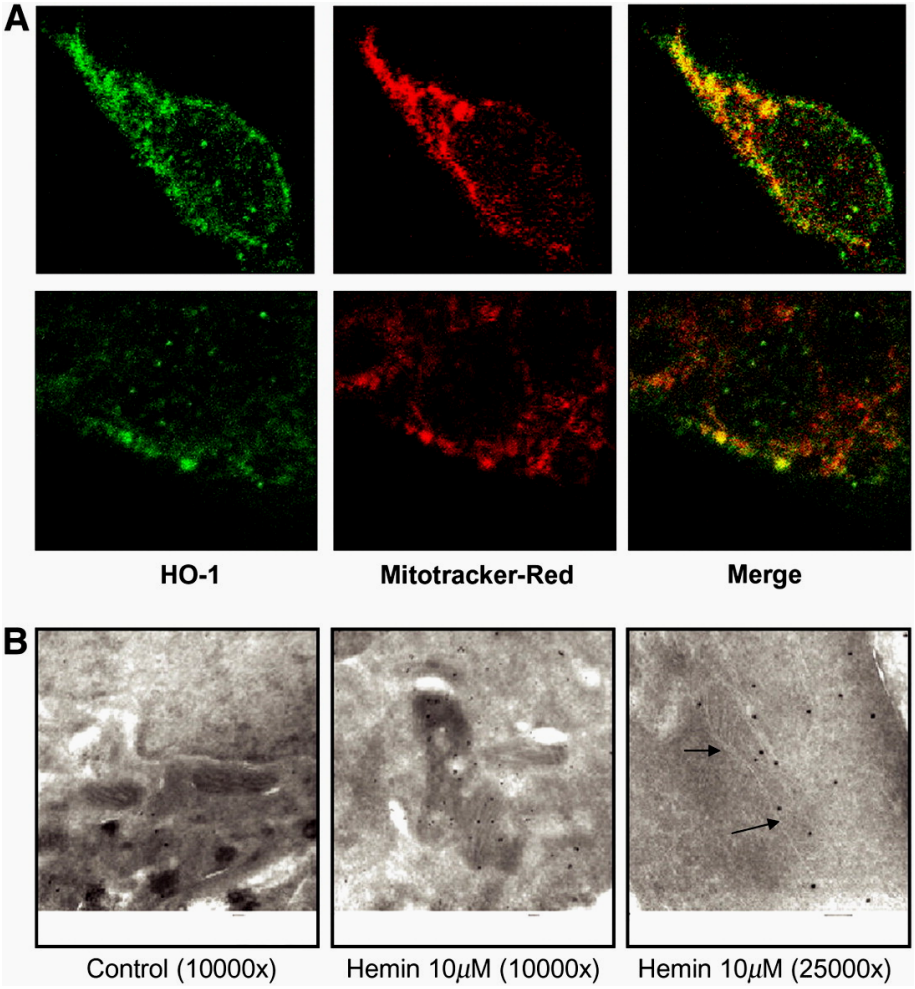

Figure 3. HO-1 co-localizes with mitochondria. Beas-2b cells were starved overnight in growth factor–free media, and then treated with hemin (10 μM) for 18 h. (A) Cells were stained with mitotracker Red, and immunostained with HO-1 antibody as described in Material and Methods. Upper and lower panels are two representative series from different cells. (B) Alternatively, cells were immunogold-stained for HO-1 and analyzed with scanning electron microscopy. The arrows show the position of the mitochondrial membrane.

CSE Induces Both Apoptosis and Necrosis in Lung Epithelial Cells

To investigate the CSE-induced cell death process in lung epithelial cells, Beas-2b cells were exposed to a high concentration of CSE (50%) for 0–5 h, and apoptosis

and necrosis were assessed simultaneously by using the annexin V–FITC/PI assay (Fig. 4A and 4B). A peak in the annexin V–FITC signal appeared after 1 h exposure, and decreased in the hours thereafter. The percentage of PI (necrotic cells) however, increased after the first hour, and continued to increase until the last hour measured (5 h).

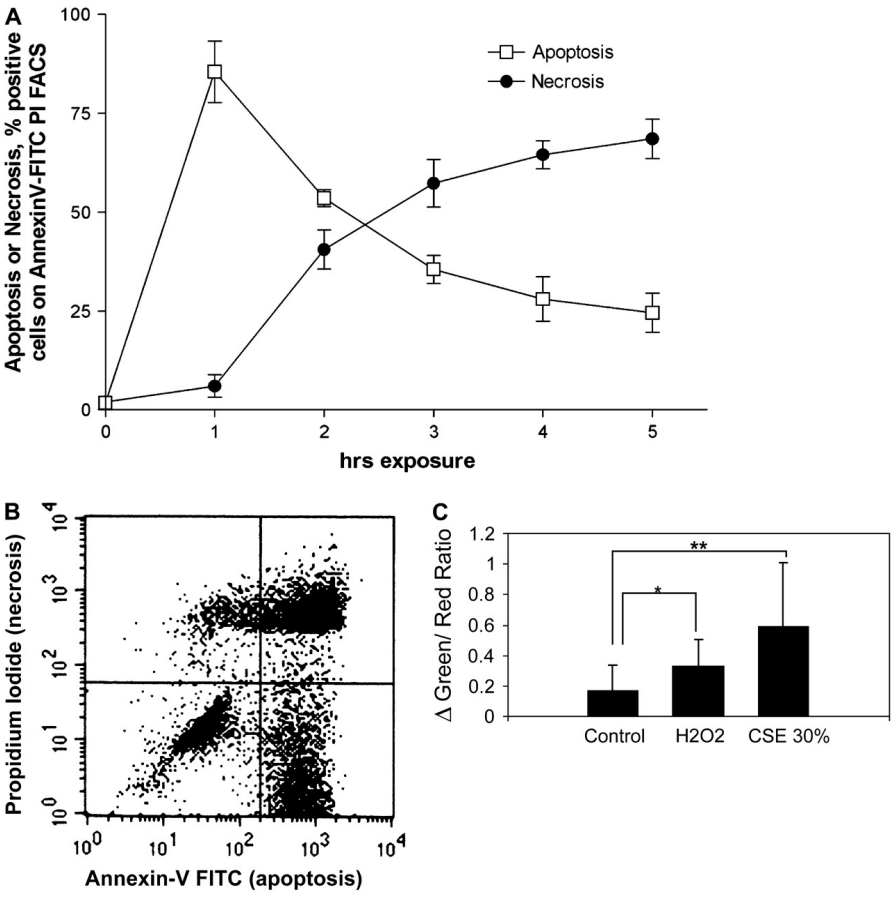

Figure 4. CSE induces apoptotic and necrotic cell death in Beas-2b cells. (*A*) Beas-2b cells were starved overnight in growth factor–free media, and then treated with 50% CSE for various time intervals (0–5 h). The percentage of cells positive for apoptosis or necrosis was determined by Annexin V–FITC/PI fluorescence-activated cell sorter analysis. Each data point represents the mean ± SD of three independent experiments. (*B*) A representative quadrant from cells exposed to 50% CSE for 3 h is displayed. (*C*) Normal Beas-2b at 50% confluence were loaded with JC-1 and then exposed to CSE (30%) or H_2O_2 (1 mM) as described in MATERIALS AND METHODS. The green:red fluorescence ratio, an indicator of mitochondrial depolarization, was taken at 30-s intervals at five different positions (20 cells each). Data represent the difference between the ratio at 20 min exposure and time of reagent addition, normalized to average baseline. Data are representative of the mean and SD, the average green:red ratio change of 20 cells at three to five positions per well. $^{**}P < 0.01$, $^{*}P < 0.05$.

To examine the dose-dependency of the occurrence of apoptosis and necrosis, we exposed the Beas-2b cells to different concentrations of CSE for 3 h. Below a concentration of 30% CSE, almost exclusively annexin V–FITC positive cells (apoptosis) were observed. The percentage of apoptotic cells increased linearly and dose-dependently between CSE concentrations of 0–20%, reaching an apparent maximum at 20% CSE, whereas the appearance of cellular necrosis began at concentrations of CSE at 30% and higher (data not shown). We furthermore observed the time-dependent activation of caspase-3 after exposure of Beas-2b cells to 30% CSE, beginning as early as 30 min after exposure and persisting at least 12 h (data not shown).

At a concentration of 30%, CSE caused rapid mitochondrial membrane depolarization, a hallmark of apoptosis, which exceeded that produced by addition of 1 mM H_2O_2 (Fig. 4C).

HO-1 Expression Protects Epithelial Cells from CSE-Induced Cell Death and ATP Depletion

Beas-2b cells were infected with an adenoviral construct containing *ho-1* cDNA (Ad-HO-1) or *LacZ* cDNA (Ad-LacZ). HO-1–overexpressing cells or corresponding Ad-LacZ–infected controls were subjected to challenge with 30% CSE for 3 h, or to an equivalent amount of complete growth media for 3 h. CSE dramatically reduced cellular ATP levels in Ad-LacZ–infected controls, which were further depressed by inclusion of the HO inhibitor tin-protoporphyrin-IX (SnPPIX, 20 μM). In contrast, CSE failed to depress cellular ATP levels in HO-1–expressing cells. Inclusion of SnPPIX reversed the protection conferred by Ad-HO-1, and resulted in depleted ATP levels (Fig. 5A). CSE treatment (30%) for 3 h caused necrotic cell death in LacZ-expressing controls. HO-1 expression as a result of Ad-HO-1 infection reduced cellular necrosis relative to LacZ controls, after CSE challenge (30%, 3 h) (Fig. 5A). These experiments demonstrate a general protective effect of HO-1 against necrosis and associated depletion of cellular energy charge during exposure to CSE.

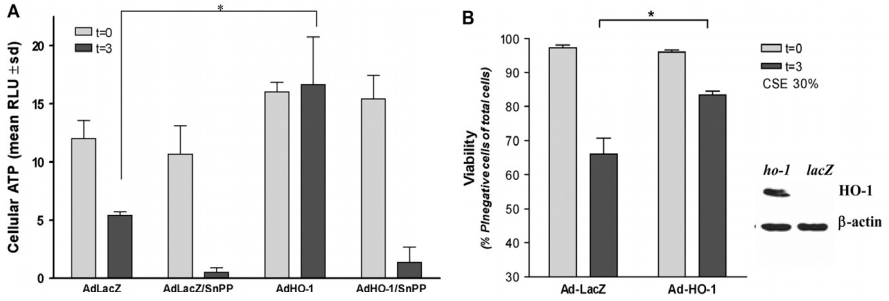

Figure 5. HO-1 protects against CSE-induced cell death and loss of ATP. Beas-2b cells were starved overnight in growth factor–free media, and then infected with Ad-HO-1 or Ad-LacZ for 6 h. At 24 h after transfection, cells were treated with 30% CSE for an additional 3 h, or sham treatment, in the absence or presence of SnPPIX (20 μM). After treatments, cells were analyzed for total ATP content (*A*), or assayed for cell viability by PI exclusion (*B*). Expression of HO-1 from the adenovirus was confirmed by Western immunoblot analysis (*B*, *insert*). β-Actin served as a standard for protein loading. *$P < 0.01$.

Chronic CS Exposure Up-Regulates HO-1 Expression in the Lungs of Mice
We examined the expression of *ho-1* in the lung after chronic exposure to CS *in vivo*. Mice exposed to CS displayed dramatically elevated expression of *ho-1* mRNA after 2 wk of chronic CS exposure relative to air-exposed controls. The elevated *ho-1* mRNA expression persisted up to 12 wk of CS exposure. *ho-1* mRNA expression returned to control values after the 24th week of continuous CS exposure (Fig. 6).

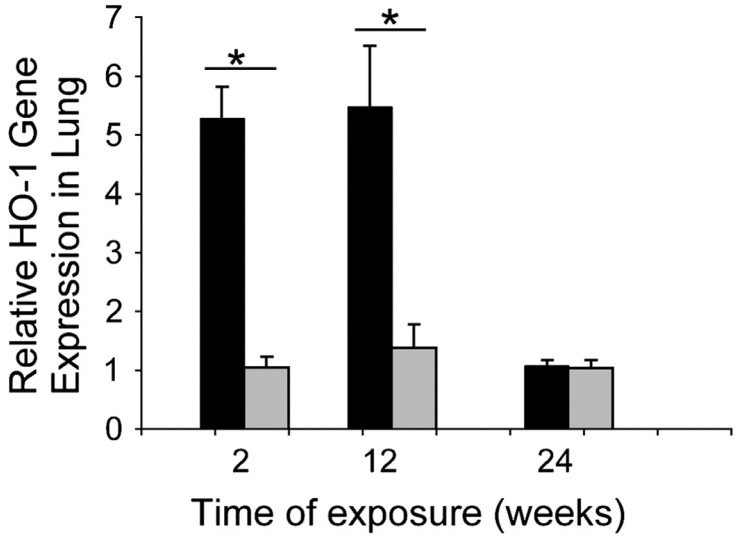

Figure 6. AKR/J mice were exposed to 24 wk of CS exposure (*black bars*) or air (*gray bars*) as described in Materials and Methods. At 2, 12, and 24 wk exposure lungs were excised. Relative HO-1 gene expression in lung tissue was determined at each indicated exposure time, by real-time PCR as described in Materials and Methods (n = 3–8 animals per time point per exposure condition). *$P < 0.01$.

DISCUSSION

Injury of the alveolar epithelium by CS constituents plays a role in the pathogenesis of COPD (2). The mechanisms underlying CS-induced epithelial cell death, however, remain unclear. It has been shown that CSE causes dose- and time-dependent cell death in A549 alveolar epithelial cells (27). Furthermore, low concentrations of CSE induce apoptosis, whereas higher concentrations induce necrosis in these cells (27). Similar transition from apoptotic to necrotic phenotype with increasing CSE dose was also observed in a human premonocytic line (U-937) (28). Apoptotic phenotypes appeared in other lung cell types exposed to CSE, including alveolar macrophages (29) and human lung fibroblasts (30), as well as in mainstream CS-treated rat bronchial/bronchiolar epithelial cells (31). Antioxidant compounds (N-acetyl-L-cystein) alone, or in combination with other scavengers (e.g., aldehyde oxidase) protected against CSE-mediated apoptosis in several models, implying the involvement of CSE-derived and/or intracellular reactive species (27–29). In alveolar macrophages, CSE induced apoptosis by activating an intrinsic mitochondria-dependent pathway, involving increased ROS generation, mitochondrial dysfunction, Bax accumulation, cytochrome-c release, independently

of p53, Fas, or caspase activation (28). Similar observations of ROS- and mitochondria-dependent apoptosis were observed after CSE exposure in various nonpulmonary cell types (28, 32–34). In human gastric adenocarcinomas and umbilical vein endothelial cells, caspase-3 activation also mediated CSE-induced apoptosis (32–34). In contrast, Wickenden and colleagues recently reported that CSE-exposure caused strictly necrosis in A549 cells, with associated inhibition of apoptosis (35). In this model, the anti-apoptotic effects of CSE involved upstream inhibition of caspase-3/9 activation, and postmitochondrial regulation of apoptosis-related factors to inhibit active apoptosome formation (35). Liu and coworkers also reported exclusively necrotic phenotypes in CSE-treated Beas-2b cells, with no activation of caspase-3 (36). In such studies, variations in experimental findings may occur in cell type–specific fashion, and may be further complicated by incomplete standardization of methodologies for experimental generation of CS, leading to variations in the strength of reported extract concentrations between individual laboratories. Additional limitations of CSE as a model of smoke exposure include the fact that some volatile compounds present in CS may be lost upon preparation of the extracts. Furthermore, the chemical composition of CSE may change upon handling or storage. Nevertheless recent consensus indicates that CSE remains a useful model of smoke exposure applicable to *in vitro* experiments with cultured cells (37).

In the current study we observe both apoptotic and necrotic cell death in Beas-2b cells exposed to CSE, with a transition from apoptosis to necrosis occurring with increasing duration (> 1 h) of CSE exposure (Fig. 4A). This cellular death was associated with the early activation of caspase-3 (data not shown). CSE caused a depletion of cellular energy charge (ATP levels) in control cells (Fig. 5A). Since mitochondria supply energy (ATP) for the apoptotic process, ATP levels may play a crucial role in the routing of cells to die by apoptosis or necrosis (11). Thus, depletion of cellular ATP by CSE may drive early apoptotic cells to switch to necrosis.

The inducible stress protein HO-1 confers protection against oxidative cellular injury and apoptosis in many disease models where ROS are implicated, including ischemia/reperfusion injury, hyperoxic stress/ acute lung injury, and atherosclerosis (19). Furthermore, adenoviral-mediated expression of HO-1 has also been shown to protect the mouse against experimental elastase–induced emphysema (38). We examined the potential relationship between HO-1 induction and CSE-related cell death. In attempting to characterize the general HO-1 induction response to CSE and other stress agents (hemin, LPS) in lung epithelial cells, we discovered a novel mitochondrial localization of HO-1 protein, and HO activity, which was strongest after CSE exposure. This response was observed in two types of transformed epithelial cell lines (Beas-2b, A549), as well as in a primary SAEC. Furthermore, this accumulation of HO-1 appeared dramatically more concentrated in mitochondria than in cytosol when normalized to the protein content of corresponding extracts (Figure 2C). Since its initial discovery in 1968, HO-1 has been described as a protein residing largely in the rough ER (15, 16). HO activity is abundant in microsomal (104,000 x *g*) fractions containing cellular membranes, and can be isolated in association with NADPH: cytochrome p450 reductase and NAD(P)H: biliverdin reductase (39). HO-1 contains a carboxy terminal hydrophobic

domain, which anchors this protein in cellular membranes (40, 41). Constitutive expression of the rat HO-1 cDNA in animal cells indicated an ER localization of the expression product (40). Recent studies from our laboratories have shown the potential compartmentalization of HO-1 in other subcellular domains beside the ER, including the mitochondria and caveolae (23). Using sucrose density-gradient fractionation, we observed that hemin, hypoxia, and LPS stimulation alter the subcellular distribution pattern of HO-1 in lung endothelial cells, with accumulations in cytochrome c containing fractions, and detergent-resistant plasma membrane fractions (23).

Since the constitutive isozyme heme oxygenase-2 (HO-2) is refractory to most forms of chemical induction, including the agents under study, the observed induction of HO activity in mitochondrial fractions by CSE most likely represents the chemical induction of HO-1 by CSE constituents as confirmed by immunoblot analysis. However, since HO activity assays do not discriminate between HO-1 and HO-2 activity, the relative contribution of HO-2 to basal mitochondrial HO activity remains unclear. This issue may warrant the examination of the possible occurrence of HO-2 in mitochondria, as well as other enzymes that support heme-degradative activity, including NAD(P)H: biliverdin reductase (BVR), and NADPH: cytochrome p450 reductase (NPR). NPR was detected in the mitochondria of Beas-2b cells, consistent with a functional role for mitochondrial HO activity. BVR, while not essential for HO activity, provides the second step in the heme metabolic pathway. Its absence from the mitochondrial fraction is consistent with previous reports of primarily cytosolic or microsomal localization of this enzyme in various cell types (24). This observation also suggests that biliverdin is not likely metabolized in the mitochondria.

As previously hypothesized (42), the principal function of inducible HO-1 in the mitochondria may be to degrade accumulated heme. Mitochondria are critically involved in the heme biosynthetic pathway in that they contain the rate-limiting step (δ-aminolevulinic acid synthase) as well as the final enzymatic steps (coproporphyrinogen III oxidase, protoporphyrinogen IX oxidase, ferrochelatase) of this pathway. Newly synthesized hemes are used for the synthesis of various hemoproteins, including hemoglobin, myoglobin and cytochrome p450, and the mitochondrial cytochromes a-a_3, b, and c (43, 44). Free hemes (b, c) are known substrates for HO activity, but not in their protein-bound forms (43). In the mitochondria the source of heme as substrate for HO activity likely arises from the turnover of hemoprotein pools, which may accelerate under conditions of stress or mitochondrial dysfunction such as exposure to CSE. A recent study, which observed mitochondrial localization of HO-1 in rat liver, proposed that HO-1 serves a regulatory role by reducing the bioavailability of heme to support cytochrome-c: oxidase activity (45). In the context of neurological disorders, excessive induction of HO-1 has been associated with pathological mitochondrial iron deposition (46). In the current study, however, the overexpression of HO-1 in epithelial cells clearly preserved mitochondrial ATP production and prevented cell death, in the presence of CSE, implying anti-necrotic protection (Fig. 5). Previously, HO-1 has been shown to inhibit cytokine-induced apoptosis in fibroblasts (47). Further studies are needed to elucidate the precise contributions of HO-derived end products such as CO, biliverdin, and/or iron to this metabolic protection. Among the byproducts of HO

activity, the liberation of CO has been associated with antiapoptotic processes in endothelial cells, by activating p38[?] MAPK-dependent pathways (48). CO inhibits cellular respiratory chain activity *in vitro* at high concentration, and may increase mitochondrial ROS production at low concentration (49). The functional significance of small gas production, including nitric oxide and CO in the mitochondrial compartment, remain unclear though some have proposed a physiologic relevance for down-regulation of respiratory chain activity under conditions of cellular stress (50). The discovery that inducible HO-1 localizes in part to the mitochondria may be of broad significance to the understanding of the mechanism(s) by which HO-1 confers protection against a wide variety of stimuli. An understanding of the function of the HO-1 enzyme system in the context of CSE-induced cellular and lung injury may provide potential therapeutic avenues, and increase the understanding of the etiology of smoke-related illness.

GRANTS

This study was financially supported in part by the department of internal medicine of the University Medical Center Groningen, The Netherlands to D.-J.S. and by a Dutch Kidney Foundation grant to M.v.d.T. This work was also supported by awards from the American Heart Association to S.W.R. (AHA #0335035N) and H.P.K. (AHA #0525552U), and by NIH grants R01-HL60234, R01-AI42365, and R01-HL55330 to Principal Investigator A.M.K.C.

REFERENCES

1. Pauwels RA, Rabe KF. Burden and clinical features of chronic obstructive pulmonary disease (COPD). Lancet 2004;364:613–620.
2. Barnes PJ, Shapiro SD, Pauwels RA. Chronic obstructive pulmonary disease: molecular and cellular mechanisms. Eur Respir J 2003;22:672–688.
3. Rahman I, MacNee W. Role of oxidants/antioxidants in smoking-induced lung diseases. Free Radic Biol Med 1996;21:669–681.
4. Rustemeier K, Stabbert R, Haussmann HJ, Roemer E, Carmines EL. Evaluation of the potential effects of ingredients added to cigarettes. Part 2: chemical composition of mainstream smoke. Food Chem Toxicol 2002;40:93–104.
5. Pauwels RA, Buist AS, Calverley PM, Jenkins CR, Hurd SS. GOLD Scientific Committee. Global strategy for the diagnosis, management, and prevention of chronic obstructive pulmonary disease. NHLBI/WHO Global Initiative for Chronic Obstructive Lung Disease (GOLD) Workshop summary. Am J Respir Crit Care Med 2001;163:1256–1276.
6. Shapiro SD, Ingenito EP. The pathogenesis of chronic obstructive pulmonary disease: advances in the past 100 years. Am J Respir Cell Mol Biol 2005;32:367–372.
7. Yokohori N, Aoshiba K, Nagai A. Respiratory Failure Research Group in Japan. Increased levels of cell death and proliferation in alveolar wall cells in patients with pulmonary emphysema. Chest 2004;125:626–632.

8. Imai K, Mercer BA, Schulman LL, Sonett JR, D'Armiento JM. Correlation of lung surface area to apoptosis and proliferation in human emphysema. Eur Respir J 2005;25:250–258.
9. Hageman GJ, Larik I, Pennings HJ, Haenen GR, Wouters EF, Bast A. Systemic poly (ADP-ribose) polymerase-1 activation, chronic inflammation, and oxidative stress in COPD patients. Free Radic Biol Med 2003;35:140–148.
10. Green DR, Reed JC. Mitochondria and apoptosis. Science 1998;281:1309–1312.
11. Leist M, Single B, Castoldi AF, Kuhnle S, Nicotera P. Intracellular adenosine triphosphate (ATP) concentration: a switch in the decision between apoptosis and necrosis. J Exp Med 1997;185:1481–1486.
12. Gairola C, Aleem MI. Cigarette smoke: effect of aqueous and nonaqueous fractions on mitochondrial function. Nature 1973;241:287–288.
13. Smith PR, Cooper JM, Govan GG, Harding AE, Schapira AH. Smoking and mitochondrial function: a model for environmental toxins. Q J Med 1993;86:657–660.
14. Miro O, Alonso JR, Jarreta D, Casademont J, Urbano-Marquez A, Cardellach F. Smoking disturbs mitochondrial respiratory chain function and enhances lipid peroxidation on human circulating lymphocytes. Carcinogenesis 1999;20:1331–1336.
15. Tenhunen R, Marver HS, Schmid R. Microsomal heme oxygenase, characterization of the enzyme. J Biol Chem 1969;244:6388–6394.
16. Tenhunen R, Marver HS, Schmid R. The enzymatic conversion of heme to bilirubin by microsomal heme oxygenase. Proc Natl Acad Sci USA 1968;61:748–755.
17. Morse D, Choi AM. Heme oxygenase-1: from bench to bedside. Am J Respir Crit Care Med 2005;172:660–670.
18. Slebos DJ, Ryter SW, Choi AM. Heme oxygenase-1 and carbon monoxide in pulmonary medicine. Respir Res 2003;4:7.
19. Ryter S, Otterbein LE, Morse D, Choi AM. Heme oxygenase/ carbon monoxide signaling pathways: regulation and functional significance. Mol Cell Biochem 2002;234/235:249–263.
20. Slebos DJ, Kerstjens HA, Rutgers SR, Kauffman HF, Choi AM, Postma DS. Heme oxygenase-1 expression is diminished in alveolar macrophages of patients with COPD. Eur Respir J 2004;23:652–653.
21. Yamada N, Yamaya M, Okinaga S, Nakayama K, Sekizawa K, Shibahara S, Sasaki H. Microsatellite polymorphism in the heme oxygenase-1 gene promoter is associated with susceptibility to emphysema. Am J Hum Genet 2000;66:187–195.
22. Lomas DA, Silverman EK. The genetics of chronic obstructive pulmonary disease. Respir Res 2001;2:20–26.
23. Kim HP, Wang X, Galbiati F, Ryter SW, Choi AM. Caveolae compartmentalization of heme oxygenase-1 in endothelial cells. FASEB J 2004;18:1080–1089.
24. Ryter SW, Kvam E, Tyrrell RM. Heme oxygenase activity: current methods and applications. Methods Mol Biol 2000;99:369–391.

25. Witschi H, Espiritu I, Maronpot RR, Pinkerton KE, Jones AD. The carcinogenic potential of the gas phase of environmental tobacco smoke. Carcinogenesis 1997;18:2035–2042.
26. Rangasamy T, Cho CY, Thimmulappa RK, Zhen L, Srisuma SS, Kensler TW, Yamamoto M, Petrache I, Tuder RM, Biswal S. Genetic ablation of Nrf2 enhances susceptibility to cigarette smoke-induced emphysema in mice. J Clin Invest 2004;114:1248–1259.
27. Hoshino Y, Mio T, Nagai S, Miki H, Ito I, Izumi T. Cytotoxic effects of cigarette smoke extract on an alveolar type II cell-derived cell line. Am J Physiol Lung Cell Mol Physiol 2001;281:L509–L516.
28. Vayssier M, Banzet N, Francois D, Bellmann K, Polla BS. Tobacco smoke induces both apoptosis and necrosis in mammalian cells: differential effects of HSP70. Am J Physiol 1998;275:L771–L779.
29. Aoshiba K, Tamaoki J, Nagai A. Acute cigarette smoke exposure induces apoptosis of alveolar macrophages. Am J Physiol Lung Cell Mol Physiol 2001;281:L1392–L1401.
30. Carnevali S, Petruzzelli S, Longoni B, Vanacore R, Barale R, Cipollini M, Scatena F, Paggiaro P, Celi A, Giuntini C. Cigarette smoke extract induces oxidative stress and apoptosis in human lung fibroblasts. Am J Physiol Lung Cell Mol Physiol 2003;284:L955–L963.
31. D'Agostini F, Balansky RM, Izzotti A, Lubet RA, Kelloff GJ, De Flora S. Modulation of apoptosis by cigarette smoke and cancer chemopreventive agents in the respiratory tract of rats. Carcinogenesis 2001;22:375–380.
32. Wang H, Ma L, Li Y, Cho CH. Exposure to cigarette smoke increases apoptosis in the rat gastric mucosa through a reactive oxygen species-mediated and p53-independent pathway. Free Radic Biol Med 2000;28:1125–1131.
33. Wang HY, Shin VY, Leung SY, Yuen ST, Cho CH. Involvement of bcl-2 and caspase-3 in apoptosis induced by cigarette smoke extract in the gastric epithelial cell. Toxicol Pathol 2003;31:220–226.
34. Wang J, Wilcken DE, Wang XL. Cigarette smoke activates caspase-3 to induce apoptosis of human umbilical venous endothelial cells. Mol Genet Metab 2001;72:82–88.
35. Wickenden JA, Clarke MC, Rossi AG, Rahman I, Faux SP, Donaldson K, MacNee W. Cigarette smoke prevents apoptosis through inhibition of caspase activation and induces necrosis. Am J Respir Cell Mol Biol 2003;29:562–570.
36. Liu X, Conner H, Kobayashi T, Kim H, Wen F, Abe S, Fang Q, Wang X, Hashimoto M, Bitterman P, et al. Cigarette smoke extract induces DNA damage but not apoptosis in human bronchial epithelial cells. Am J Respir Cell Mol Biol 2005;33:121–129.
37. Rennard SI. Cigarette smoke in research. Am J Respir Cell Mol Biol 2004;31:479–480.
38. Shinohara T, Kaneko T, Nagashima Y, Ueda A, Tagawa A, Ishigatsubo Y. Adenovirus-mediated transfer and overexpression of heme oxygenase 1 cDNA in lungs attenuates elastase-induced pulmonary emphysema in mice. Hum Gene Ther 2005;16:318–327.

39. Yoshinaga T, Sassa S, Kappas A. The occurrence of molecular interactions among NADPH-cytochrome c reductase, heme oxygenase, and biliverdin reductase in heme degradation. J Biol Chem 1982;257:7786–7793.
40. Shibahara S, Muller RM, Taguchi H, Yoshida T. Cloning and expression of cDNA for rat heme oxygenase. Proc Natl Acad Sci USA 1985;82:7865–7869.
41. Yoshida T, Biro P, Cohen T, Müller M, Shibahara S. Human heme oxygenase cDNA and induction of its mRNA by hemin. Eur J Biochem 1988;171:457–461.
42. Keyse SM, Tyrrell RM. Heme oxygenase is the major 32-kDa stress protein induced in human skin fibroblasts by UVA radiation, hydrogen peroxide, and sodium arsenite. Proc Natl Acad Sci USA 1989;86:99–103.
43. Maines MD. Heme oxygenase: function, multiplicity, regulatory mechanisms, and clinical applications. FASEB J 1988;2:2557–2568.
44. Ryter S, Tyrrell RM. The heme synthesis and degradation pathways, role in oxidant sensitivity. Heme oxygenase has both pro- and anti-oxidant properties. Free Radic Biol Med 2000;28:289–309.
45. Converso DP, Taille C, Carreras MC, Jaitovich A, Poderoso JJ, Boczkowski J. HO-1 is located in liver mitochondria and modulates mitochondrial heme content and metabolism. FASEB J 2006;20:1236–1238.
46. Mehindate K, Sahlas DJ, Frankel D, Mawal Y, Liberman A, Corcos J, Dion S, Schipper HM. Proinflammatory cytokines promote glial heme oxygenase-1 expression and mitochondrial iron deposition: implications for multiple sclerosis. J Neurochem 2001;77:1386–1395.
47. Petrache I, Otterbein LE, Alam J, Wiegand GW, Choi AM. Heme oxygenase-1 inhibits TNF-alpha-induced apoptosis in cultured fibroblasts. Am J Physiol Lung Cell Mol Physiol 2000;278:L312–L319.
48. Brouard S, Otterbein LE, Anrather J, Tobiasch E, Bach FH, Choi AM, Soares MP. Carbon monoxide generated by heme oxygenase-1 suppresses endothelial cell apoptosis. J Exp Med 2000;192:1015–1026.
49. Taille C, El-Benna J, Lanone S, Boczkowski J, Motterlini R. Mitochondrial respiratory chain and NAD(P)H oxidase are targets for the antiproliferative effect of carbon monoxide in human airway smooth muscle. J Biol Chem 2005;27:25350–25360.
50. Moncada S, Erusalimsky JD. Does nitric oxide modulate mitochondrial energy generation and apoptosis? Nat Rev Mol Cell Biol 2002;3:214–220.

Chapter 4

GASEOUS-PHASE CIGARETTE SMOKE IRREVERSIBLY MODIFIES

GLUTATHIONE IN AIRWAY EPITHELIAL CELLS

Marco van der Toorn[1*], Maria P. Smit-de Vries[2*], Dirk-Jan Slebos[3], Harold G. de Bruin[1], Nicolas Abello[2], Antoon J. M. van Oosterhout[1], Rainer Bischoff[2], Henk F. Kauffman[4].

[1]Laboratory of Allergology and Pulmonary Diseases, [2]Department of Analytical Biochemistry, [3]Department of Pulmonary Diseases, [4]Groningen University Institute for Drug Exploration, University Medical Center Groningen, University of Groningen, PO Box 30001, 9700 RB, The Netherlands.
[*]Equal contribution as first author.

Am J Physiol Lung Cell Mol Physiol. 2007 Aug 24;

ABSTRACT

In patients with COPD an imbalance between oxidants and anti-oxidants is acknowledged to result in disease development and progression. Cigarette smoke (CS) is known to deplete total glutathione (GSH+GSSG) in the airways. We hypothesized that components in the gaseous-phase of CS may irreversibly react with GSH to GSX, thereby causing this depletion. To understand this phenomenon, we investigated the GSH metabolism in response to CS, and identified the actual GSX compounds. Both CS and H_2O_2-control depletes reduced GSH in solution (Δ -54.1±1.7 μM, $P < 0.01$ and Δ - 39.8±0.9 μM; $P < 0.01$). However, a significant decrease of total glutathione was observed after CS exposure (Δ -75.1±7.6 μM, $P < 0.01$) but not after H_2O_2 exposure. Exposure of A549 cells and primary bronchial epithelial cells to CS decreased free sulfhydryl (–SH) groups (Δ -64.2±14.6 μM/mg protein; $P < 0.05$) and irreversibly modified total glutathione (Δ -17.7±1.9 μM; $P < 0.01$) compared to non-exposed cells or H_2O_2 control. Mass spectrometry (MS) showed that GSH was modified into glutathione-aldehyde derivatives. Further MS identification showed that GSH was bound to acrolein and crotonaldehyde, and another, yet unidentified structure. Our data shows that CS did not oxidize GSH to GSSG, but reacts to non-reducible glutathione-aldehyde derivatives, thereby depleting the total available GSH-pool.

INTRODUCTION

Smoking and genetic susceptibility are the main risk factors for the development of Chronic Obstructive Pulmonary Disease (COPD) (2, 22). One important hypothesis with respect to the pathophysiology of COPD is an imbalance between oxidants and antioxidants in the airways. This imbalance results in disease, when the anti-oxidant capacity of the lung is unable to sufficiently neutralize reactive compounds present in cigarette smoke (CS) or generated during the persistent airway inflammation present in COPD (18).

Reactive compounds in the gaseous-phase of CS are thought to constitute the main component of the oxidative stress present in COPD (15). In patients with COPD, increased levels of oxidative stress parameters have been documented in exhaled breath condensate, sputum and blood (e.g. higher H_2O_2, 8-isoprostane, malondialdehyde (MDA), and lower reduced glutathione (GSH) levels) (3, 11). Changes induced by these reactive components may result in inactivation of anti-proteases, epithelial cell injury, apoptotic and necrotic cell death, mitochondrial dysfunctions, disturbance of extracellular matrix repair, and maintenance of airway inflammation, all potentially of importance in the development of COPD (25, 32).

Since the airways of smokers are exposed to highly reactive components, the lung is always at risk of oxidative injury (26). To ensure an appropriate defense against this injury, the respiratory tract is equipped with the epithelial lining fluid (ELF) and the airway epithelium, which both contain large amounts of GSH (9). GSH plays a key role in the cellular redox balance, and is thought to be one of the most important anti-oxidant defenses against CS inhaled reactive components (4).

Under non-stress conditions, most of the intracellular GSH is 'stored' in its reduced form. However, the balance between GSH and oxidized glutathione (GSSG) can change significantly under conditions of oxidative stress, and their ratio provides information on the redox status of cells and tissues. During states of increased oxidative stress, the free sulfhydryl (-SH) groups become oxidized (33). It has been described that exposure to the gaseous-phase of CS in vitro and in vivo generally results in a loss of GSH, whereas the amount of GSSG does not increase significantly (21, 26). This was confirmed by preliminary experiments performed in our laboratory, where an irreversible loss of total glutathione in epithelial cells was observed when exposed to gaseous-phase CS.

We therefore hypothesized that components in the gaseous-phase of CS may irreversibly react with GSH to GSX. As a consequence of this, GSH derivatives that can not be reduced (GSX) may induce a chronic lack of protection against additional CS-exposure under conditions where *de novo* synthesis of GSH is rate-limiting. This may occur when there is a genetic deficiency in *de novo* synthesis of GSH, which predisposes smokers to the development of COPD (8, 14).

MATERIALS AND METHODS

Chemicals

L-cystein, bovine serum albumin (BSA), reduced glutathione (GSH), oxidized glutathione (GSSG), hydrogen peroxide (H_2O_2), 5,5'-dithiobis-(2)-nitrobenzoic acid

(DTNB), trichloroacetic acid (TCA), acrolein and crotonaldehyde were obtained from Sigma-Aldrich Chemie B.V. (Zwijndrecht, The Netherlands).

Cell cultures
The human alveolar type II epithelium-like adherent cell line, A549 was purchased from American Type Culture Collection (ATCC, Manassas, VA). Human primary bronchial epithelial cells were collected and cultured by the methods described previously (32). All cells were grown in RPMI 1640 with 25 mM HEPES, L-Glutamine (BioWitthaker, Verviers, Belgium) supplemented with 10% heat-inactivated fetal calf serum (BioWitthaker, Verviers, Belgium) and 20 µg/ml Gentamycin (Centafarm Services, Etten-Leur, The Netherlands). All cells were grown in 25 cm_2 plastic culture flasks (Costar, Cambridge, MA) at 37°C in an atmosphere of 5% CO_2 until 80-90% confluency was reached. Before the experiments both the A549 cells and the human primary bronchial epithelial cells were incubated for 16 h in serum free RPMI 1640 media.

Exposure of a GSH solution to different oxidants
A solution of GSH (150 µM in pure H_2O, pH 4.2) was exposed to air, the gaseous-phase of one cigarette (CS) or two cigarettes (CS (2x)), or a solution of H_2O_2 (1 mM). Briefly, 25 ml solution was placed in a 50 ml Falcon tube (BD Biosciences, Alphen aan den Rijn, The Netherlands) at 37°C. Kentucky 2R4F research-reference cigarettes (The Tobacco Research Institute, University of Kentucky, Lexington, KY) were smoked using a peristaltic pump. Just before the experiments, filters were cut from the cigarettes. Each cigarette was smoked in exactly 5 min at a flowrate of 8 L/h and bubbled through the GSH solution. This solution was used immediately for the experimental procedures. Air, produced with the same peristaltic pump, but without the use of a cigarette, was used as a negative control under the same conditions. The oxidative agent H_2O_2 (final concentration 1 mM) was used as a positive control.

Exposure of airway epithelial cells to CS
A549 cells were exposed to air, CS or a solution of 5 mM H_2O_2. Briefly, A549 cells were grown in 25 cm2 plastic culture flasks as described above. Just before the experiments, medium was removed and the culture flask was positioned up-side down, allowing a direct contact of smoke with epithelial cells. Kentucky 2R4F research reference cigarettes were smoked using a peristaltic pump. Just before the experiments, filters were cut from the cigarettes. Each cigarette was smoked in exactly 5 min at a rate of 8 L/hr. Gaseous-phase CS was directly distributed inside the culture flasks, by blowing the smoke inside through a small plastic tube. After the exposure, cells were washed with PBS, lysed with water and analyzed. Air was used as negative control under the same conditions as CS. As positive control, H_2O_2 (final concentration 5 mM) was incubated at room temperature for 5 min, after which the cells were washed with PBS, lysed with water and analyzed.

Quantitative determination of total -SH groups
A549 cells were washed with PBS and lysed by one freeze-thaw cycle in 2.5 ml pure H_2O. Total protein concentration was determined by the Bradford method (7), using BSA as standard (Bio-Rad Laboratories, The Netherlands). Ellman's reagent (12) was used for the determination of free -SH groups in cell culture and a cell-free solution of GSH. Ellman's reagent (12 mM DTNB) was added to the lysed cells or GSH solution to a final concentration of 6 mM DTNB followed by 10 min incubation. Thereafter, samples were centrifuged at 1000 g for 5 min. The supernatant was used in the assay and measured at 405 nm in a Biotek EL808 microplate reader (Bio-Tek Instruments, Abcoude, The Netherlands). The amount of free thiol groups was calibrated against a standard curve of L-cystein.

Quantitative determination of total glutathione using the Tietze assay
The sum of reduced and oxidized glutathione in different samples was determined by the enzymatic method of Tietze (31). Briefly, cells were washed with PBS and treated with 5% TCA. The samples of the GSH solution were also treated with 5% TCA. All samples were centrifuged at 10.000 g for 5 min, at 4°C. 150 µL of each standard and sample were pipetted into a 96-wells Elisa plate. 25 µL Ellman reagents (DTNB) and 5 µL glutathione reductase (GR) were added. This supernatant was enzymatically reduced by the added GR and immediately before reading, NADPH was added and the increase absorbance at 405 nm was recorded for 10 min at room temperature on a Biotek EL808 microplate reader. The results were compared with a standard curve of GSH.

Mass spectrometry
Before analyzing A549 cell lysates, primary bronchial epithelial cell lysates, and solutions of GSH and GSSG by mass spectrometry (MS), samples were filtrated using an Amicon Ultra 5-kDa cut-off centrifugal filter device (Millipore Co., Cork, Ireland). The collected ultrafiltrate was diluted in a 1:1 ratio with 0.1% (v/v) formic acid (Merck, Haarlem, The Netherlands) in acetonitrile (Merck, Haarlem, The Netherlands). The samples were analyzed by direct infusion at 5 µL/min into an SL ion trap mass spectrometer (Agilent, Santa Clara, USA) equipped with an electrospray ionization source operated in positive mode, using the following conditions: capillary voltage (3000V), nebulizer gas (N_2, 10 psi), drying gas (N_2, 4 L/min) at 275ºC. MS data were acquired over a scan range of 50-650 m/z (mass/charge) and with a scan rate of 5,500 m/z per second. The target m/z was 615, the compound stability was set at 70%. Data were collected for 10 min prior to mass spectrum averaging and analyzed using data analysis software for LC/MSD Trap version 3.2 (Bruker Daltonics, Bremen, Germany). Peaks of interest were fragmented using manual MS/MS (MS2) settings (width of precursor ion selection: 1.0-1.5 Da; amplitude of 0.8-1.0 V). MS2 data were collected for 5 min.

Statistical Analysis
Data were analyzed using Prism 4 for Windows (GraphPad Software, inc., San Diego, USA). Comparisons between different experimental groups were performed with Dunnet's multiple comparison test (figure 1 A, B and 3 A, B). $P < 0.05$ was

considered significant. Results are presented as mean values (±SEM) unless otherwise mentioned.

RESULTS

Cigarette smoke decreases total glutathione in solution

GSH is one of the most important anti-oxidants present in the ELF and participates in the defense of pulmonary epithelial cells against inhaled reactive components of CS. To test whether these CS components are able to modify the free thiol groups of GSH, a solution of GSH was exposed to CS. While air, used as negative control, did not affect the level of free -SH groups of GSH, exposure to gaseous-phase CS (CS (2x), Δ -54.1±1.7 μM, $P < 0.01$; Fig. 1A) or the addition of 1 mM H_2O_2 (Δ -39.8±0.9 μM, $P < 0.01$; Fig. 1A) resulted in a dose-dependent decrease of free -SH groups. To determine whether CS oxidizes GSH to GSSG, the enzymatic reducing cycle of Tietze was used. A significant reduction of total glutathione (GSH+GSSG) was observed after exposure to gaseous-phase CS (CS (2x): Δ -75.1±7.6 μM, $P < 0.01$; Fig. 1B) whereas H_2O_2, which has been proven to oxidize GSH (Fig. 1A), did not affect the total glutathione concentration compared to control (Fig. 1B).

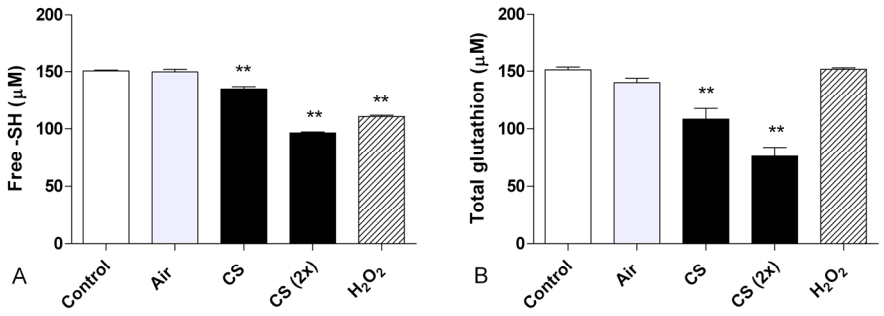

Figure 1. The effect of cigarette smoke, control air and H_2O_2 on the level of free –SH groups of GSH in solution. Free –SH groups were studied using Ellman's reagent (A). Total glutathione was studied using the enzymatic reducing cycle system of Tietze (B). CS = exposure to 1 cigarette, CS (2x) = exposure to 2 cigarettes. Data are expressed as mean values ± SEM and are referred to 4 experiments. **, $p<0.01$ vs control by Dunnet's multiple comparison test.

MS analysis of CS-exposed GSH in solution

To understand why CS decreases free –SH groups in solution, samples were analyzed by mass spectrometry using direct infusion. Figure 2A and B show the MS background of pure water and water exposed to the gaseous-phase of two cigarettes. Water exposed to CS shows a substantial background between m/z 80-300. Because the background was less prominent above m/z 300 we were able to study glutathione modification (m/z 308.1, singly charged protonated GSH, Fig. 2C). In figure 2D two peaks corresponding to GSSG can be seen. The peak with the m/z value of 307.1 indicates double charged GSSG, and the peak of m/z 613.2 indicates single charged GSSG. MS analysis of GSH in solution exposed to the gaseous-phase of two cigarettes did not result in the formation of oxidized GSSG. However, two

additional components (component 1 and 2) were observed with m/z values of 364.1 and 378.1 respectively (Fig. 2E). Addition of H_2O_2 to GSH in solution, as control experiment, resulted in two peaks of m/z 307.2 and 613.2, proving the direct oxidation of GSH into GSSG (Fig. 2F).

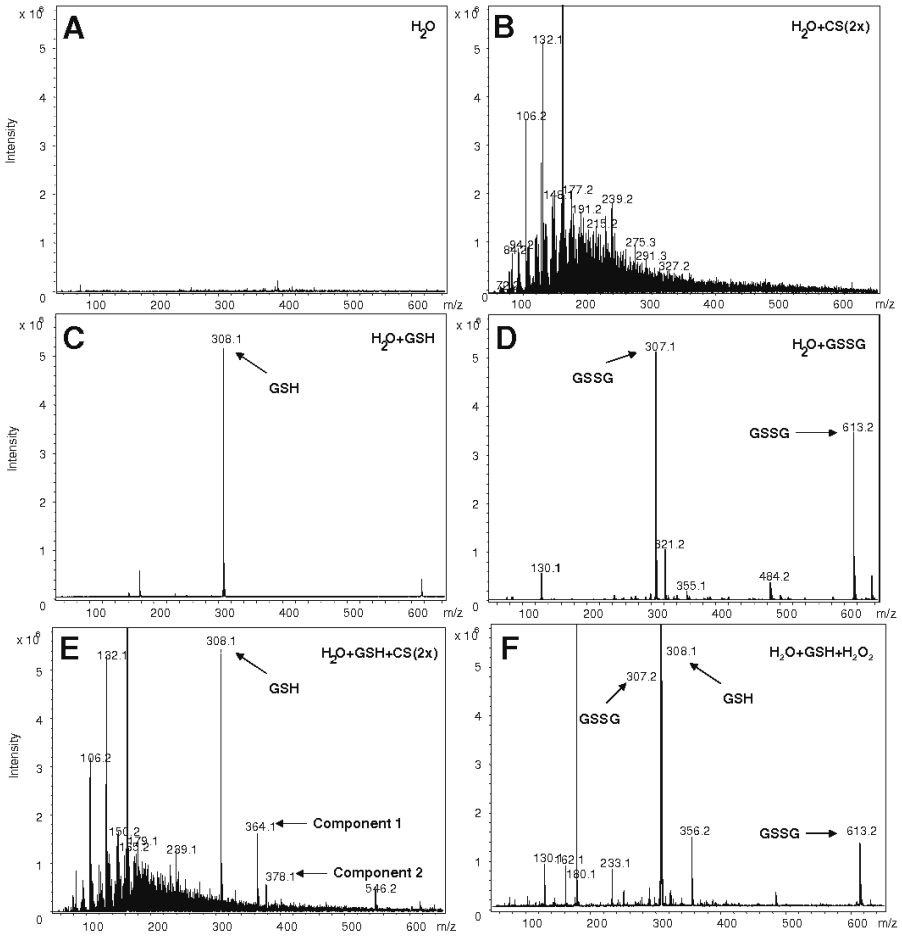

Figure 2. The effect of cigarette smoke and H_2O_2 on the modification of a cell-free GSH solution by mass spectrometry. A) sample solution (pure H_2O); B) exposure of H_2O to 2 cigarettes (H_2O+CS(2x)); C) solution of GSH (final concentration 150 μM) (H_2O+GSH); D) exposure of GSH to 2 cigarettes (H_2O+GSH+CS(2x)); E) solution of GSSG (final concentration 150 μM) (H_2O+GSSG); F) exposure of GSH to H_2O_2 (final concentration 1 mM) (H_2O+GSH+H_2O_2). The mass spectra are representative of one experiment out of three.

Cigarette smoke decreases total –SH groups in airway epithelial cells

To investigate the effect of CS on the redox status of free -SH groups, airway epithelial cells were directly exposed to CS. Air exposure used as a negative control did not affect free -SH groups in the cells, whereas the gaseous-phase of CS significantly decreased this level by -64.2±14.6 μM/mg protein, $P < 0.05$ (Fig. 3A). H_2O_2 used as positive control, did not show an effect, which might be due to the short time of incubation (30).

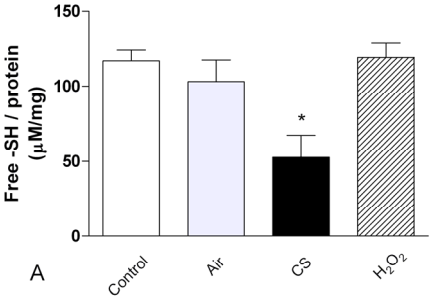

Figure 3A. The effect of cigarette smoke on free –SH groups in A549 cells. Free –SH groups in A549 cells were measured using Ellman's reagent. Data are expressed as mean values ± SEM and are referred to 4 experiments. *, $P < 0.05$ vs control by Dunnet's multiple comparison test.

Cigarette smoke decreases total glutathione in airway epithelial cells

To examine whether glutathione was irreversibly modified after CS exposure, total glutathione was determined using the enzymatic GSSG-reducing cycle system described by Tietze (31). A significant reduction of total glutathione was observed after the A549 cells were exposed to gaseous-phase CS (CS, Δ -17.7±1.9 μM, $P < 0.01$; Fig. 3B). Exposure to air and H_2O_2 did not affect the total glutathione concentration in the epithelial cells compared with control cells.

Figure 3B. To examine irreversible modification of glutathione after exposure of A549 cells to cigarette smoke, total glutathione was measured using the enzymatic reducing cycle system of Tietze. Data are expressed as mean values ± SEM and are referred to 4 experiments. **, $P < 0.01$ vs control by Dunnet's multiple comparison test.

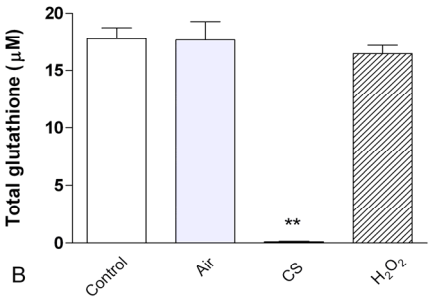

MS analysis of airway epithelial cells

A549 cells were exposed directly to the gaseous-phase of CS and thereafter lysed. This lysate was directly analyzed by MS by direct infusion. Non-exposed A549 cells (Fig. 4A) and cells exposed to air (Fig. 4B) show a peak at m/z 308.1, corresponding to the reduced form of GSH. We observed a decreased signal for GSH in the CS-exposed cells (Fig. 4C) compared to the untreated- or air exposed cells and observed the appearance of three different components (Component 1, 2 and 3). The first two components were also observed in the CS-exposed GSH solution: the peaks at m/z 364.1 (Component 1) and 378.1 (Component 2). Furthermore, a new peak appeared

corresponding with an m/z value of 391.2 (Component 3). Short exposure of A549 cells to H_2O_2 did not alter GSH, compared to the non-exposed cells (Fig. 4D). Interestingly GSSG (peaks at m/z of 307.1 and 613.2) was not detectable in any of the A549 cultures.

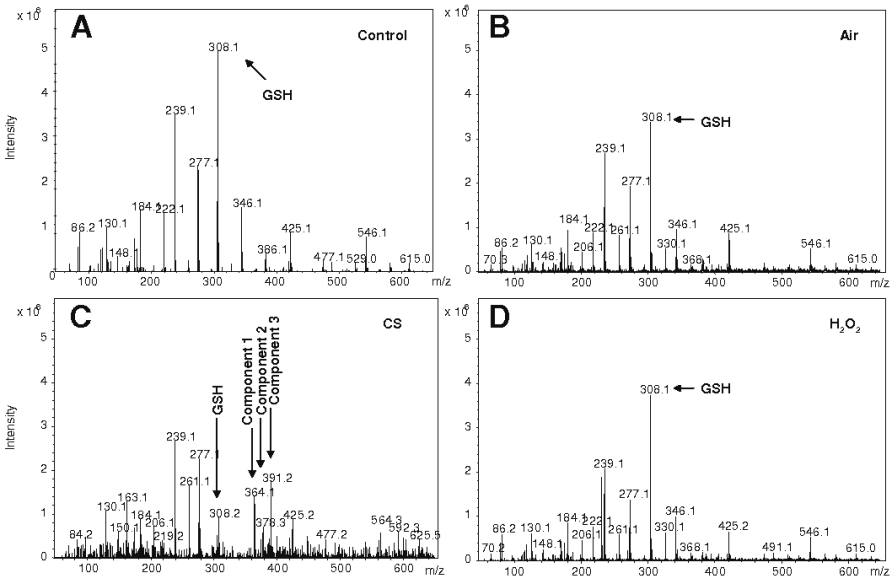

Figure 4. The effect of cigarette smoke and H_2O_2 on modification of GSH in A549 cells by mass spectrometry. A) control cells (no exposure); B) exposure to air; C) exposure to cigarette smoke (CS); D) exposure to H_2O_2 (final concentration 5 mM). Characterization of the peaks at m/z 364.1 (Component 1), 378.1 (Component 2) and 391.2 (Component 3) was done by MS2 spectrometry (Fig. 5). The mass spectra are representative of one experiment out of three.

Mass spectrometry showed GSH modification into glutathione-aldehyde derivatives

MS analysis of CS-exposed A549 cells resulted in a decreased peak at m/z 308.1, reduced GSH, and additional peaks at m/z values of 364.1 (Component 1), 378.1 (Component 2) and 391.2 (Component 3). The isotope distribution confirmed that these m/z values corresponded to singly-charged molecules. By subtracting the mass of these components from the mass of GSH we were able to select a few candidate molecules that would fit the observed mass difference including acrolein or crotonaldehyde. After incubation of GSH with acrolein and crotonaldehyde we were able to detect peaks at m/z values of 364.1 and 378.1 respectively (Fig. 5A and B). Identification of these peaks was done by MS2 fragmentation. The fragments obtained from the A549 cells exposed to gaseous-phase CS were compared to GSH incubated with acrolein (GSH+acrolein) or crotonaldehyde (GSH+crotonaldehyde). These findings were also confirmed by MS2 fragmentation of primary bronchial epithelial cell lysates under the same experimental conditions as the A549 cells (Fig. 5C and D). Fragmentation confirmed the identity of the peaks to be GSH-acrolein (Component 1) and GSH-crotonaldehyde (Component 2) (Fig. 5C and D). The same

cell lysate also showed a peak at m/z 391.2 (Component 3). So far we have not been able to identify this peak, apart from the fact that it did not derive from a phthalate contamination. Phthalates are well known contaminants in MS, coming from plastic bottles, flasks and packing materials (13). MS2 fragmentation of peak m/z 391.2 (Component 3) obtained from traces of phthalate contamination differs from the MS2 fragmentation of peak m/z 391.2 obtained from the cell lysate (Fig. 5E and F).

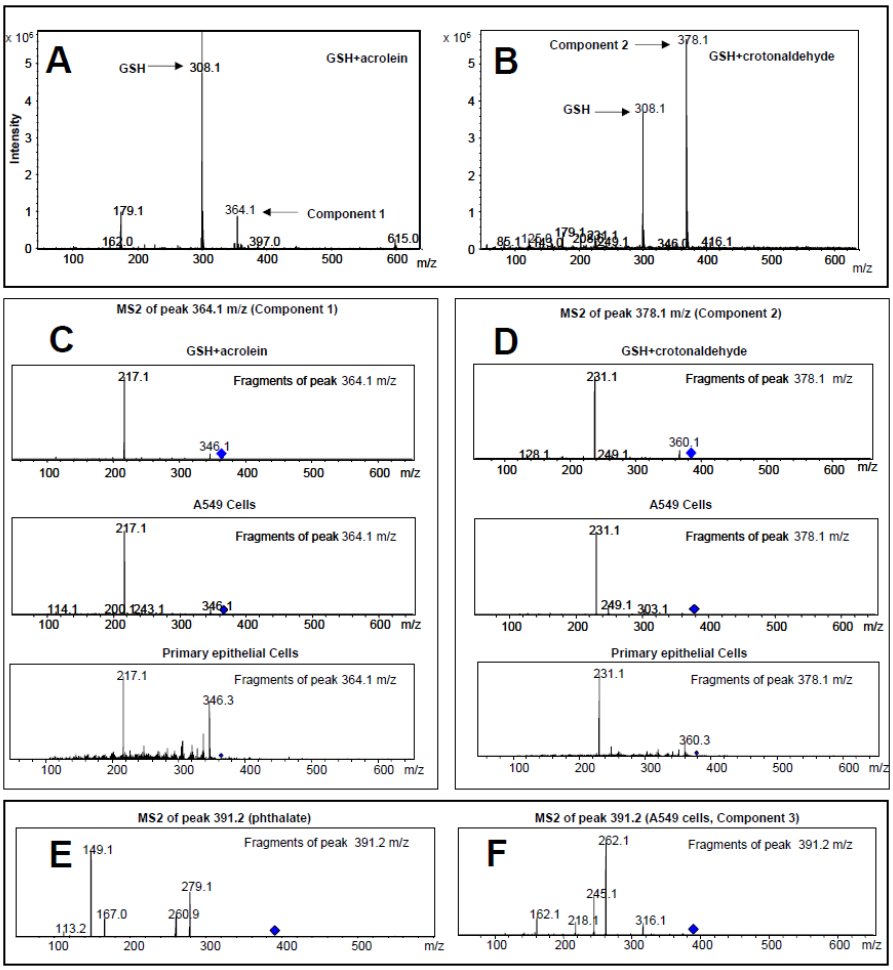

Figure 5. Identification of GSH-acrolein (m/z 364.1, component 1) and GSH-crotonaldehyde (m/z 378.1, component 2) derivatives by MS2. The mass spectra of GSH + acrolein (A) and GSH + crotonaldehyde are shown (B). First daughter ion spectra of GSH+acrolein, A549 cells and primary bronchial epithelial cells are shown (C) and the first daughter ion spectra of GSH+crotonaldehyde, A549 cells and primary bronchial epithelial cells are shown (D). First daughter spectra of phthalate (E) and the unknown component from A549 cells (Component 3) are shown (F). The mass spectra are representative of one experiment out of three.

DISCUSSION

In this study we investigated the modification of glutathione (GSH) and more general the total reduced thiol content of airway epithelial cells by the gaseous-phase of CS. We hypothesized that CS can irreversibly modify GSH, rendering it unavailable for the enzymatic reducing cycle system that is thought to play an important role in protection of airway epithelial cells against oxidative stress. Our results clearly showed that the gaseous-phase of CS decreases free -SH groups of GSH in solution and in airway epithelial cells. We observed that the reactive components present in the gaseous-phase of CS did not oxidize GSH to the disulfide-containing GSSG. Instead of this physiological reaction, GSH was irreversibly modified by unsaturated aldehydes that are being generated during the combustion of tobacco. In vitro experiments showed that exposure of CS changed almost the entire pool of GSH into GSH-aldehyde components.

These findings shed new light on the GSH redox cycle in airway epithelial cells. The enzymatic redox cycle, which is normally activated after oxidative stress and the formation of GSSG, could not be activated because of the depletion of GSH into nonreducible glutathione components, with loss of the GSH pool. This exhaustion of the pool of reduced GSH may induce a chronic lack of anti-oxidant protection. Persistent smokers may in that case inhale more ROS than can be scavenged by the residual anti-oxidants, resulting in increased vulnerability to oxidative stress. This makes the synthesis of GSH essential for cellular survival and protection of the lung.

The development of COPD is associated with increased oxidative stress and reduced antioxidant resources (5; 6; 18). Smoking cigarettes is the most important factor for the development of COPD, which is currently the 5th leading cause of death worldwide (19). Cellular stress induced by CS is critically dependent on the intracellular reduced GSH concentration. For instance, intracellular GSH depletion significantly facilitates stress signal transduction pathways, cell proliferation, apoptosis and inflammation (1). Studies performed by Rahman *et al.* showed that a GSH/GSSG ratio of less than 90% influences a variety of cellular signaling processes, such as phosphorylation of stress kinases JNK, p38, MAPK and PI-3K as well as activation of the transcription factors AP-1 and NFκB (23, 27). In these publications it has been demonstrated that increasing the intracellular levels of GSH can provide protection. In other respiratory diseases like cystic fibrosis a significant decrease of GSH efflux from cells, which leads to deficiency of GSH in the ELF of the lung, as well as in other compartments, including cells of the immune system and the gastrointestinal tract, was observed (16).

Although reduced GSH has been shown to be elevated in the ELF of chronic smokers, CS acutely lowers intracellular levels of GSH (17, 24). An animal study by Cotgreave *et al.* showed that acute effects of CS inhalation by rats caused significant depletion of GSH in the whole lung, lavage cells and lavage fluid. The depleted GSH could not be reduced by a reducing agent like dithiothreitol. They suggested that GSH was irreversible conjugated with electrophilic components of the CS (10). In line with these results, intratracheal instillation of CS condensate in the rat resulted in depletion of intracellular GSH, concomitant formation of GSH-conjugates without significant elevation of oxidized GSSG nor any GSH efflux from

the cells (24). These studies are in agreement with our current findings. We showed in a GSH solution that GSH exposed to gaseous-phase CS was not oxidized into GSSG but became irreversibly modified into glutathione derivatives (Fig. 1 and 2). Where addition of the enzyme GR to a solution of GSH exposed to H_2O_2 resulted in a restoration of the initial GSH concentration, this enzyme was not able to reduce the components in the GSH solution exposed to CS, indicating that GSH had been irreversibly modified. However, this enzyme was not able to reduce the components in the GSH solution exposed to CS, indicating that GSH had been irreversibly modified. Exposure of cultured alveolar A549 cells to the gaseous-phase of CS also showed that GSH was irreversibly modified into the same GSH derivatives, whereas incubation with H_2O_2 for 5 minutes did not alter the intracellular pool of GSH.

MS showed that the depletion of GSH could be attributed to the formation of glutathione-aldehyde derivatives. Direct infusion of cell lysate into the mass spectrometer showed three peaks (m/z 364.1, 378.1 and 391.2), while the peak of GSH (m/z 308.1) was diminished. We confirmed by MS2 that two of the three peaks were GSH aldehyde derivatives, respectively GSH-acrolein (m/z 364.1) and GSH-crotonaldehyde (m/z 378.1). In line, a recent study by Reddy *et al.* demonstrated that exposure of neutrophils to the gaseous-phase of CS also resulted in the formation of GSH-acrolein (29). In contrast to our observations, Reddy *et al.* were not able to show GSH-aldehyde derivatives in airway epithelial cells. This may be due either to a lower exposure to CS, to a longer incubation time of the cells allowing the release of the toxic components into the culture medium or to the use of cell culture medium resulting in no direct contact of smoke with the cultured epithelial cells. In our system, medium was removed from the cells with only a very thin layer of medium covering the cells, allowing a more direct contact of the gaseous phase of CS with the epithelial cells. After the exposure, cells were rapidly lysed and analyzed by MS by direct infusion. Reported EC50 values of a variety of aldehydes that are able to deplete GSH, showed that acrolein was by far the most effective one to bind to GSH followed by formaldehyde and crotonaldehyde (20). In contrast to our data from airway epithelial cells, the third peak (m/z 391.2) was not seen within the CS-exposed GSH solution. This peak is similar to a well known contaminant in MS, coming from phthalate compounds in plastic, however, fragmentation of the peak by MS2 showed that it was not a phthalate compound (13). It may be proposed that this component is derived from membrane degradation by radicals in CS, but the mass of this component could not be ascribed to known membrane degradation products.

The presence of oxidative stress and decreased anti-oxidant capacity has important consequences for the pathogenesis of COPD. Activation of redox-sensitive transcription factors enhances pro-inflammatory mediators and protective anti-oxidant gene expression. In biochemistry, *de novo* synthesis of GSH from glutamate, cysteine and glycine is catalyzed sequentially by the two cytosolic enzymes, γ-GCS and GS. It is already known that epithelial cells of the lung respond rapidly and sensitively to oxidative stress, and that this adaptive response is mediated by an increase of γ-GCS mRNA and enzyme activity (28). Although CS is the main environmental risk factor for developing COPD, only about 15-20% of smokers develop COPD. Genetic factors are likely to modify the risk of developing COPD. It can therefore be hypothesized that restricted ability to synthesize sufficient GSH may be due to polymorphisms in genes linked to *de novo* synthesis of GSH

leading to COPD. A few studies are available involving polymorphisms in genes related to GSH synthesis and lung disease (8; 14). Therefore, further research on the variability among genes encoding for *de novo* GSH synthesis in smokers would be of great interest in human genetics of COPD.

For the first time, we have demonstrated by direct infusion MS combined with enzymatic assays, that a substantial amount of GSH in epithelial cells is irreversibly modified into GSH-acrolein and GSH-crotonaldehyde derivatives and a yet unknown component. Under these circumstances, a chronic lack of protection against oxidative stress might be induced, especially when a genetic predisposition of rate-limiting *de novo* synthesis of GSH is present. These findings might be a possible biochemical mechanism of CS induced toxicity which has been found in patients with COPD.

GRANTS

This work was supported by research grants of the J.K. de Cock foundation (MvdT and DJS) and from GlaxoSmithKline (HGdB). NA is the recipient of an Ubbo Emmius fellowship from the University of Groningen. The authors have no conflicting financial interests.

REFERENCE LIST

1. Armstrong JS, Steinauer KK, Hornung B, Irish JM, Lecane P, Birrell GW, Peehl DM and Knox SJ. Role of glutathione depletion and reactive oxygen species generation in apoptotic signaling in a human B lymphoma cell line. Cell Death Differ 9: 252-263, 2002.

2. Barnes PJ, Shapiro SD and Pauwels RA. Chronic obstructive pulmonary disease molecular and cellular mechanisms. Eur Respir J 22: 672-688, 2003.

3. Beier J, Beeh KM, Semmler D, Beike N and Buhl R. Increased concentrations of glutathione in induced sputum of patients with mild or moderate allergic asthma. Ann Allergy Asthma Immunol 92: 459-463, 2004.

4. Biswas S, Chida AS and Rahman I. Redox modifications of protein-thiols: emerging roles in cell signaling. Biochem Pharmacol 71: 551-564, 2006.

5. Boots AW, Haenen GR and Bast A. Oxidant metabolism in chronic obstructive pulmonary disease. Eur Respir J Suppl 46: 14s-27s, 2003.

6. Bowler RP, Barnes PJ and Crapo JD. The role of oxidative stress in chronic obstructive pulmonary disease. COPD 1: 255-277, 2004.

7. Bradford MM. A rapid and sensitive method for the quantitation of microgram quantities of protein utilizing the principle of protein-dye binding. Anal Biochem 72: 248-254, 1976.

8. Calikoglu M, Tamer L, Ates Aras N, Karakas S and Ercan B. The Association Between Polymorphic Genotypes of Glutathione S-Transferases and COPD in the Turkish Population. Biochem Genet 44: 307-319, 2006.

9. Cantin AM, North SL, Hubbard RC and Crystal RG. Normal alveolar epithelial lining fluid contains high levels of glutathione. J Appl Physiol 63: 152-157, 1987.

10. Cotgreave IA, Johansson U, Moldeus P and Brattsand R. The effect of acute cigarette smoke inhalation on pulmonary and systemic cysteine and glutathione redox states in the rat. Toxicology 45: 203-212, 1987.
11. Dekhuijzen PN, Aben KK, Dekker I, Aarts LP, Wielders PL, van Herwaarden CL and Bast A. Increased exhalation of hydrogen peroxide in patients with stable and unstable chronic obstructive pulmonary disease. Am J Respir Crit Care Med 154: 813-816, 1996.
12. Ellman GL. Tissue sulfhydryl groups. Arch Biochem Biophys 82: 70-77, 1959.
13. Ende M and Spiteller G. Contaminants in mass spectrometry. Mass Spectr Rev 1: 29-62, 1982.
14. He JQ, Ruan J, Connett JE, Anthonisen NR, Pare PD and Sandford AJ. Antioxidant gene polymorphisms and susceptibility to a rapid decline in lung function in smokers. Am J Respir Crit Care Med 166: 323-328, 2002.
15. Huang MF, Lin WL and Ma YC. A study of reactive oxygen species in mainstream of cigarette. Indoor Air 15: 135-140, 2005.
16. Hudson VM. New insights into the pathogenesis of cystic fibrosis: pivotal role of glutathione system dysfunction and implications for therapy. Treat Respir Med 3: 353-363, 2004.
17. Li XY, Donaldson K, Rahman I and MacNee W. An investigation of the role of glutathione in increased epithelial permeability induced by cigarette smoke in vivo and in vitro. Am J Respir Crit Care Med 149: 1518-1525, 1994.
18. MacNee W. Pulmonary and systemic oxidant/antioxidant imbalance in chronic obstructive pulmonary disease. Proc Am Thorac Soc 2: 50-60, 2005.
19. Mannino DM, Buist AS, Petty TL, Enright PL and Redd SC. Lung function and mortality in the United States: data from the First National Health and Nutrition Examination Survey follow up study. Thorax 58: 388-393, 2003.
20. Meacher DM and Menzel DB. Glutathione depletion in lung cells by low-molecular-weight aldehydes. Cell Biol Toxicol 15: 163-171, 1999.
21. Park EM, Park YM and Gwak YS. Oxidative damage in tissues of rats exposed to cigarette smoke. Free Radic Biol Med 25: 79-86, 1998.
22. Pauwels RA, Buist AS, Calverley PM, Jenkins CR and Hurd SS. Global strategy for the diagnosis, management, and prevention of chronic obstructive pulmonary disease. NHLBI/WHO Global Initiative for Chronic Obstructive Lung Disease (GOLD) Workshop summary. Am J Respir Crit Care Med 163: 1256-1276, 2001.
23. Rahman I, Gilmour PS, Jimenez LA and MacNee W. Oxidative stress and TNF-alpha induce histone acetylation and NF-kappaB/AP-1 activation in alveolar epithelial cells: potential mechanism in gene transcription in lung inflammation. Mol Cell Biochem 234-235: 239-248, 2002.
24. Rahman I, Li XY, Donaldson K, Harrison DJ and MacNee W. Glutathione homeostasis in alveolar epithelial cells in vitro and lung in vivo under oxidative stress. Am J Physiol 269: L285-L292, 1995.
25. Rahman I and MacNee W. Role of oxidants/antioxidants in smoking-induced lung diseases. Free Radic Biol Med 21: 669-681, 1996.
26. Rahman I and MacNee W. Lung glutathione and oxidative stress: implications in cigarette smoke-induced airway disease. Am J Physiol 277: L1067-L1088, 1999.

27. Rahman I and MacNee W. Regulation of redox glutathione levels and gene transcription in lung inflammation: therapeutic approaches. Free Radic Biol Med 28: 1405-1420, 2000.
28. Ray S, Watkins DN, Misso NL and Thompson PJ. Oxidant stress induces gamma-glutamylcysteine synthetase and glutathione synthesis in human bronchial epithelial NCI-H292 cells. Clin Exp Allergy 32: 571-577, 2002.
29. Reddy S, Finkelstein EI, Wong PS, Phung A, Cross CE and van der Vliet A. Identification of glutathione modifications by cigarette smoke. Free Radic Biol Med 33: 1490-1498, 2002.
30. Smit-de Vries MP, van der Toorn M, Bischoff R and Kauffman HF. Resistance of quiescent and proliferating airway epithelial cells to H2O2 challenge. Eur Respir J 29: 633-642, 2007.
31. Tietze F. Enzymic method for quantitative determination of nanogram amounts of total and oxidized glutathione: applications to mammalian blood and other tissues. Anal Biochem 27: 502-522, 1969.
32. van der Toorn M, Slebos DJ, de Bruin H, Leuvenink H, Bakker S, Gans R, Koeter G, van Oosterhout A and Kauffman H. Cigarette smoke induced blockade of the mitochondrial respiratory chain switches lung epithelial cell apoptosis into necrosis. Am J Physiol Lung Cell Mol Physiol 2007.
33. Wang W and Ballatori N. Endogenous glutathione conjugates: occurrence and biological functions. Pharmacol Rev 50: 335-356, 1998.

Chapter 5

RESISTANCE OF QUIESCENT AND PROLIFERATING AIRWAY EPITHELIAL CELLS TO H_2O_2 CHALLENGE

Maria P. Smit-de Vries[1], Marco van der Toorn[2], Rainer Bischoff[1], Henk F. Kauffman[3].

[1]Department of Analytical Biochemistry, [2]Laboratory of Allergology and Pulmonary Diseases, [3]Groningen University Institute for Drug Exploration, University Medical Center Groningen, University of Groningen, PO Box 30001, 9700 RB, The Netherlands.

Eur Respir J. 2007 Apr;29(4):633-42. Epub 2007 Jan 24.

ABSTRACT

Alveolar epithelial cell injury and recovery are important in the pathogenesis of oxidant-induced lung damage. The alveolar cell line A549 was used to study responses of proliferating and quiescent cells in culture to time- and dose-dependent hydrogen peroxide (H_2O_2) challenges. Recovery was monitored after 24 h of incubation in fresh medium with 10% serum. The adherent cells were counted and the resistance and recovery of the attached cells was assessed by appearance, by measuring the number of viable, apoptotic and necrotic cells using fluorescent-activated cell sorting, and by determining the intracellular free thiol content. A549 cells recovered from a 1-h challenge with up to 1 mM H_2O_2 but could not sustain a more prolonged challenge (6 or 24 h) with 0.5 mM or 1.0 mM H_2O_2. These more severe conditions resulted in: loss of cells by detachment from the plate surface; reduced numbers of viable cells primarily due to necrosis; and a strong reduction of the intracellular free thiol content. Quiescent cells proved to be more sensitive to oxidative stress than proliferating cells. Intracellular free thiol levels apparently play a decisive role in cell survival, preferentially protecting proliferating cells.

INTRODUCTION

Oxidative stress is, on a cellular level, a combination of: an increase in reactive oxygen species (ROS) exposure; a decrease in antioxidant protection; and a failure to repair oxidative damage. Oxidative stress and the damage that may result from it have been implicated in a wide number of disease processes, including inflammation, neuronal degeneration and cancer (1, 2).

Lungs are exposed to high levels of oxygen and, in the case of smokers, high levels of radicals (10^{14} radicals per puff) are inhaled (3). Chronic obstructive pulmonary disease (COPD), which develops in 20% of smokers, encompasses both chronic bronchitis and emphysema, currently the fourth leading cause of death in the western world (4). Emphysema due to oxidative stress and continuous inflammation are major hallmarks of COPD (5). ROS, either directly from inhaled smoke and/or indirectly from inflammatory cells, may play a role in inflammation (6, 7) through the formation of lipid peroxidation products, the activation and phosphorylation of mitogen-activated protein kinases (MAPKs), and through the activation of redox-sensitive transcription factors, such as nuclear factor-κB and activator protein-1 (8).

Damage by ROS can induce apoptosis (programmed cell death) or necrosis of lung epithelial cells, which is followed by recovery and repair by the proliferation of residual cells (9). To obtain a detailed description of recovery of cells after an oxidative challenge, the response of the alveolar epithelial cell line A549 to various concentrations of hydrogen peroxide (H_2O_2) was investigated. The effect of H_2O_2 on pulmonary epithelial cells has been studied in earlier investigations using different concentrations and different culture conditions (10–15). However, the different abilities of proliferating and quiescent lung epithelial cells to recover from various concentrations of H_2O_2 have not been studied in a time-dependent manner. A549 is an adenocarcinoma cell line but is related to alveolar epithelial cells, as previous studies show (11, 16), and is known to be sensitive to morphological changes under different stress conditions (17).

Inflamed lung tissue of smokers is exposed to high H_2O_2 concentrations. This is reflected in elevated H_2O_2 levels in exhaled breath condensate of smokers or patients with exacerbated COPD, compared with ex-smokers or nonsmokers (18). However, the level of H_2O_2 found in healthy or in inflamed lung epithelial cells is unknown. The current authors hypothesized that resistance and recovery would be dependent not only on the concentration of the oxidative agent but also on the duration of exposure and on the quiescent or proliferating state of airway epithelial cells. To address the hypothesis of the present study, conditions under which A549 cultures were quiescent were established, in order to enable comparisons with proliferating cultures. To define the concentrations of H_2O_2 that lead to survival or irreversible damage, and to determine whether these concentrations are different for quiescent *versus* proliferating cells, the morphology of the adherent cells was assessed, as well as their viability and apoptotic and necrotic status.

Various studies describe H_2O_2 as an agent that may indirectly oxidize the free thiol groups of cysteines in peptides and proteins within different types of human cells. In order to sustain their antioxidant defense, cells regenerate the oxidized peptides or proteins *via* enzymatic reduction and by increasing the expression of antioxidant peptides and proteins. Two major components of thiol-reducing systems,

glutathione (GSH) and thioredoxin (TRX), have been identified from various kinds of tissue and appear to dominate the cellular thiol redox potential (19, 20). In the present article it is hypothesized that the resistance and recovery of airway epithelial cells to H_2O_2 is determined by the pool of reduced thiol components. Therefore, the effect of H_2O_2 on the redox state of airway epithelial cells was monitored by measuring the total free thiol content before and after a 24-h recovery period for both proliferating and quiescent cells.

MATERIALS AND METHODS

Study design

Basal conditions (no H_2O_2) were used as controls for the 1, 6 and 24 h of incubation of quiescent (nondividing) and proliferating cultures with 0, 0.1, 0.5 and 1.0 mM H_2O_2, followed by a 24-h recovery period (Fig. 1a). The parameters that were studied to assess resistance and recovery of A549 cultures were cell morphology, number of adherent cells, cell viability, apoptosis, necrosis and the intracellular free thiol content relative to the protein content (thiol redox state).

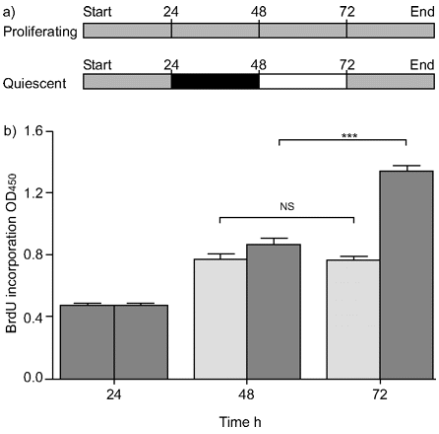

Figure 1. **a)** Experimental design to study the effect of hydrogen peroxide (H_2O_2) on proliferating and quiescent A549 cells. After 24 h of proliferation, the cultures were made quiescent by replacing the medium with serum-free medium and incubating for another 24 h. At time point "48", H_2O_2 (0.1, 0.5 or 1 mM) was added to the cultures and the cells were exposed to this oxidative stress for 1, 6 or 24 h. Exposure to H_2O_2 was stopped by either harvesting the cells for analysis or by replacing the medium containing H_2O_2 with fresh medium supplemented with 10% fetal calf serum (FCS; exemplified as time point "72"). Cultures were allowed to recover for another 24 h before analysis ("End"). Proliferating cell cultures were maintained in medium containing 10% FCS throughout the entire duration of the experiment. Control cultures were treated identically but without H_2O_2; ■: medium with 10% serum; ■: serum-free medium; □: incubation with 0.1, 0.5, or 1.0 mM H_2O_2 for 1, 6, or 24 h. **b)** Determination of the quiescent and proliferating state of A549 cell cultures. The increased optical density of a sample, measured at 450 nm (OD_{450}), correlates directly to the amount of bromodeoxyuridine (BrdU) that has been incorporated into the DNA. After 24 h in serum-free medium, the cultures were nondividing (quiescent; ■) throughout the duration of the oxidative stress period (until 72 h), while the cultures in serum-containing medium continued to proliferate (■). ***: $p<0.001$, n = 4, paired t-test; NS: nonsignificant.

A549 epithelial cells

The human alveolar type II epithelium-like adherent cell line, A549 (ATCC number CCL-185), was maintained in continuous culture, split ratio 1:5, at 37°C, 5% CO_2 in RPMI-1640 with L-glutamine (Cambrex, Verviers, Belgium), 20 $\mu g \cdot mL^{-1}$ gentamicin (Centafarm Services, Etten-Leur, the Netherlands) and 10% fetal calf serum (FCS; Cambrex). PCR tests for mycoplasma were negative.

Cell proliferation
Proliferation of A549 cells was measured using a cell proliferation ELISA assay (Amersham, Diegem, Belgium). Briefly, 5,000 cells were cultured in a 96-well microtitre plate at a final volume of 100 µL RPMI-1640 supplemented with 10% FCS and bromodeoxyuridine (BrdU; 10 µM) in each well. After 24 h the medium was removed. For quiescent cells, the cells were re-incubated overnight in serum-free medium and BrdU. Proliferating cells were maintained in medium with 10% FCS and BrdU. BrdU incorporation was measured at 450 nm after 24 h (both 10% FCS), 48 h (with and without 10% FCS) and 72 h (with and without 10% FCS), according to the manufacturer's instructions.

Challenge of proliferating or quiescent epithelial cells with H_2O_2
For proliferating cultures, $0.8x10^5$ A549 cells·well^{-1} were seeded in sterile 24-well culture dishes (Costar Europe Ltd, Badhoevedorp, the Netherlands) and incubated for 48 h in the presence of serum. For quiescent cultures, the medium with 10% FCS was removed after 24 h of incubation and the cultures were incubated for another 24 h in serum-free medium. Measures of 0.1, 0.5 and 1 mM H_2O_2 (Sigma, St Louis, MO, USA) were added to the cultures and incubated at 37°C for 1, 6 and 24 h. After incubation, the medium with H_2O_2 was removed and the cells were either washed with sterile PBS (Ca^{2+} and Mg^{2+} free; pH 7.4) and analyzed or washed and incubated for a further 24 h in fresh medium with 10% FCS (recovery phase). The remaining adherent cells were photographed using a Leica phase contrast microscope (5x; Leica Microsystems GmbH, Wetzlar, Germany) and Leica digital camera (Leica Camera AG, Solms, Germany) to assess the morphology of the cells in the cultures.

Flow cytometry
After H_2O_2 challenge and the subsequent recovery phase, cells were washed and the adherent cells were detached by a 5-min incubation with 0.05% trypsin in 0.53 mM ethylenediamine tetraacetic acid (EDTA; GIBCO, Invitrogen Company, Burlington, ON, Canada) at 37°C, collected, centrifuged (300*g* for 5 min) and stained for fluorescent-activated cell sorting (FACS) analysis of apoptosis (annexin V-FITC) and necrosis (propidium iodide (PI)). The Annexin V–FITC/PI Apoptosis/Necrosis Detection Kit was used according to the manufacturer's instructions (Immune Quality Products (IQP), Groningen, the Netherlands). Cell suspensions were analyzed on a FACS Calibur instrument with CellQuest software (Becton Dickinson, Heidelberg, Germany). For each sample, 10,000 events were collected and all analyses of whole cells were performed using appropriate scatter gates to exclude cellular debris and aggregates. Unlabeled cells and labeled basal cultures were used to set the limit of the quadrants; the boundaries of the first quadrant (annexin V^{low}-PI^{low}) were set to contain 100% of an unlabelled cell suspension and 95% of the labeled cells of basal cultures. These settings were used to analyze all labeled cell suspensions.

Total protein and free thiol measurements
Cells were washed and lysed by one freeze–thaw cycle in 200 µL of dematerialized water, and 50 µL were used for protein determination by the Bradford assay (21), using a bovine serum albumin (BSA; Sigma) standard curve. The samples were

measured at 595 nm in a Bio-Tek EL808 microplate reader (Beun de Ronde, Abcoude, the Netherlands). 12 mM 5,5'-dithiobis-(2-nitrobenzoic acid) (DTNB; Sigma) in 0.1 mM potassium phosphate buffer (pH 7.0; Merck, Haarlem, the Netherlands) was added to the rest of the lysed cells to a final concentration of 6 mM DTNB. After 10 min the samples were measured at 405 nm (22). The amount of free thiols was calibrated against a standard curve of L-cystein (Sigma).

Direct oxidation of BSA and L-cystein
In order to assess the potential for direct oxidation, 250 µM BSA in PBS containing 1 mM EDTA, or 250 µM L-cystein in PBS containing 1 mM EDTA, were incubated for 10 min in the dark with 0, 0.1, 0.5 and 1.0 mM H_2O_2. Before adding DTNB, the excess H_2O_2 was inactivated with catalase. To 100-µL aliquots of the reaction, DTNB was added to achieve a final concentration of 6 mM, and after a 5-min incubation the thiol content was measured at 405 nm. The amount of free thiols was calibrated against a standard curve of L-cystein.

Statistical analysis
The t-test for paired observations was used for comparisons between the basal (nonstressed) values and the values directly after H_2O_2 incubation and recovery, and for the comparisons between proliferating and quiescent values. Data are expressed as mean±SEM of four to six determinations per experiment. Each determination corresponded to one generation of A549. Differences were considered to be statistically significant when $P < 0.01$.

RESULTS

Proliferation and quiescence
The schematic outline of the experimental design is depicted in figure 1a. The incorporation of BrdU was measured to determine the state of quiescence and proliferation. Figure 1b shows that in the absence of serum, cultures become quiescent within 24 h and remain quiescent for 72 h.

Morphological analysis of A549 cells
The morphology of a cell is defined by its form and appearance, which can change in response to stimuli. Two clearly distinguishable morphologies could be discriminated (Fig. 2). Morphology I (MI) relates to cells that are flat with a visible nucleus (Fig. 2a), where each cell has a diameter of 20 µm and is contacting neighbouring cells. Morphology II (MII) shows rounded cells that have shrunk in size to 10 µm in diameter (Fig. 2b), often losing contact with neighbouring cells. In basal cultures at 80% confluence, 95±3% of cells (proliferating and quiescent) show MI (Fig. 2c). When cultures contained >15% rounded cells (Fig. 2d), the designation MII has been added to table 1, which summarizes the status of the cultures under various conditions of oxidative stress. When cultures contained >85% rounded cells (Fig. 2e) the cultures were considered to be entirely MII.

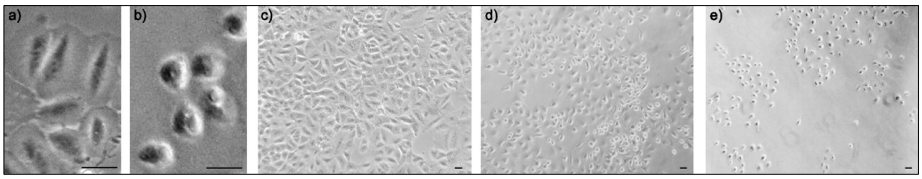

Figure 2. Observed morphological changes in A549 cells exposed to H_2O_2-mediated oxidative stress. a) Morphology I shows cells that are flat, on average 20 µm in size, and have cell–cell contact. b) Morphology II shows rounded cells that have shrunk in size to ~10 µm in diameter due to oxidative stress. Most cells have lost contact with neighbouring cells. Basal, unstressed cells are mainly of morphology I but contain 5±3% cells of morphology II (c). Both morphologies can occur in a single culture (d), as shown for quiescent cells that were exposed to 0.1 mM H_2O_2 for 6 h. Under severe stress situations (24 h of 0.5 mM H_2O_2) all remaining cells are of morphology II (e). Scale bars = 10 µm.

TABLE 1 Morphology of proliferating and quiescent 75–85% confluent A549 cultures after exposure to hydrogen peroxide (H_2O_2) and subsequent recovery, based on two different appearances (morphologies I and II; fig. 2)

H_2O_2 incubation	1 h		6 h		24 h	
	Pro	Qui	Pro	Qui	Pro	Qui
Basal morphology no H_2O_2	I	I	I	I	I	I
After 24 h incubation 10% serum	I	I	I	I	I	I
0.1 mM H_2O_2 after stress	I	I	I	I, II	I	I,II
0.1 mM H_2O_2 after recovery	I	I	I	I	I	I,II
0.5 mM H_2O_2 after stress	I	I, II	I, II	I, II	II	II
0.5 mM H_2O_2 after recovery	I	I	II	II	II	II
1.0 mM H_2O_2 after stress	I	I, II	I, II	II	II	II
1.0 mM H_2O_2 after recovery	I	I	II	II	II	II

Distinct morphologies are: large, flat cells with clear nuclei (I) and small, rounded cells (II). Both morphologies can exist in one culture, which is indicated in this table when one morphology exceeds 15% of the total cell number. Pro: proliferating cultures; Qui: quiescent cultures.

Most cells in the cultures incubated for 1 h with 0.5 mM and 1.0 mM H_2O_2 showed an overall MI indicative of healthy cells. As the time of incubation with 0.5 and 1.0 mM H_2O_2 increased from 1 to 6 and 24 hours, the overall culture changed from MI to MII. Once a culture contained >85% of MII cells it could not recover in 24 h to a MI culture. Judging by the number of cells that had changed to MII, quiescent cultures were slightly more sensitive to oxidative stress than proliferating cultures (table 1).

Cell numbers and cell viability

In MII cultures, a part of the cells became detached from the cell culture dish. The severity of H_2O_2 stress was assessed by counting the cells that remained attached to the plate (Fig. 3) and analyzing their viability by FACS (Fig. 4). As a control for the cell counts (and the loss of cells), the total protein content of basal and stressed cultures was measured. The results of the protein assay corresponded to the cell counts (data not shown). FACS analysis showed that the number of viable cells in basal cultures and in the presence of H_2O_2 is generally lower in quiescent than in proliferating cultures. After 1 h of stress, the proliferating cultures showed a decrease of cell numbers as compared with the unstressed cultures, along with an increase in apoptotic and necrotic cells. The quiescent cultures did not show this dose response after 1 h and contained even more viable cells after 1 h of 1.0 mM H_2O_2 challenge than the basal cultures. After 6 h of stress the cultures did not show a dose response, as the number of cells remained constant, but the number of necrotic cells increased with increasing H_2O_2 concentration. This was more profound for quiescent cultures.

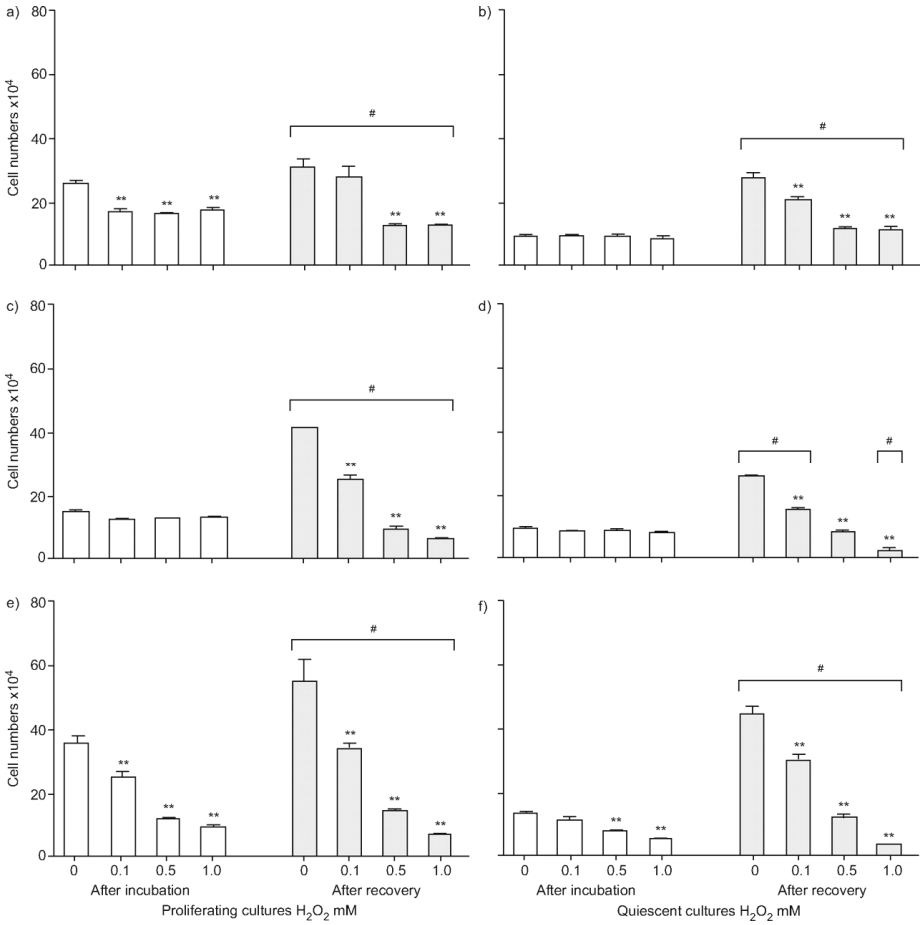

Figure 3. Effect of oxidative stress on cell numbers of proliferating and quiescent A549 cultures. Proliferating and quiescent A549 cell cultures were analyzed after 1 h (a and b), 6 h (c and d) and 24 h (e and f) of incubation with 0 (basal), 0.1, 0.5 and 1.0 mM hydrogen peroxide (H_2O_2;□) and after 24 h of recovery in the presence of serum-containing medium (■). $^{\#}$: $P < 0.01$ difference of cultures after recovery *versus* cell numbers directly after incubation, $n = 4$; **: $P < 0.01$ difference of stressed samples *versus* basal cell numbers

During the 24-h stress period a decrease of cell numbers corresponding to increasing H_2O_2 concentrations was observed, which was stronger for proliferating cultures than quiescent cultures. However, the residual adherent proliferating cells were more resilient to the challenge with 1.0 mM H_2O_2, as reflected by the higher number of viable cells than in quiescent cultures. After the recovery period, the basal cultures obviously had increased cell numbers. It was observed that epithelial cells recovered from exposure to increasing H_2O_2 concentrations after 1 h of incubation, as was

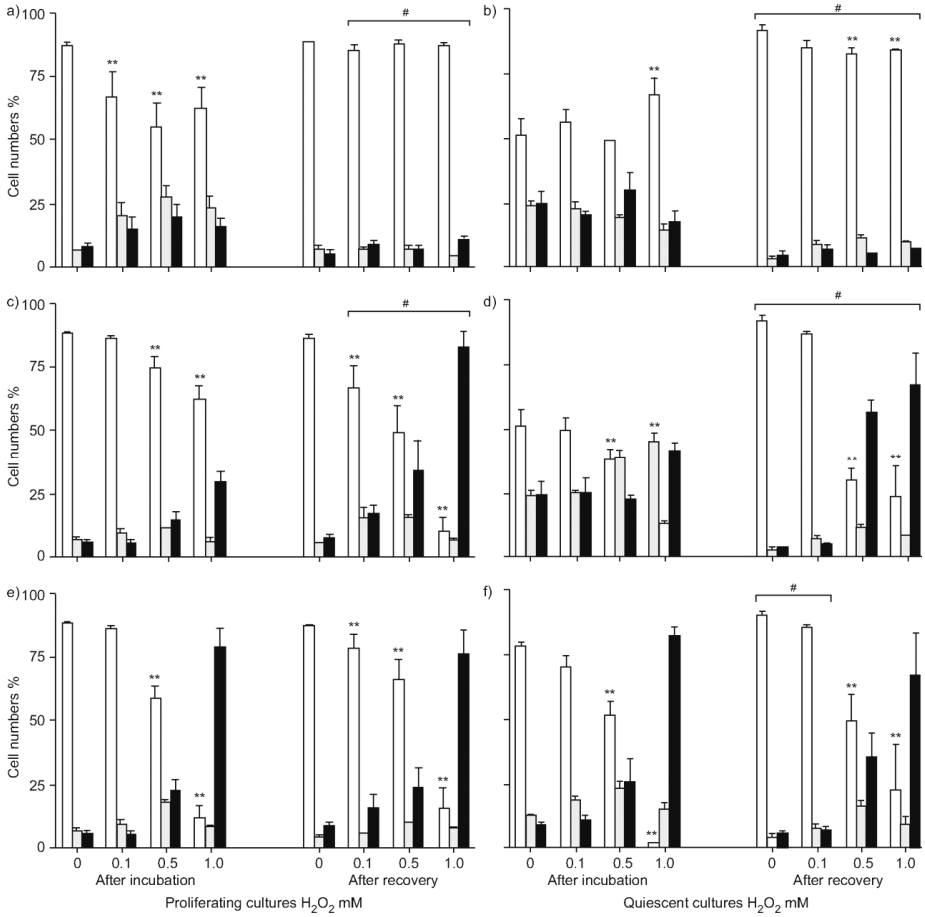

Figure 4. Percentage of viable, apoptotic and necrotic cells of proliferating and quiescent A549 cultures with hydrogen peroxide (H_2O_2) at various concentrations for increasing time periods (a and b, 1 h; c and d, 6 h; e and f, 24 h). Cells with polarized, intact membranes (annexin V^{low}-propidium iodide $(PI)^{low}$) were considered viable (□). Cells with distorted membranes (annexin V^{high}-PI^{low}) were considered early apoptotic (■). All cells with damaged membranes (annexin V^{low}-PI^{high} and annexin V^{high}-PI^{high}) were considered to be necrotic cells (■). Directly after incubation with H_2O_2 or after a 24-h recovery period, 10^4 cells·culture^{-1} were counted. #: $P < 0.01$ difference of cultures after recovery versus viable cells in cultures directly after incubation, $n = 5$; **: $P < 0.01$ difference of viable cells in stressed cultures versus basal viable cultures.

shown by the increased viability of the remaining adherent cells. Similarly, epithelial cells recovered from 0.1 mM H_2O_2 independent of exposure time. However, cell numbers did not reach the "recovered" unstressed culture values (except for the 1-h incubation of proliferating cells). During the recovery period after 6 h of stress, the cell numbers had decreased, as reflected by an increase of mainly necrotic cells. This increase in necrotic cells was more profound for quiescent cultures, especially after recovery from 0.5 mM H_2O_2. After recovery from 24 h of stress, the cell numbers

had increased slightly after 0.5 mM H_2O_2 and had decreased slightly after 1.0 mM H_2O_2. The difference between proliferating and quiescent cultures becomes clear when analyzing cell viability. The relative number of viable and necrotic cells did not change in proliferating cultures during the recovery period. However, in quiescent cultures after recovery from 1.0 mM H_2O_2 the remaining adherent cells were significantly more viable than directly after the stress.

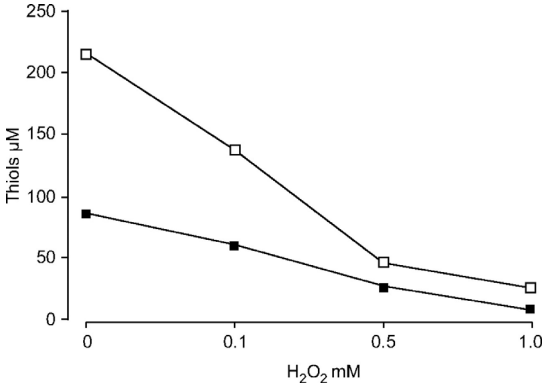

Figure 5. Direct oxidation of free thiol groups by hydrogen peroxide (H_2O_2). The effect of 15-min incubation of 250 µM of BSA (■) and L-cystein (□) with increasing concentrations of H_2O_2 in the absence of ultraviolet light and in the presence of ethylenediamine tetraacetic acid.

Oxidation of free (cellular) thiol groups

H_2O_2 is considered to be a precursor for radicals generated by mitochondrial metabolism. However, incubation of H_2O_2 in the presence of the metal chelator EDTA, and in the absence of light, showed a rapid oxidation of cysteines (Fig. 5). The ratio between oxidized and reduced thiol groups can be considered to be an indicator of oxidation. Since free thiol groups play an important role in the defense against oxidative stress, the effect of H_2O_2 on the total cellular level of free thiols was measured relative to the protein content (Fig. 6). Cellular oxidative stress by H_2O_2 was reflected in a lower free thiol/protein ratio of most cultures, compared with basal unstressed values. First of all it was observed that basal quiescent cultures had a higher thiol/protein ratio than proliferating basal cultures. However, the free thiol/protein ratio in quiescent cultures had diminished more strongly compared with the basal values, especially after 24 h of stress, in contrast to the proliferating cultures. After the recovery period, the quiescent cultures had returned to a proliferating state and subsequently showed lower free thiol/protein ratios. Based on these changed basal values, the quiescent cultures subjected to 0.1 mM H_2O_2 had recovered. At higher stress levels (0.5 and 1.0 mM), recovery of the thiol to protein ratio was still observed after 1 h of stress and, remarkably, even after 24 h of 0.5 mM H_2O_2. After the recovery period of proliferating cultures, it was observed that the cultures recovered from all H_2O_2 concentrations for 1 h of stress and from 0.1 mM H_2O_2 for 6 and 24 h.

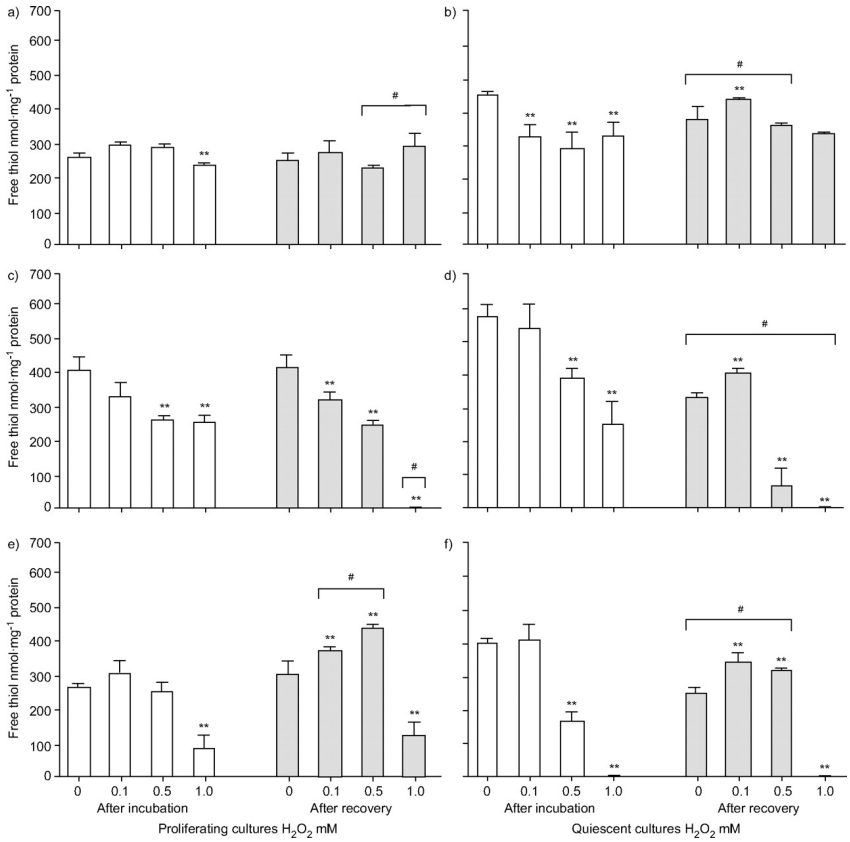

Figure 6. Oxidation of free thiols expressed as thiol/protein ratio (nmol·mg^{-1}) in A549 cells after exposure to hydrogen peroxide (H_2O_2) at various concentrations for increasing time periods. Proliferating and quiescent cell cultures were incubated with 0, 0.1, 0.5 and 1.0 mM H_2O_2 for 1 h (a and b), 6 h (c and d) and 24 h (e and f). The free thiol redox balance was calculated directly after challenge (□) and after recovery (■). $^{\#}$: $P < 0.01$ difference of cultures after recovery *versus* the thiol redox balance directly after incubation, $n = 4$; **: $P < 0.01$ difference of stressed cultures *versus* the basal cultures.

Remarkably, proliferating cultures showed a high free thiol/protein ratio after recovery from 6 and 24 h of 0.5 mM H_2O_2. Another remarkable result was the presence of free thiols after recovery from 24 h of 1.0 mM H_2O_2 in proliferating cultures, whereas in quiescent cultures these values had diminished to zero. This indicates that some of the remaining attached cells of MII morphology (mainly necrotic cells), had responded to the challenge by strongly increasing their thiol redox balance. By measuring the total GSH content (GSH and disulfide-bound GSH (GSSG)), similar results were obtained (data not shown). Cells entering necrosis have a low free thiol/protein ratio. Figure 7 relates the average thiol concentration in nmoles·mL to the percentage of necrotic cells. As the morphology is a visual indication of the stress level, figure 7 also includes the different morphologies. In

general, a trend was observed that cultures with a low thiol concentration contained the most MII cells and necrotic cells.

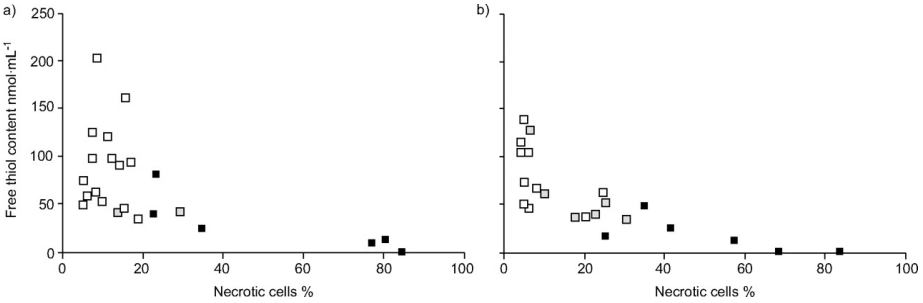

Figure 7. Correlation between the number of necrotic cells and the thiol content of A549 cultures. a) Proliferating and b) quiescent cultures were analyzed for free thiol content and percentage of necrotic cells after hydrogen peroxide (H_2O_2) administration and after a recovery period. All cells with damaged membranes (annexin V^{low}-propidium iodide $(PI)^{high}$ and annexin V^{high}-PI^{high}) were considered to be necrotic cells. The morphology of the cells in proliferating and quiescent cultures is shown: morphology I (□), cultures of mixed morphologies I and II (▩) and cultures with cells of morphology II (■; table 1).

DISCUSSION

H_2O_2 is one of the oxidants formed through oxygen metabolism and during inflammation as part of the oxidative burst. In studies on A549 and other cells, widely different conditions for H_2O_2 incubations have been used (10–13, 15); this prompted the current authors to perform a detailed time-dependent dose–response study and to define limits for in vitro resistance and recovery. For this purpose, cells were challenged with H_2O_2 at concentrations above levels implicated in cell signaling (50 μM) (23) but below levels that would lead to cell death within minutes (10 mM). In most described cases, A549 cells are maintained in medium containing serum up to the moment the experiment starts (11, 12, 15). When the cultures are not 100% confluent it is likely that they are still proliferating at the start of the experiment.

In the present report it has been demonstrated that differences in cell viability and the relative content of free thiols of basal quiescent and proliferating cultures influence their ability to recover from oxidative stress. FACS analysis (Fig. 4) showed that a higher percentage of cells are viable in basal proliferating cultures compared to quiescent cultures. This indicates that cells are in a more viable state when they are growing in a medium containing 10% serum.

In contrast, basal quiescent cultures maintained a higher protein/thiol ratio (Fig. 6). These basal quiescent cultures showed a remarkable decrease in free thiols after the addition of serum, indicating that in general the thiol redox balance of proliferating cells is lower. It is important to note that the observations argue against a simple correlation between the free thiol/protein ratio and antioxidant defense during stress-free conditions. Quiescent cells have a higher thiol redox balance than proliferating cells but are nevertheless more sensitive to oxidative stress. Differences are most prominent after 6- and 24-h exposures, especially to 0.5 mM H_2O_2 and

subsequent recovery, where it was observed that quiescent cultures are more vulnerable (figs 3, 4 and 6).

When the proliferating and quiescent cultures were stressed with H_2O_2 and subsequently incubated for recovery, morphological differences and changes in cell numbers were observed. These differences prompted the current authors to investigate whether they could be related to a different physiology of quiescent cultures opposed to proliferating cultures. Furthermore, a causal relation was found between cell morphology, free thiol content and the number of necrotic cells for proliferating cultures, and it was also found that this correlation was less strong for quiescent cultures (Fig. 7). These differences were not influenced by the thiol content of the external medium. The thiol content of the medium was measured prior to the addition of H_2O_2 and it was found that the thiol content was not significantly different in the medium of proliferating cultures compared with that of quiescent cultures (data not shown).

The present data help define a threshold of H_2O_2 stress up to which A549 cells can recover when supplemented with serum-containing medium. All cultures could recover from short-term (1 h) exposure to 0.1–1.0 mM H_2O_2, or from long-term exposure (up to 24 h) to low H_2O_2 (0.1 mM) concentrations. However, cells underwent irreversible changes after incubation times longer than 1 h with higher H_2O_2 concentrations (0.5–1.0 mM), as indicated by a modified morphology (cell shrinkage), decreased cell viability and an increased number of cells detaching from the plate surface. This is consistent with previous findings in the literature (14). This recovery from oxidative stress may mimic, to some extent, the situation in vivo, where epithelial cells may be exposed to oxidative stress followed by a recovery period (*e.g.* after a smoking episode).

It is of interest to study how both quiescent and proliferating epithelial cells cope with oxidative stress, as there are indications that cells start to proliferate upon lung damage. When the lungs are damaged, both quiescent and proliferating cells are likely to respond differently to oxidative stress. It has been reviewed that upon tissue damage, growth factors are responsible for proliferation and remodeling of airway epithelium to repair the damage in COPD (24). However, reliable data on the in vivo rate of proliferation in the human lung is not available. An indication of the proliferation rate is derived from literature on pulmonary gene therapy studies in mouse lungs, where 28 days after transient transfection with an adenoviral vector the expressed transfected gene product had disappeared (25). In current experiments described in the literature, it is not always clear whether the cells were incubated with or without serum previous to the experiment.

In vitro quiescent cultures form a homogenous population of cells in the same state, facilitating analysis. Mammalian cells deprived of serum stop proliferating and become arrested, usually between mitosis and S-phase, in a specialized, nonproliferating G0 state, called quiescence. It is known that the cellular redox potential varies during the lifespan of a cell. For example, the cellular redox state has characteristic set points depending on whether cells are quiescent, proliferating, differentiating or apoptotic (26, 27). The current authors hypothesize that these differences explain in part the sensitivity of quiescent cultures to oxidative stress. The proliferating cultures are heterogeneous, as cells are in different phases of mitosis, all responding more or less strongly to oxidative stress. However, the cells

in the homogenous quiescent cultures will all respond similarly, marking the sensitivity and the lack of recovery of the cultures after 6 h of 0.5 mM H_2O_2.

The lung epithelium in vivo is constantly exposed to high concentrations of oxygen and other oxidants from endogenous and exogenous sources, especially during smoking (28). ROS causes cellular injury *via* reactions leading to more reactive species, such as hydroxyl radicals and lipid peroxidation products. A source of ROS is H_2O_2, which is known to cause oxidative stress through depletion of free thiols. H_2O_2 is directly generated during cigarette smoking (~22–37 μg H_2O_2 per aqueous tar extract from one cigarette) (29). Additionally, H_2O_2 is produced within epithelial cells as a result of mitochondrial metabolism, reduced nicotinamide adenine dinucleotide phosphate oxidase (14), glycollate and monoamine oxidase activity (23), and by superoxide dismutase in the cytoplasm. In this report it has been shown that H_2O_2 is able to directly oxidize free thiols without the need for cellular metabolism as exemplified by the in vitro oxidation of BSA and L-cystein (Fig. 5).

In studies conducted by the current authors, A549 cells went into a state of necrosis without any pronounced signs of apoptosis, which led to a study of the activation state of caspase-3, a cysteine proteinase, during a selected number of experimental conditions. Interestingly, there was no indication of caspase-3 activation at 0.5 or 1 mM H_2O_2 after long-term incubation, as studied by Western blotting (data provided by D.J. Slebos (Groningen, the Netherlands), not shown), which may explain the lack of apoptosis. Although not proven, it is likely that the active site cysteine in caspase-3 was directly oxidized by H_2O_2 or its metabolites, thus inactivating the enzyme (30, 31). This is in line with results reported here that H_2O_2 can directly oxidize free thiol groups, *e.g.* in BSA and cysteine.

CONCLUSION

Quiescent cultures appear to be more sensitive than proliferating cultures, especially to prolonged incubations with higher H_2O_2 concentrations. The aim of the present study was to define the upper concentration limit of H_2O_2 from which quiescent and proliferating cells can recover when returned to serum-containing medium, for the purpose of future studies on the analysis of proteins involved in the recovery process. This upper concentration limit appears to be 0.1 mM H_2O_2, as all cultures were able to recover from this concentration. Another important factor is the time of exposure, as incubations with 0.5 and 1.0 mM H_2O_2 for >1 h resulted in loss of attached cells and an increase in necrotic cells. In proliferating cultures there are a limited number of cells remaining viable after severe oxidative stress, and it appears that they have adapted to this condition by increasing their thiol/protein ratio considerably after recovery.

Many regulatory proteins contain critical cysteine residues that are sensitive to: oxidation to sulfenic acids; the formation of intra- and intermolecular disulfides; or mixed disulfides with glutathione (32). In general, free (reduced) thiol groups play an important role in the defense against oxidative stress and healthy cells are generally found in a reduced state, having a large excess of reduced compared with oxidized thiols. The maintenance of this state is critical and is dependent on the equilibrium between oxidized and reduced thiols. The current authors are studying how the free thiols in proteins of cultures react to these borderline conditions of

oxidative stress, in order to elucidate protective mechanisms that aid stress resistance and to correlate this to recovery or cell death. These studies may elucidate the inter-individual differences in susceptibility to oxidation-mediated tissue damage and inflammation, as is observed in the 20% of smokers that develop chronic obstructive pulmonary disease, whereas the remaining 80% do not show pulmonary limitations.

ACKNOWLEDGEMENTS

The authors appreciate the work done by D.J. Slebos (Groningen, the Netherlands), the excellent technical assistance of H.G. de Bruin (Groningen, the Netherlands) and the financial support of the Jan Kornelis de Cock Foundation (Groningen, the Netherlands).

REFERENCES

1. Floyd RA. Role of oxygen free radicals in carcinogenesis and brain ischemia. FASEB J 1990;4:2587–2597.
2. Finkel T. Oxidant signals and oxidative stress. Curr Opin Cell Biol 2003;15:247–254.
3. Pryor WA. Cigarette smoke radicals and the role of free radicals in chemical carcinogenicity. Environ Health Perspect 1997;105: Suppl. 4 875–882.
4. Viegi G, Scognamiglio A, Baldacci S, Pistelli F, Carrozzi L. Epidemiology of chronic obstructive pulmonary disease (COPD). Respiration 2001;68:4–19.
5. Rutgers SR, Postma DS, ten Hacken NH, et al. Ongoing airway inflammation in patients with COPD who do not currently smoke. Thorax 2000;55:12–18.
6. Maestrelli P, Saetta M, Mapp CE, Fabbri LM. Remodeling in response to infection and injury. Airway inflammation and hypersecretion of mucus in smoking subjects with chronic obstructive pulmonary disease. Am J Respir Crit Care Med 2001;164:S76–S80.
7. Boots AW, Haenen GRMM, Bast A. Oxidant metabolism in chronic obstructive pulmonary disease. Eur Respir J 2003;22: Suppl. 46 14s–27s.
8. Rahman I. Oxidative stress in pathogenesis of chronic obstructive pulmonary disease: cellular and molecular mechanisms. Cell Biochem Biophys 2005;43:167–188.
9. Rutgers SR, Timens W, Kauffman HF, Postma DS. Markers of active airway inflammation and remodelling in chronic obstructive pulmonary disease. Clin Exp Allergy 2001;31:193–205.
10. Rahman I, Li XY, Donaldson K, Harrison DJ, MacNee W. Glutathione homeostasis in alveolar epithelial cells in vitro and lung in vivo under oxidative stress. Am J Physiol 1995;269:L285–L292.
11. Anseth JW, Goffin AJ, Fuller GG, Ghio AJ, Kao PN, Upadhyay D. Lung surfactant gelation induced by epithelial cells exposed to air pollution or oxidative stress. Am J Respir Cell Mol Biol 2005;33:161–168.
12. Rahman I, Mulier B, Gilmour PS, et al. Oxidant-mediated lung epithelial cell tolerance: the role of intracellular glutathione and nuclear factor-B. Biochem Pharmacol 2001;62:787–794.

13. Rahman I, Gilmour PS, Jimenez LA, MacNee W. Oxidative stress and TNF-induce histone acetylation and NF-B/AP-1 activation in alveolar epithelial cells: potential mechanism in gene transcription in lung inflammation. Mol Cell Biochem 2002;234–235:239–248.
14. Dandrea T, Hellmold H, Jonsson C, et al. The transcriptosomal response of human A549 lung cells to a hydrogen peroxide-generating system: relationship to DNA damage, cell cycle arrest, and caspase activation. Free Radic Biol Med 2004;36:881–896.
15. Lehtonen ST, Markkanen PMH, Peltoniemi M, Kang SW, Kinnula VL. Variable overoxidation of peroxiredoxins in human lung cells in severe oxidative stress. Am J Physiol Lung Cell Mol Physiol 2005;288:L997–L1001.
16. Lannan S, Donaldson K, Brown D, MacNee W. Effect of cigarette smoke and its condensates on alveolar epithelial cell injury in vitro. Am J Physiol 1994;266:L92–L100.
17. Kauffman HF, Tomee JF, van de Riet MA, Timmerman AJ, Borger P. Protease-dependent activation of epithelial cells by fungal allergens leads to morphologic changes and cytokine production. J Allergy Clin Immunol 2000;105:1185–1193.
18. Dekhuijzen PN, Aben KK, Dekker I, et al. Increased exhalation of hydrogen peroxide in patients with stable and unstable chronic obstructive pulmonary disease. Am J Respir Crit Care Med 1996;154:813–816.
19. Arner ES, Holmgren A. Physiological functions of thioredoxin and thioredoxin reductase. Eur J Biochem 2000;267:6102–6109.
20. Rahman I, MacNee W. Lung glutathione and oxidative stress: implications in cigarette smoke-induced airway disease. Am J Physiol 1999;277:L1067–L1088.
21. Bradford MM. A rapid and sensitive method for the quantitation of microgram quantities of protein utilizing the principle of protein-dye binding. Anal Biochem 1976;72:248–254.
22. Deakin H, Ord MG, Stocken LA. 'Glucose 6-phosphate-dehydrogenase' activity and thiol content of thymus nuclei from control and X-irradiated rats. Biochem J 1963;89:296–304.
23. Halliwell B, Clement MV, Long LH. Hydrogen peroxide in the human body. FEBS Lett 2000;486:10–13.
24. Chung KF. Cytokines in chronic obstructive pulmonary disease. Eur Respir J 2001;18: Suppl. 34 50s–59s.
25. Koehler DR, Sajjan U, Chow YH, et al. Protection of Cftr knockout mice from acute lung infection by a helper-dependent adenoviral vector expressing Cftr in airway epithelia. Proc Natl Acad Sci USA 2003;100:15364–15369.
26. Shackelford RE, Kaufmann WK, Paules RS. Oxidative stress and cell cycle checkpoint function. Free Radic Biol Med 2000;28:1387–1404.
27. Schafer FQ, Buettner GR. Redox environment of the cell as viewed through the redox state of the glutathione disulfide/glutathione couple. Free Radic Biol Med 2001;30:1191–1212.
28. Cross CE, van der Vliet A, O'Neill CA, Louie S, Halliwell B. Oxidants, antioxidants, and respiratory tract lining fluids. Environ Health Perspect 1994;102: Suppl. 10 185–191.

29. Yan F, Williams S, Griffin GD, et al. Near-real-time determination of hydrogen peroxide generated from cigarette smoke. J Environ Monit 2005;7:681–687.
30. Hampton MB, Stamenkovic I, Winterbourn CC. Interaction with substrate sensitises caspase-3 to inactivation by hydrogen peroxide. FEBS Lett 2002;517:229–232.
31. Baker A, Santos BD, Powis G. Redox control of caspase-3 activity by thioredoxin and other reduced proteins. Biochem Biophys Res Commun 2000;268:78–81.
32. Fratelli M, Demol H, Puype M, et al. Identification by redox proteomics of glutathionylated proteins in oxidatively stressed human T lymphocytes. Proc Natl Acad Sci USA 2002;99:3505–3510.

Chapter 6

CYCLOSPORIN A-INDUCED OXIDATIVE STRESS IS NOT THE CONSEQUENCE OF AN INCREASE IN MITOCHONDRIAL MEMBRANE POTENTIAL

Marco van der Toorn[1], Henk F. Kauffman[2], Margaretha van der Deen[3], Dirk-Jan Slebos[4], Gerard H. Koëter[4], Rijk O. B. Gans[5], Stephan J. L. Bakker[5]

[1]Laboratory of Allergology and Pulmonary Diseases, [2]Groningen University Institute for Drug Exploration, [3]Department of Medical Oncology, [4]Department of Pulmonary diseases, [5]Department of Internal Medicine, University Medical Center Groningen, University of Groningen, PO Box 30001, 9700 RB, The Netherlands.

FEBS J. 2007 Jun;274(12):3003-12. Epub 2007 May 17.

ABSTRACT

Cyclosporin A induces closure of the mitochondrial permeability transition pore. We aimed to investigate whether this closure results in concomitant increases in mitochondrial membrane potential ($\Delta\psi_m$) and the production of reactive oxygen species. Fluorescent probes were used to assess $\Delta\psi_m$ (JC-1, 5,5',6,6'-tetrachloro-1,1',3,3'-tetraethyl-benzimidazolyl-carbocyanine iodide), reactive oxygen species [DCF, 5- (and 6)-chloromethyl-2',7'-dichlorodihydrofluorescein diacetate, acetyl ester] and [Ca^{2+}] [Fluo-3, glycine N-[4-[6-[(acetyloxy)methoxy]-2,7-dichloro-3-oxo-3H-xanthen-9-yl]-2-[2-[2-[bis[2-[(acetyloxy)methoxy]-2-oxyethyl]amino]-5-methyl-phenoxy]ethoxy]phenyl]-N-[2-[(acetyloxy)methoxy]-2-oxyethyl]-(acetyloxy)methyl ester] in human kidney cells (HK-2 cells) and in a line of human small cell carcinoma cells (GLC4 cells), because these do not express cyclosporin A-sensitive P-glycoprotein. We used transfected GLC4 cells expressing P-glycoprotein as control for GLC4 cells. NIM811 (N-methyl-4-isoleucinecyclosporin) and PSC833 (SDZ-PSC833) were applied as selective mitochondrial permeability transition pore and P-glycoprotein blockers, respectively. To study the effect of cyclosporin A on mitochondrial function, we isolated mitochondria from fresh pig livers. Cyclosporin A and PSC833 induced a more than two-fold increase in JC-1 fluorescence in HK-2 cells, whereas NIM811 had no effect. None of the three substances induced a significant increase in JC-1 fluorescence in GLC4 cells. Despite this, cyclosporin A, NIM811 and PSC833 induced a 1.5-fold increase in DCF fluorescence ($P < 0.05$) and a two-fold increase in Fluo-3 fluorescence ($P < 0.05$). Studies in isolated mitochondria showed that blockage of mitochondrial permeability transition pores by cyclosporin A affected neither $\Delta\psi_m$, ATP synthesis, nor respiration rate. The mitochondrial permeability transition pore blockers cyclosporin A and NIM811, but also the non-mitochondrial permeability transition pore blocker PSC833, induced comparable degrees of reactive oxygen species production and cytosolic [Ca^{2+}]. Neither mitochondria, effects on P-glycoprotein nor inhibition of calcineurin therefore play a role in cyclosporin A-induced oxidative stress and disturbed Ca^{2+} homeostasis.

INTRODUCTION

Immunosuppressive treatment with cyclosporin A (CsA) is accompanied by accelerated atherosclerosis and fibrosis, which contribute to the development of chronic transplant dysfunction (1). It has been suggested that reactive oxygen species (ROS) play an important underlying role (2–4). Different studies have shown that CsA is able to increase levels of superoxide anion (O_2^{-}), hydrogen peroxide, malondialdehyde, and thiobarbituric acid reactive substances (5,6). Mitochondrial enzymes with antioxidative properties, including superoxide dismutase, catalase, and glutathione peroxidase, become upregulated upon exposure to CsA (7). It is evident that CsA induces oxidative stress, but its origin remains speculative.

Mitochondria represent a major source of intracellular ROS, and play a crucial role in cellular Ca^{2+} homeostasis, which affects various cell signaling pathways (8). The primary function of mitochondria is production of ATP, a process linked to the action of the electron transfer chain. Normally, electrons supplied by metabolic fuel (NADH and $FADH_2$) are transferred along the electron transfer chain to oxygen. Optimally, the terminal enzyme of the electron transfer chain, cytochrome c oxidase, binds oxygen until it has accepted four electrons, when it is released as water. Most of the energy released during the transfer of these electrons is used to pump protons from the mitochondrial matrix towards the inner membrane space, thereby creating a proton gradient. The energy stored in the proton gradient is used to drive the process of oxidative phosphorylation of ADP to ATP. When the intramitochondrial ADP concentration drops (e.g. under conditions of low energy demand), the proton gradient will rise as a consequence of decreased consumption (9–12). This increased proton gradient impairs the flow of electrons along the electron transfer chain, which results in accumulation of electrons along the electron transfer chain (13). This results in an increased likelihood of leakage of electrons from the chain, with increased ROS production as a consequence (14).

One mechanism by which the mitochondrial membrane potential ($\Delta\psi_m$) can decrease is through opening of the mitochondrial permeability transition pore (MPTP) (15–17). CsA is well known as an inhibitor of calcineurin and P-glycoprotein, but it is also a strong inhibitor of the MPTP (18,19). Indeed, it has been suggested that in several cell types CsA prevents opening of the MPTP, thereby leading to an increased $\Delta\psi_m$ (17,20). The CsA analog N-methyl-4-isoleucine-cyclosporin (NIM811) is also known as an inhibitor of MPTP, and to lead to an increase in $\Delta\psi_m$ (21). Fluorescent probes used to assess $\Delta\psi_m$ are pumped out of cells by P-glycoprotein (22). Thus, probe accumulation caused by CsA may result from effects on P-glycoprotein as well as effects on MPTP. The CsA analog SDZ-PSC833 (PSC833) may serve as a useful control substance in this context, because it is an inhibitor of P-glycoprotein rather than MPTP, and is devoid of calcineurin-inhibiting properties (23).

We hypothesized that an increase in steady-state $\Delta\psi_m$ underlies increased ROS production in association with CsA exposure. We set out to investigate the effects of CsA on $\Delta\psi_m$ in relation to the production of ROS, with NIM811 and PSC833 as control.

MATERIALS AND METHODS

Chemicals
The cyclosporin analogs CsA, NIM811 and PSC833 were kindly provided by Novartis (Basel, Switzerland). DNP was obtained from Merck & Co., Inc. (Haarlem, the Netherlands), and sodium succinate, ATP, ADP, KCN and oligomycin were obtained from Sigma-Aldrich Chemie B.V. (Zwijndrecht, the Netherlands). Vincristine sulfate was purchased from Abic Ltd (Netanya, Israel). JC-1, DCF and Fluo-3 were purchased from Molecular probes Europe BV (Leiden, the Netherlands).

Cell culture
Human-derived renal proximal tubular epithelial cells (HK2), obtained from the ATCC (Manassas, VA, USA) were grown in keratinocyte serum-free medium (Gibco-BRL, Breda, the Netherlands), supplemented with 5 $ng \cdot ml^{-1}$ epidermal growth factor, 40 $\mu g \cdot ml^{-1}$ bovine pituitary extract and 20 $\mu g \cdot ml^{-1}$ gentamicin (Centafarm Services, EttenLeur, the Netherlands). The human small cell lung cancer (GLC4) cell line and GLC4 cell line transfected the human multidrug resistance 1 gene were kindly provided by EGE de Vries (Department of Medical Oncology, University Medical Center Groningen, the Netherlands). The cells were grown in RPMI-1640 with 25 mM Hepes and L-glutamine (BioWitthaker, Verviers, Belgium), supplemented with 10% heat-inactivated fetal bovine serum (BioWitthaker) and 20 $\mu g \cdot ml^{-1}$ gentamicin. The multidrug resistance 1-transfected GLC4 cell line expressing P-glycoprotein was grown with a drug pressure of vincristine sulfate (50 nM) until 1 week before the experiments. All cells were grown in 75 cm^2 plastic flasks (Costar, Cambridge, MA) at 37 °C in an atmosphere of 5% CO2.

Immunocytochemical staining of P-glycoprotein
Cytospins of GLC4 and GLC4/P-glycoprotein cells were incubated for 1 min with hematoxylin for staining of nuclei. To assess the localization of P-glycoprotein expression in the membranes, stained cells were evaluated by immunohistochemistry. Monoclonal antibody to P-glycoprotein (C219) (Alexis, San Diego, CA) was used to detect P-glycoprotein expression. An irrelevant antibody was used as isotype control. GLC4 cells without expression of P-glycoprotein did not show P-glycoprotein staining. GLC4 cells expressing P-glycoprotein showed strong and homogeneous membrane-bound staining of P-glycoprotein.

Flow cytometry analyses
Cells at 90% confluence were washed with Hank's buffered saline solution (UMCG, Groningen, the Netherlands) and cultured for 24 h in serum-free medium. After starvation, the cells were resuspended in NaCl/Pi, loaded with a fluorescent probe,

and incubated for 20 min at room temperature in the dark. At the end of the incubation period, cells were washed twice with NaCl/Pi. The loaded cells were incubated for 1 h with different concentration of CsA, NIM811 and PSC833 in an incubator, and analyzed using a FACSCalibur flow cytometer (Becton Dickinson Medical Systems, Sharon, MA).

Isolation of mitochondria from pig liver

Mitochondria were isolated from fresh pig liver using a commercial mitochondria isolation kit (Sigma-Aldrich Chemie B.V.). Briefly, fresh liver tissue (obtained within 1 h of sacrifice) was washed twice with two volumes of extraction buffer (10 mM Hepes, 200 mM mannitol, 70 mM sucrose and 1 mM EGTA, pH 7.5). The liver was cut into small portions and homogenized with 10 volumes of extraction buffer containing 2 mg/ml delipidated BSA (Sigma-Aldrich Chemie B.V.), using a pestle and glass tube. The homogenate was centrifuged at 600 g for 5 min using an Eppendorf centrifuge 5417R, rotor F45-30-11, Eppendorf AG, Hamburg, Germany (all centrifugation carried out using same centrifuge and rotor types). The supernatant was collected and centrifuged at 11 000 g for 10 min. The supernatant was then removed, and the pellet was resuspended in 10 volumes of extraction buffer and centrifuged at 600 g for 5 min. Finally, the supernatant was centrifuged at 11 000 g for 10 min. The supernatant was removed, and the isolated mitochondria were resuspended in respiratory buffer (120 mM KCl, 5 mM K_2PO_4, 3 mM Hepes, 1 mM EGTA, brought to pH 7.2 with 5 mM KH_2PO_4). Mitochondrial protein was estimated by the Bradford method (Bio-Rad Laboratories, Veenendaal, the Netherlands) according to the manufacturer's instructions. To stabilize the mitochondria, respiration buffer was supplemented with 0.2% delipidated BSA (m/v).

Mitochondrial swelling assay

Mitochondria were resuspended in respiration buffer (without EGTA) containing 4 mg mitochondrial protein/ml. The mitochondria were energized with succinate (final concentration 5 mM). The suspension was pipetted into the wells (100 μL per well) of a 96-well polystyrene microtiter plate (Greiner Bio-One B.V., Alphen aan den Rijn, the Netherlands). CsA and its analogs (0.1–10 μM) were added. Five minutes after addition of the CsA and its analogs, $CaCl_2$ (final concentration 1 mM) was added to each well. Immediately after addition of $CaCl_2$, the plate was measured in an EL808 spectrophotometer using a 550 nm filter (Bio-Tek Instruments, Abcoude, the Netherlands). Measurements were repeated every 30 s for a period of 30 min. Measurements were performed at room temperature.

$\Delta\psi_m$ in isolated mitochondria
Isolated mitochondria were resuspended (final protein concentration 100 μg·ml^{-1}) in 1 mL of respiration buffer. Mitochondria were stained with 0.2 μg·ml^{-1} JC-1 probe for 10 min at 37 °C according to the manufacturer's instruction. State III respiration was reached after addition of succinate (final concentration 5 mM) and ADP (final concentration 1 mM). The loaded mitochondria were then suspended in the wells of a 96-well fluorescent plate (Costar) and exposed to 10 μM CsA for 15 min at 37 °C. DNP (final concentration 20 μM) served as negative control. $\Delta\psi_m$ was measured with an excitation wavelength of 485 nm through a 590 nm bandpass filter in a FL500 fluorescent plate reader (Bio-Tek Instruments).

Luminescence monitoring of mitochondrial ATP
Mitochondria (final protein concentration 100 μg·ml^{-1}) were resuspended in respiration buffer. All experiments were done in state III respiration. DNP (final concentration 20 μM) and state IV respiration served as negative controls. Mitochondria were incubated for 15 min at 37 °C. At the end of the incubation period, ATP synthesis was stopped by freezing the samples in) 196 °C nitrogen. Mitochondrial ATP levels were measured using the Enliten ATP assay (Promega, Leiden, the Netherlands) and a Berthold microplate luminometer (Berthold Detection Systems GmbH, Pforzheim, Germany).

Mitochondrial respirometry
Mitochondria (final concentration 2 mg·ml^{-1}) were resuspended in a 1 mL respiration chamber with air-saturated respiration buffer (209 μM O_2). CsA (final concentration 10 μM) was preincubated for 5 min. State III respiration was started after addition of succinate (final concentration 5 mM) and ADP (final concentration 0.5 mM). Mitochondrial respiration was measured at 37 °C with a commercial Clark-type oxygen electrode (U-53002-50; Cole-Parmer, Schiedam, the Netherlands) covered with a high-sensitivity membrane (Yellow Springs Instruments Co., Inc., Ohio, USA), continuously registered with the Oxystat interface and STRATHKELVIN 928 oxygen system software (U-53002-05; Cole-Parmer).

Mitochondrial ROS production
Mitochondrial ROS were measured using the procedure of Garcia-Ruiz et al. (39). Briefly, production of ROS was monitored using the fluorescent probe DCF. Freshly isolated mitochondria (100 μg·ml^{-1}) were incubated in respiratory buffer (without EGTA) with 1 μM DCF in the absence or presence of 1 mM Ca^{2+}. The effects of CsA (10 μM) were tested under conditions of state III respiration. Antimycin A was used to stimulate maximal ROS production by inhibiting complex III of the electron transfer chain. The mitochondrial suspension was incubated for 15 min at 37 °C. DCF fluorescence was monitored with an excitation

wavelength of 485 nm through a 530 nm bandpass filter in an FL500 fluorescent plate reader.

Statistical analysis

Data were analyzed using PRISM 4 for Windows (GraphPad Software, Inc., San Diego, CA). Two-way ANOVA was used for assessment of dose–response experiments (Figs 2 and 4). Comparisons between different experimental groups were performed with the Newman–Keuls multiple comparison test (Figs 1, 3 and 5). $P < 0.05$ was considered significant. Results are presented as mean (± SEM) unless otherwise mentioned.

RESULTS

Closure of the MPTP and $\Delta\Psi_m$

Human kidney (HK-2) cells are known to express P-glycoprotein (24,25). Both CsA and PSC833 induced a dose-dependent increase in 5,5',6,6'-tetrachloro-1, 1', 3,3'-tetraethyl-benzimidazolyl-carbocyanine iodide (JC-1) fluorescence in these cells (Fig. 1). NIM811, however, did not induce a significant increase in JC-1 fluorescence.

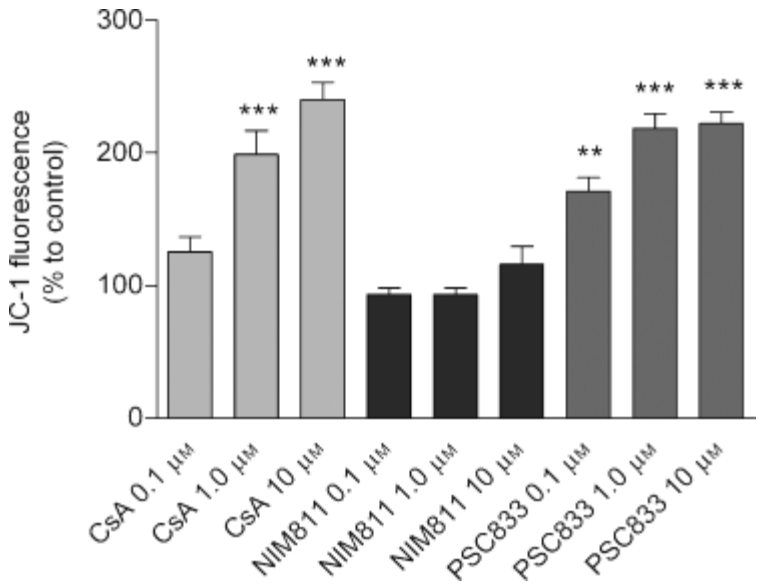

Figure 1. Effect of CsA and its analogs on mitochondrial membrane potential in HK-2 cells. JC-1 probe (5 $\mu g \cdot mL^{-1}$) was used to study mitochondrial membrane potential. Data are expressed as mean value ± SEM, and refer to three experiments. *$P < 0.05$ versus control, **$P < 0.01$ versus control, ***$P < 0.001$ versus control by Newman–Keuls multiple comparison test.

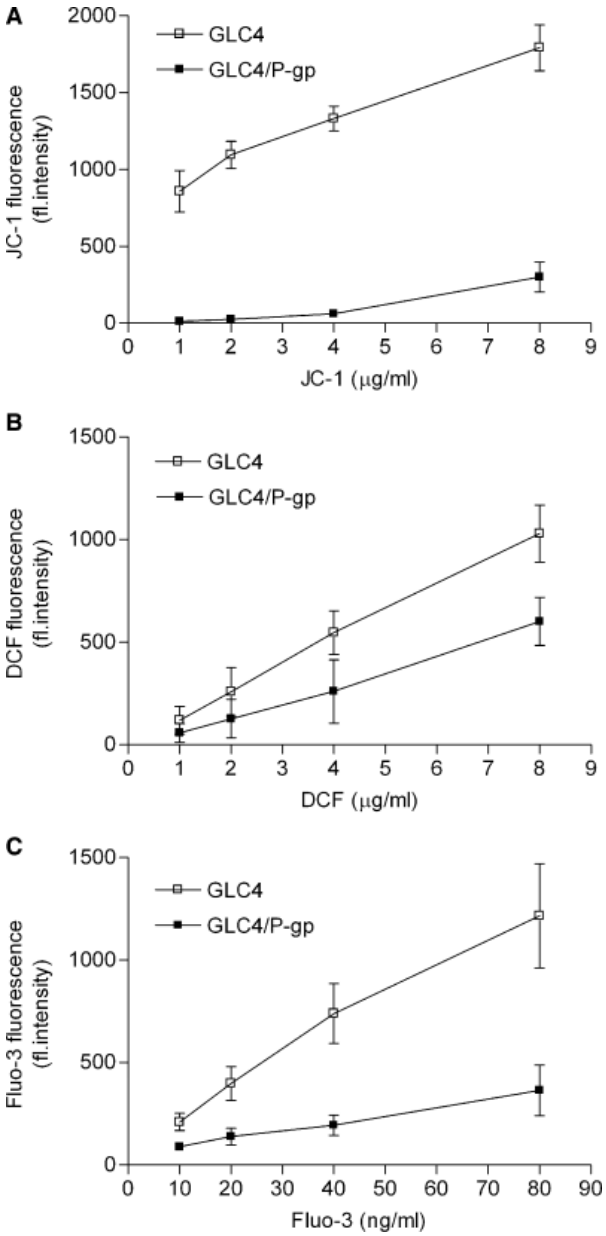

Figure 2. Probe accumulation in GLC4 cells without expression of P-glycoprotein (GLC4) and GLC4 cells with expression of P-glycoprotein (GLC4/P-gp). After loading of cells with probes and subsequent washing, they were kept in culture medium for 1 h, and then measured by flow cytometry. (A) Dose–response curve of JC-1 (mitochondrial membrane potential). (B) Dose–response curve of DCF (intracellular levels of ROS). (C) Dose–response curve of Fluo-3 (intracellular levels of Ca^{2+}). The data presented are from at least three independent experiments, and represent the mean value ± SEM. If no error bar appears, it is hidden by the marker for the mean value.

We used human small cell carcinoma (GLC4) cells and GLC4/P-glycoprotein cells to investigate the effects of CsA and its analogs on $\Delta\Psi_m$. There were no significant increases in JC-1 fluorescence in response to either CsA or its analogs in GLC4 cells. Inhibition of P-glycoprotein by CsA and its analogs, including NIM811, resulted in significant increases in JC-1 fluorescence as compared to GLC4/P-glycoprotein control cells untreated with CsA and its analogs (Fig. 3A).

We also used GLC4 cells to investigate CsA and its analogs in the absence of disturbing effects mediated by inhibition of P-glycoprotein pumps. Analyses with DCF as probe for assessment of ROS production showed, for all three analogs, a significant, more than 1.5-fold, increase in fluorescence (Fig. 3B). Treatment with the antioxidant vitamin E blunted these increases in DCF fluorescence. The Fluo-3 measurements presented in Fig. 3C suggest increases in cytosolic [Ca^{2+}] in response to CsA and its analogs. Both the intracellular Ca^{2+} chelator BAPTA and the extracellular Ca^{2+} chelator EGTA caused significant attenuation of the effects of CsA and its analogs on Fluo-3 fluorescence.

Effects of CsA and its analogs on mitochondrial function

We concluded that experiments in isolated mitochondria were necessary to discern whether mitochondria could be a source of increased ROS production, because we observed ROS production with CsA and both of its analogs even in GLC4 cells that were devoid of P-glycoprotein. To perform these experiments, we used mitochondria that were isolated from fresh liver obtained from pigs. We first confirmed that CsA and NIM811 actually inhibit the MPTP, using the mitochondrial swelling assay. As shown in Fig. 4, isolated mitochondria undergo large-amplitude swelling that is dependent on Ca^{2+}, which is a classical inducer of MPTP opening. Pretreatment of mitochondria with CsA (1 and 10 μM) and NIM811 (10 μM) significantly reduced mitochondrial swelling, whereas CsA (0.1 μM) and PSC833 (10 μM) did not.

Isolated mitochondria

To further examine whether closure of the MPTP results in an increase in $\Delta\Psi_m$, isolated mitochondria were loaded with JC-1. After addition of succinate and ADP, state III respiration was reached. Figure 5A shows that CsA did not result in an increase in JC-1 fluorescence. In response to induction of state IV respiration, however, JC-1 fluorescence increased by 13.5 ± 2.8%. The protonophore 2,4-dinitrophenol (DNP), which dissipates $\Delta\Psi_m$, resulted in a significant (50.7 ± 12.9%, $P < 0.001$) decrease.

Mitochondrial ATP levels were monitored during state III respiration. CsA did not result in an increase in ATP production (Fig. 5A). State IV respiration and DNP were used as negative controls. State IV respiration could not result in ATP production, because there was no supply of ADP. Addition of DNP, an established uncoupler of oxidative phosphorylation, resulted in a decrease in ATP to 28.9 ± 4.5% ($P < 0.01$) as compared to state III.

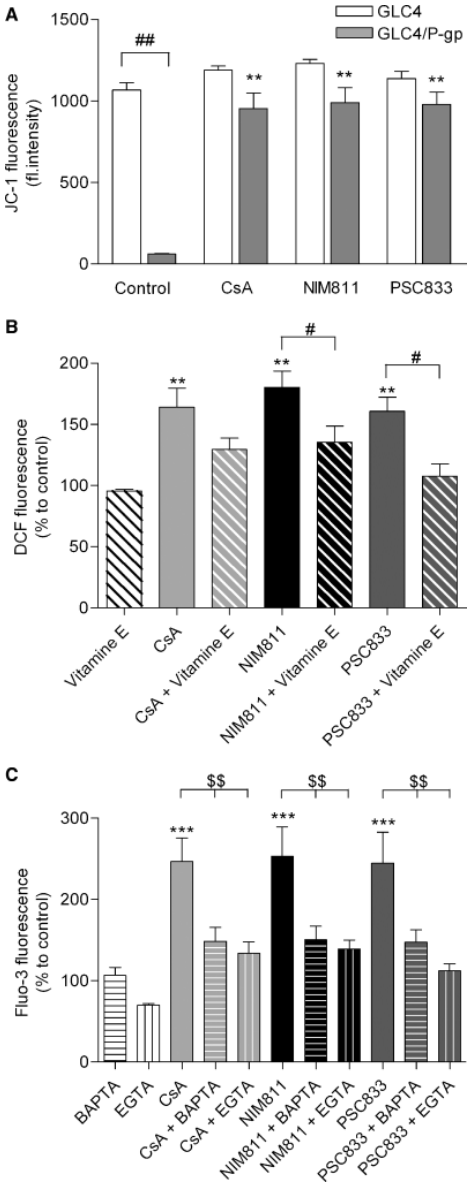

Figure. 3. Effects of CsA (10 μM), NIM811 (10 μM) and PSC833 (10 μM) in GLC4 cells without expression of P-glycoprotein (GLC4) and GLC4 cells expressing P-glycoprotein (GLC4/P-gp). (A) JC-1 (5 μg·mL^{-1}) was used to assess mitochondrial membrane potential. (B) DCF (5 μg·mL^{-1}) was used to detect the generation of ROS. (C) Fluo-3 (50 ng·mL^{-1}) was used to determine Ca^{2+} levels. The data presented are from four independent experiments, and represent the mean value ± SEM. (A) $^{\#\#}P < 0.01$ versus GLC4; $^{**}P < 0.01$ versus control. (B) $^{**}P < 0.01$ versus control; $^{\#}P < 0.05$ versus vitamin E (200 μM) treatment. (C) $^{***}P < 0.001$ versus control; $\$\$P < 0.01$ versus BAPTA (10 μM) or EGTA (0.1 mM). *P*-values are according to the Newman–Keuls multiple comparison test.

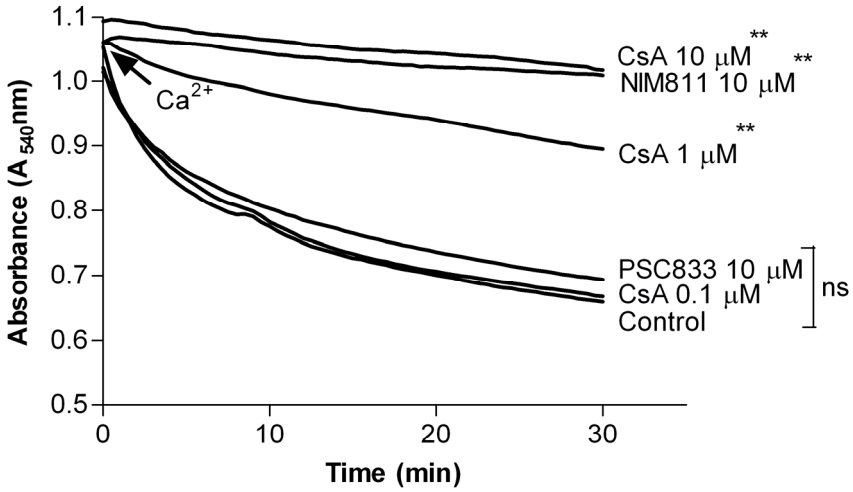

Figure. 4. Effects of different concentrations of CsA and its analogs on the Ca^{2+}-dependent induction of opening of the MPTP. The data are representative of four experiments. A concentration of 1 mM Ca^{2+} was used to induce opening of the MPTP. CsA (1 and 10 μM) and NIM811 (10 μM) caused significant inhibition of mitochondrial swelling. $^{**}P < 0.01$ versus control; ns, not significant by two-way ANOVA.

Oxygen consumption was monitored with sequential addition of succinate, ADP (to induce state III respiration) and CsA, until state IV respiration was reached again, when all ADP was converted to ATP. DNP was then added, followed by KCN (Fig. 5B). Isolated mitochondria were incubated in an oxygraph sample chamber with air-saturated respiration buffer in these experiments. After addition of succinate as metabolic substrate, mitochondria start to respire (4.8 ± 0.5 nmol $O_2 \cdot min^{-1} \cdot mg^{-1}$). Addition of ADP causes a burst of oxygen uptake (15.4 ± 1.8 nmol $O_2 \cdot min^{-1} \cdot mg^{-1}$). The respiratory control index was 3.2 ± 0.3. Addition of CsA during state III respiration did not cause a significant change in oxygen consumption as compared to state III control. DNP was used as positive control. Uncoupling of the mitochondria caused a burst of oxygen uptake (17.8 ± 4.0 nmol $O_2 \cdot min^{-1} \cdot mg^{-1}$). KCN, a blocker of complex IV, was used as negative control. Addition of KCN acutely blocked respiration of the uncoupled mitochondria (2.2 ± 6.8 nmol $O_2 \cdot min^{-1} \cdot mg^{-1}$).

Finally, we examined whether CsA exposure induces changes in ROS production during state III respiration in the presence and absence of 1 mM Ca^{2+}. Mitochondrial ROS production was monitored with DCF in these experiments. Figure 5C shows that addition of Ca^{2+} results in a significant increase in DCF fluorescence. Antimycin A, a blocker of complex III and a well-known inducer of ROS production (26), was used as positive control. Addition of CsA resulted in significant attenuation of DCF fluorescence during state III respiration, both in the absence and in the presence of Ca^{2+}, with no significant difference between the latter two conditions.

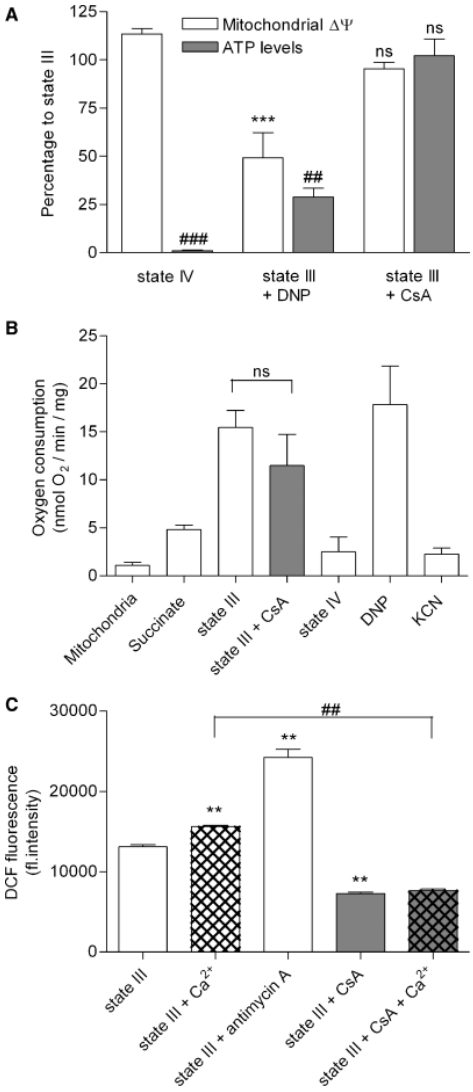

Fig. 5. Effects of 10 μM CsA in isolated liver mitochondria. (A) Mitochondrial membrane potential ($\Delta\Psi_m$) and ATP levels. (B) Respiration rate. (C) ROS. Measurements for assessment of $\Delta\Psi_m$, ATP levels and ROS were performed under different conditions. Measurements of oxygen consumption for assessment of respiration rate represent four experiments in which isolated mitochondria were subsequently exposed to different conditions, starting with respiration medium with mitochondria alone (indicated as mitochondria) and ending with addition of KCN (indicated as KCN). JC-1 (0.2 μg·mL^{-1}) probe was used to monitor mitochondrial membrane potential. Mitochondrial ATP levels were quantified by using a chemiluminescent ATP assay. Mitochondrial respiration rate was measured using an oxygraph. DCF (1 μg·mL^{-1}) was used to quantify ROS. Data are expressed as mean value ± SEM and are representative of four experiments. (A) (mitochondrial $\Delta\Psi_m$) $^{***}P < 0.001$ versus state III; ns, not significant. (A) (ATP levels) $^{\#\#}P < 0.01$ versus state III; $^{\#\#\#}P < 0.001$ versus state III; ns, not significant. (B) ns, not significant; (C) $^{**}P < 0.01$ versus state III; $^{\#\#}P < 0.01$ versus state III + Ca^{2+}. *P*-values are according to the Newman–Keuls multiple comparison test.

DISCUSSION

In this study, we found that CsA induces increases in the production of ROS and in cytosolic [Ca^{2+}]. In contrast to expectations, we found that these increases cannot be explained by blockage of the MPTP by CsA. We also found that both the MPTP-blocking CsA analog NIM811 and the P-glycoprotein-blocking CsA analog PSC833 induced comparable increases in ROS and cytosolic [Ca^{2+}] to those induced by CsA. All three compounds induced a comparable degree in ROS production in cells devoid of P-glycoprotein. Unlike CsA, both NIM811 and PSC833 do not inhibit calcineurin. Together, these results suggest that neither mitochondria, inhibition of calcineurin nor blockage of P-glycoprotein play a role in the comparable induction of ROS production by CsA and its analogs.

We found that CsA induces a strong increase in JC-1 fluorescence in intact human kidney cells. Studies in human neuroblastoma cells have found the same phenomenon [20,27]. It was suggested by these authors that this action of CsA derives from its inhibition of the MPTP at the level of mitochondria. Our experiments with PSC833, which we confirmed to be a potent inhibitor of P-glycoprotein pumps, but not of the MPTP, showed that it induced comparable increases in JC-1 fluorescence as CsA (Fig. 1). P-glycoprotein is located at the plasma membrane, and is expressed in almost every cell type, including human kidney and neuroblastoma cells [28–30]. This pump is able to excrete many different fluorescent probes [22,31]. Our data imply that the fluorescent probe JC-1 accumulates in cells as a consequence of P-glycoprotein inhibition, resulting in an apparent increase in $\Delta\Psi_m$. We also subsequently tested whether P-glycoprotein pumps are involved in the accumulation of other fluorescent probes, because this might disturb the interpretation of our data concerning these probes. Parallel experiments with the fluorescent probes JC-1, DCF and Fluo-3 in GLC4 cells with and without expression of P-glycoprotein provided evidence that probe accumulation and probe excretion were influenced by the presence of these pumps (Fig. 2A–C). Cells that did not express P-glycoprotein accumulated the probes, resulting in a strong fluorescence signal. We can conclude that P-glycoprotein expression gives rise to false-positive results that do not correspond to the increases in $\Delta\Psi_m$, ROS production and [Ca^{2+}] that the investigated probes were intended to assess. This is a major problem in the interpretation of studies, because many pharmacologic agents can influence the efflux of probes mediated by P-glycoprotein pumps [20,27,32].

In order to investigate the effect of MPTP blockage by CsA in the absence of disturbance by probe efflux effects due to P-glycoprotein pumps, we used GLC4 cells without these pumps. Our study is the first to compare the effect of CsA on intracellular probe accumulation between non-P-glycoprotein-containing cells and the same cells transfected in such a way that they express this protein. We demonstrated that in cells that do not contain P-glycoprotein, neither CsA, NIM811 nor PSC833 was able to induce a significant increase in JC-1 fluorescence (Fig. 3A). This was confirmed at the level of isolated mitochondria (Fig. 5A). CsA blockage of the temporary opening of the MPTP in state III respiration did not result in an increase in JC-1 fluorescence. If closure of the MPTP by CsA altered the flow of electrons along the electron transfer chain, mitochondrial ATP synthesis and

respiration rate would be expected to alter. Our results showed that neither ATP synthesis nor mitochondrial respiration rate was influenced by CsA, which is similar to the observations by Sanchez *et al*. [33]. Strzelecki *et al*. showed that CsA inhibited the process of spontaneous Ca^{2+} discharge in isolated mitochondria [34]. CsA also inhibited the swelling and respiration induced by accumulated Ca^{2+} in these experiments. The authors concluded that CsA at an immunosuppressive level impairs Ca^{2+}-induced membrane permeability. Our findings show that Ca^{2+}-induced increases in mitochondrial ROS production can be prevented by CsA, thereby virtually excluding mitochondria as source of increased ROS production in response to exposure of cells to CsA. Elzinga *et al*. showed that Ca^{2+} uptake by mitochondria isolated from renal cortical cells of rats that had been treated with CsA for 2 weeks was significantly lower than Ca^{2+} uptake by mitochondria isolated from control rats [35]. It was not investigated whether there was an increased concentration gradient as a consequence of prior intramitochondrial Ca^{2+} accumulation. If this was the case, it could be that long-term treatment with CsA results in a net zero effect on mitochondrial ROS production under steady-state conditions *in vivo*.

We showed in experiments in isolated mitochondria that the classic MPTP inducer Ca^{2+} leads to mitochondrial swelling, and that this can be blocked by CsA and NIM811, but not by PSC833. Our experiments in whole cells suggested that both CsA, NIM811 and PSC833 induce an increase in cytosolic [Ca^{2+}] and production of ROS. The discrepancy in the effects of PSC833 between GLC4 cells and isolated mitochondria versus the consistency in the effects of CsA and NIM811 in these experiments suggests that MPTP blockage plays a role neither in the observed increases in cytosolic [Ca^{2+}] nor in increases in ROS production. To further substantiate this suggestion, we performed experiments in the presence and absence of 1 mM Ca^{2+} in isolated mitochondria. We found significant stimulation of ROS production after addition of Ca^{2+} during state III respiration, whereas CsA resulted in a significant attenuation of ROS production.

We observed the same degree of increased ROS production in response to CsA and its analogs NIM811 and PSC833. The increased production was not of mitochondrial origin. It is also unlikely that the calcineurin-inhibiting properties of CsA play a role, because neither NIM811 nor PSC833 inhibit calcineurin. It is furthermore also unlikely that the P-glycoprotein-inhibiting properties of CsA play a role, because CsA, NIM811 and PSC833 all increased ROS production to the same degree in cells that were devoid of P-glycoprotein. ROS-forming candidates that may explain this side-effect of CsA are NADPH oxidase, endoplasmic reticulum cytochrome P450, and glycolate oxidase. Recently, a study by Vetter *et al*. suggested that CsA activates NADPH oxidase and generates release of $O_2^{\cdot-}$ [36]. Other studies have found increased arachidonic acid omega-hydroxylation activity by CsA. The omega-hydroxylation of arachidonic acid is an activity associated with members of the cytochrome P450 family [37,38].

In conclusion, our results showed induction of increased ROS production and cytosolic [Ca^{2+}] by CsA and its analogs. However, mitochondria, involvement of P-glycoprotein and inhibition of calcineurin are unlikely to play a role in CsA-induced oxidative stress and disturbed Ca^{2+} homeostasis. Care must be taken in the use of fluorescent probes in P-glycoprotein-expressing cells when substances with P-glycoprotein-blocking properties, such as CsA, are investigated, because this may

result in false-positive signals. More detailed *in vitro* studies are required to further elucidate the mechanisms responsible for the CsA-induced toxicity.

ACKNOWLEDGEMENTS

We thank Inge de Vegt and Harold G. de Bruin for their valuable technical support in carrying out experimental studies, and the Dutch Kidney Foundation for financial support (Co1.1923).

REFERENECES

1. Kopp JB & Klotman PE (1990) Cellular and molecular mechanisms of cyclosporin nephrotoxicity. JAm Soc Nephrol 1, 162–179.
2. Redondo-Horcajo M & Lamas S (2005) Oxidative and nitrosative stress in kidney disease: a case for cyclosporine A. J Nephrol 18, 453–457.
3. Hong F, Lee J, Song JW, Lee SJ, Ahn H, Cho JJ, Ha J & Kim SS (2002) Cyclosporin A blocks muscle differentiation by inducing oxidative stress and inhibiting the peptidyl-prolyl-cis–trans isomerase activity of cyclophilin A: cyclophilin A protects myoblasts from cyclosporin A-induced cytotoxicity. FASEB J 16, 1633–1635.
4. Buetler TM, Cottet-Maire F, Krauskopf A & Ruegg UT (2000) Does cyclosporin A generate free radicals? Trends Pharmacol Sci 21, 288–290.
5. Perez de Lema G, Arribas I, Prieto A, Parra T, de Arriba G, Rodriguez-Puyol D & Rodriguez-Puyol M (1998) Cyclosporin A-induced hydrogen peroxide synthesis by cultured human mesangial cells is blocked by exogenous antioxidants. Life Sci 62, 1745–1753.
6. Wang C & Salahudeen AK (1995) Lipid peroxidation accompanies cyclosporine nephrotoxicity: effects of vitamin E. Kidney Int 47, 927–934.
7. Parra Cid T, Conejo Garcia JR, Carballo Alvarez F & de Arriba G (2003) Antioxidant nutrients protect against cyclosporine A nephrotoxicity. Toxicology 189, 99–111.
8. Brookes PS, Yoon Y, Robotham JL, Anders MW & Sheu SS (2004) Calcium, ATP, and ROS: a mitochondrial love–hate triangle. Am J Physiol Cell Physiol 287, C817–C833.
9. Azzone GF, Schmehl I, Canton M & Luvisetto S (1994) The effect of the protonmotive force on the redox state of mitochondrial cytochromes. Biochim Biophys Acta 1187, 140–144.
10. Brown GC & Brand MD (1985) Thermodynamic control of electron flux through mitochondrial cytochrome bc1 complex. Biochem J 225, 399–405.
11. Capitanio N, De Nitto E, Villani G, Capitanio G & Papa S (1990) Protonmotive activity of cytochrome c oxidase: control of oxidoreduction of the heme centers by the protonmotive force in the reconstituted beef heart enzyme. Biochemistry 29, 2939–2945.
12. Duszynski J & Wojtczak L (1985) The apparent non-linearity of the relationship between the rate of respiration and the protonmotive force of mitochondria can be explained by heterogeneity of mitochondrial preparations. FEBS Lett 182, 243–248.

13. Skulachev VP (1996) Role of uncoupled and noncoupled oxidations in maintenance of safely low levels of oxygen and its one-electron reductants. Q Rev Biophys 29, 169–202.

14. Bakker SJ, IJzerman RG, Teerlink T, Westerhoff HV, Gans RO & Heine RJ (2000) Cytosolic triglycerides and oxidative stress in central obesity: the missing link between excessive atherosclerosis, endothelial dysfunction, and beta-cell failure? Atherosclerosis 148, 17–21.

15. Fall CP & Bennett JP Jr (1999) Visualization of cyclosporin A and Ca2 +-sensitive cyclical mitochondrial depolarizations in cell culture. Biochim Biophys Acta 1410, 77–84.

16. Huser J & Blatter LA (1999) Fluctuations in mitochondrial membrane potential caused by repetitive gating of the permeability transition pore. Biochem J 343 (Part 2), 311–3 17.

17. Smaili SS & Russell JT (1999) Permeability transition pore regulates both mitochondrial membrane potential and agonist-evoked Ca2 + signals in oligodendrocyte progenitors. Cell Calcium 26, 121–130.

18. Crompton M, Virji S, Doyle V, Johnson N & Ward JM (1999) The mitochondrial permeabiity transition pore. Biochem Soc Symp 66, 167–179.

19. Halestrap AP, Connern CP, Griffiths EJ & Kerr PM (1997) Cyclosporin A binding to mitochondrial cyclophilin inhibits the permeability transition pore and protects hearts from ischaemia/reperfusion injury. Mol Cell Biochem 174, 167–172.

20. Cassarino DS, Swerdlow RH, Parks JK, Parker WD Jr & Bennett JP Jr (1998) Cyclosporin A increases resting mitochondrial membrane potential in SY5Y cells and reverses the depressed mitochondrial membrane potential of Alzheimer's disease cybrids. Biochem Biophys Res Commun 248, 168–173.

21. Waldmeier PC, Feldtrauer JJ, Qian T & Lemasters JJ (2002) Inhibition of the mitochondrial permeability transition by the nonimmunosuppressive cyclosporin derivative NIM811. Mol Pharmacol 62, 22–29.

22. Diaz G, Diana A, Falchi AM, Gremo F, Pani A, Batetta B, Dessi S & Isola R (2001) Intra- and intercellular distribution of mitochondrial probes and changes after treatment with MDR modulators. IUBMB Life 51, 121–126.

23. Boesch D, Gaveriaux C, Jachez B, Pourtier-Manzanedo A, Bollinger P & Loor F (1991) In vivo circumvention of P-glycoprotein-mediated multidrug resistance of tumor cells with SDZ PSC 833. Cancer Res 51, 4226– 4233.

24. Iqbal T, Kinjo M & Dowling TC (2005) Determination of Rhodamine 123 in cell lysate by HPLC with visible wavelength detection. J Chromatogr B Anal Technol Biomed Life Sci 814, 259–262.

25. Nieri P, Romiti N, Adinolfi B, Chicca A, Massarelli I & Chieli E (2006) Modulation of P-glycoprotein activity by cannabinoid molecules in HK-2 renal cells. Br J Pharmacol 148, 682–687.

26. Indo HP, Davidson M, Yen HC, Suenaga S, Tomita K, Nishii T, Higuchi M, Koga Y, Ozawa T & Majima HJ (2006) Evidence of ROS generation by mitochondria in cells with impaired electron transport chain and mitochondrial DNA damage. Mitochondrion 7, 106–118.

27. Kowaltowski AJ, Smaili SS, Russell JT & Fiskum G (2000) Elevation of resting mitochondrial membrane potential of neural cells by cyclosporin A, BAPTA-AM, and bcl-2. Am J Physiol Cell Physiol 279, C852–C859.

28. Bordow SB, Haber M, Madafiglio J, Cheung B, Marshall GM & Norris MD (1994) Expression of the multidrug resistance-associated protein (MRP) gene correlates with amplification and overexpression of the N-myc oncogene in childhood neuroblastoma. Cancer Res 54, 5036–5040.
29. Ernest S, Rajaraman S, Megyesi J & Bello-Reuss EN (1997) Expression of MDR1 (multidrug resistance) gene and its protein in normal human kidney. Nephron 77, 284–289.
30. Romiti N, Tramonti G & Chieli E (2002) Influence of different chemicals on MDR-1 P-glycoprotein expression and activity in the HK-2 proximal tubular cell line. Toxicol Appl Pharmacol 183, 83–91.
31. Koizumi S, Konishi M, Ichihara T, Wada H, Matsukawa H, Goi K & Mizutani S (1995) Flow cytometric functional analysis of multidrug resistance by Fluo-3: a comparison with rhodamine-123. Eur J Cancer 31A, 1682–1688.
32. Ho GT, Moodie FM & Satsangi J (2003) Multidrug resistance 1 gene (P-glycoprotein 170): an important determinant in gastrointestinal disease? Gut 52, 759–766.
33. Sanchez H, Bigard X, Veksler V, Mettauer B, Lampert E, Lonsdorfer J & Ventura-Clapier R (2000) Immunosuppressive treatment affects cardiac and skeletal muscle mitochondria by the toxic effect of vehicle. J Mol Cell Cardiol 32, 323–331.
34. Strzelecki T, Kumar S, Khauli R & Menon M (1988) Impairment by cyclosporine of membrane-mediated functions in kidney mitochondria. Kidney Int 34, 234–240.
35. Elzinga LW, Mela-Riker LM, Widener LL & Bennett WM (1989) Renal cortical mitochondrial integrity in experimental cyclosporine nephrotoxicity. Transplantation48, 102–106.
36. Vetter M, Chen ZJ, Chang GD, Che D, Liu S & Chang CH (2003) Cyclosporin A disrupts bradykinin signaling through superoxide. Hypertension 41, 1136–1142.
37. Ahmed SS, Napoli KL & Strobel HW (1995) Oxygen radical formation during cytochrome P450-catalyzed cyclosporine metabolism in rat and human liver microsomes at varying hydrogen ion concentrations. Mol Cell Biochem 151, 131–140.
38. Nakamura M, Imaoka S, Miura K, Tanaka E, Misawa S & Funae Y (1994) Induction of cytochrome P450 isozymes in rat renal microsomes by cyclosporin A. Biochem Pharmacol 48, 1743–1746.
39. Garcia-Ruiz C, Colell A, Morales A, Kaplowitz N & Fernandez-Checa JC (1995) Role of oxidative stress generated from the mitochondrial electron transport chain and mitochondrial glutathione status in loss of mitochondrial function and activation of transcription factor nuclear factor-kappa B: studies with isolated mitochondria and rat hepatocytes. Mol Pharmacol 48, 825–834.

SUMMARY AND MAIN CONCLUSIONS

In this thesis we studied the effects of cigarette smoke (CS) on mitochondrial function and oxidative stress in epithelial cells and discussed the potential of these phenomena in the pathogenesis of chronic obstructive pulmonary diseases (COPD). In the first three chapters we demonstrated that CS disturbs mitochondrial function, increase reactive oxygen species (ROS) generation and alters the regulation of cell death. In chapter 4 and 5 we investigated the effects of gaseous-phase CS and H_2O_2 on the antioxidant glutathione and thiol proteins regulating redox state, morphology and cell death pathways in airway epithelial cells. In chapter 6 we studied the negative side effects of cyclosporine A (CsA), an immunosuppressive drug and potent inducer of mitochondrial permeability transition pore (MPTP) closure, on mitochondrial membrane potential ($\Delta\psi_m$), oxidative stress and calcium homeostasis in relation to chronic renal allograft dysfunction.

In **chapter 1** of this thesis we investigated the effects of CS extract (CSE) on mitochondrial function and mode of cell death in human lung epithelial cells. Therefore, at first we isolated mitochondria and examined the effects of CSE on complex I and II activity of the electron transfer chain (ETC), $\Delta\psi_m$, proton motive force, oxygen consumption and examined the effects of CSE on intracellular energy production and cell death in lung epithelial cells. We demonstrated that CSE acts as a blocking agent of complex I and II of the ETC. Inhibition of the two entry points of the ETC caused a decrease in $\Delta\psi_m$ and proton motive force. As a result of that, oxygen consumption and production of ATP were diminished. Furthermore, we demonstrated that CSE inhibited caspase-3 and -7 activities in early apoptotic cells and switched epithelial cell apoptosis into necrosis. We concluded that compounds in CSE act as blocking agents of the mitochondrial ETC and that the loss of intracellular ATP generation switches early apoptotic epithelial cells into necrosis.

In COPD patients markers of increased oxidative stress are present. ROS in the gaseous-phase of CS are thought to constitute the main component of the oxidative stress present in COPD. In **chapter 2** we described that ROS present in the gaseous-phase of CS are not able to diffuse through the membranes of the epithelial cells of the lungs. Despite this fact, evidence of systemic oxidative stress parameters such as higher malondialdehyde (MDA) levels, lower serum vitamin C and reduced glutathione (GSH) levels have been found in smokers and patients with COPD. We hypothesized that instead of ROS, lipophilic compounds present in CS enter the cell and induce an intracellular burst of ROS by disturbing mitochondrial function. Therefore, we investigated the acute effects of CSE and lipophilic free CSE on mitochondrial function. We also used A549 alveolar epithelial cells and A549-ρ0 cells that lack a functional ETC and examined if CSE was able to induce an intracellular burst of ROS production. Furthermore, we used an ancient method, the Narghile or so called waterpipe, to quench ROS from the gaseous-phase of CS to investigate the effects of intracellular generated ROS on thiol redox status in lung epithelial cells. We demonstrated that CSE deteriorates the intracellular levels of ATP, most probably trough inhibition of the ETC (**chapter 1**). Removal of lipophilic compounds from CSE significantly restored the intracellular levels of

ATP. Exposure of CSE to A549 and A549-ρ0 cells showed an increase in ROS generation in A549 cells whereas A549-ρ0 cells did not. We furthermore showed that ROS in the gaseous-phase of CS directly induces thiol oxidation in A549 cells whereas water-filtered CS did not. We concluded that lipophilic compounds present in CS disturbed mitochondrial function leading to increased generation of intracellular ROS. A functional mitochondrial ETC was essential in this ROS generation. Furthermore, ROS inside the gaseous-phase of CS and generated by the mitochondria themselves were both responsible for the oxidation of free thiol groups.

In **chapter 3** we described the significance of heme oxygenase-1 (HO-1), a stress protein, which contributes to the protection of the airway epithelium against toxic compounds present in CS. HO-1 catalysis the rate-limiting step in the oxidative degradation of heme, confers protection against exogenous stresses and inhibits apoptotic cell death. In ex-smoking patients with COPD compared with ex-smoking healthy control subjects, lower expression of HO-1 were found. In this study we hypothesized that HO-1 exerts a potential regulatory and protective function in COPD by preserving mitochondrial function, and by inhibiting cell death associated with CS exposure. Therefore at first we characterized the localization of HO-1 in the epithelial cells. In mice we examined the mRNA expression of HO-1 in the lung after exposure of CS. Thereafter we examined the functional activity of HO-1 in whole cells and mitochondrial extracts after treatments with hemin (substrate of HO-1) and CSE. To investigate the protective role of HO-1 in CSE-induced cell death process, we used Beas-2b bronchial epithelial cells overexpressing HO-1 and control Beas-2b cells. We demonstrated that HO-1 levels were significantly increased in cytosolic and mitochondrial fractions of alveolar A549 cells and bronchial Beas-2b cells. The mitochondrial localization of HO-1 was confirmed using immunogold-electron and confocal microscopy. HO-1 activity increased dramatically in mitochondrial fraction and whole cell extract after exposure of hemin and CSE. HO-1 mRNA expression levels were elevated in the lungs of mice exposed to CS. Furthermore, over expression of HO-1 levels inhibited CSE-induced cell death and preserved cellular ATP levels. We concluded that functional compartmentalization of HO-1 in the mitochondria of airway epithelial cells preserved mitochondrial ATP production and prevented cell death, in the presence of CSE.

In patients with COPD, increased levels of oxidative stress parameters have been documented suggesting that antioxidants may be insufficient to prevent oxidative damage from CS. To ensure an appropriate defense against lung injury, the respiratory tract is equipped with the epithelial lining fluid (ELF) and the airway epithelium, which both contain large amounts of the reduced GSH. GSH plays a key role in the cellular redox balance and is thought to be one of the most important antioxidant defenses in the airways. CS is known to deplete total glutathione (GSH + GSSG) in the airways. In **chapter 4** we investigated if compounds of the gaseous-phase of CS react irreversibly with the reduced form of GSH to form GSH derivatives that cannot be reduced, thereby causing this depletion. Therefore at first we tested whether CS compounds were able to modify the free thiol (-SH) groups of

GSH in solution compared to hydrogen peroxide (H_2O_2). Thereafter we investigated if gaseous-phase CS irreversibly modified GSH in A549 cells and primary bronchial epithelial cells. Enzymatic assays combined with mass spectrometry were used to quantify the amount of total glutathione and identify the GSH modification. We demonstrated in a solution of GSH and in airway epithelial cells that gaseous-phase CS irreversibly reduces the amount of total glutathione whereas H_2O_2 did not. Mass spectrometry showed that GSH was modified to glutathione-aldehyde derivatives. Identification by MS2 showed that GSH was bound to acrolein and crotonaldehyde and another, yet to be identified structure. We concluded that CS does not oxidize reduced GSH to oxidized GSSG but, rather, reacts to nonreducible glutathione-aldehyde derivatives, thereby depleting the total available GSH pool. Under these circumstances, a chronic lack of protection against oxidative stress might be induced.

The airways of smokers are constantly exposed to high levels of ROS. These reactive compounds may directly participate in specific tissue injury and cell death, which is followed by recovery and repair by the proliferation of the remaining cells. In **chapter 5** we investigated the response and recovery of A549 cells after various concentrations of H_2O_2. We hypothesized that resistance and recovery would be dependent on the concentration of the oxidative agent, duration of exposure and on the quiescent or proliferating state of the cells. Therefore at first we studied morphological changes in quiescent or proliferating A549 cells exposed to different concentration of H_2O_2 and incubation time. Because free thiol groups play an important role in the defense against oxidative stress, the effect of H_2O_2 on the cellular level of free thiol groups were measured relative to the protein content. Thereafter, cell numbers, cell viability and recovery were tested. We demonstrated that proliferating A549 cells recovered a 1-h challenge with up to 1 mM H_2O_2 whereas quiescent A549 cells did not. Proliferating A549 cells did not sustain a more prolonged challenge (6 or 24 h) with 0.5 mM or 1.0 mM H_2O_2. The severe conditions resulted in loss of cells by detachment from the plate surface, reduced numbers of viable cells primarily due to necrosis and a strong reduction of the intracellular free thiol content. Furthermore, a relation was found between cell morphology, free thiol content and the number of necrotic cells for proliferating A549 cells. This correlation was less strong for quiescent A549 cells. We concluded that quiescent cells were more sensitive to oxidative stress than proliferating cells. Intracellular free thiol levels apparently played a decisive role in cell survival, preferentially protecting proliferating cells.

Immunosuppressive therapy with cyclosporine A (CsA) to prevent rejection of transplanted solid organs is associated with undesired effects that promote deterioration of transplant function and accelerated atherogenesis. It has been suggested that ROS plays an important underlying role. CsA is also a potent inhibitor of the mitochondrial permeability transition pore (MPTP). In **chapter 6** we investigated whether closure of the MPTP by CsA resulted in a concomitant increase in $\Delta\psi_m$ and increased production of mitochondrial ROS. We used fluorescent probes to asses $\Delta\psi_m$, ROS and $[Ca^{2+}]$ in human kidney cells (HK-2) and a line of human small cell lung carcinoma (GLC4), because these do not express CsA-sensitive P-

glycoprotein. Transfected GLC4 cells were used expressing P-glycoprotein as control for GLC4 cells. NIM811 and PSC833 were applied as selective MPTP and P-glycoprotein blockers. We also isolated mitochondria from fresh pig livers and studied the effects of CsA on mitochondrial function. We demonstrated that CsA and PSC833 induced a more than two-fold increase in $\Delta\psi_m$ in HK-2 cells, whereas NIM811 had no effect. None of the three cyclosporine analogs induced an increase in $\Delta\psi_m$ in GLC4 cells. The MPTP blockers CsA and NIM811, but also the non-MPTP blocker PSC833, induced comparable degrees of increased ROS production and cytosolic [Ca^{2+}]. Furthermore, blockade of the MPTP in isolated mitochondria by CsA affected neither $\Delta\psi_m$, ATP synthesis, nor respiration rate. During state III respiration and in the presence of Ca^{2+} mitochondrial ROS generation was increased. Addition of CsA resulted in significant attenuation of generation of mitochondrial ROS. We concluded that CsA and its analogs induce ROS generation and cytosolic Ca^{2+}. However, neither mitochondria, nor involvement of P-glycoprotein nor inhibition of calcineurin play a role in CsA-induced oxidative stress and disturbed Ca^{2+} homeostasis. One must be very cautious when using fluorescent probes in P-glycoprotein-expressing cells when effects of substances with P-glycoprotein-blocking properties, such as CsA, are investigated, because this may result in false-positive signals.

MAIN CONCLUSIONS OF THE STUDIES IN THIS THESIS

About the effects of CSE on isolated mitochondria and intact cells

1 CSE acts as a blocking agent of the mitochondrial ETC

2 CSE-induced depletion of cellular ATP switches lung epithelial cell apoptosis into necrosis

3 Overexpression of HO-1 levels in airway epithelial cells inhibited CSE-induced cell death and preserved cellular ATP levels

4 CSE induces the activity of HO-1 protein

About the effects of gaseous-phase CS on intact cells

5 ROS inside the gaseous-phase of CS and generated by the mitochondria themselves are able to change the thiol redox state of the cell

6 CS induces mRNA expression of HO-1 in the lungs of mice

7 Lipophilic compounds in CS disturb mitochondrial function and induce mitochondrial ROS generation

8 Gaseous-phase CS is able to deplete free thiol groups

9 Unsaturated aldehydes generated during the combustion of tobacco irreversibly modify GSH into GSH-aldehyde compounds

About the effects of oxidative stress on intact cells

10 Quiescent alveolar A549 cells are more sensitive to oxidative stress than proliferating A549 cells

11 Intracellular free thiol levels apparently play a decisive role in cell survival after oxidative stress challenges

About the effects of CsA on isolated mitochondria and intact cells

12 The MPTP blockers CsA and NIM811, but also the non-MPTP blocker PSC833 induce increased production of ROS and cytosolic Ca^{2+} in GLC4 cells

13 Neither mitochondria, involvement of P-glycoprotein or inhibition of calcineurin play a role in CsA-induced oxidative stress and disturbed Ca^{2+} homeostasis

14 Ca^{2+} induced generation of mitochondrial ROS can be prevented by CsA

15 One must be cautious when using fluorescent probes in P-glycoprotein-expressing cells when substances with P-glycoprotein-blocking properties, such as CsA, are investigated, because this may result in false-positive signals

GENERAL CONCLUSIONS AND FUTURE PERSPECTIVES

The aim of this thesis was to study the effects of CS on mitochondrial function as a potential pathophysiological mechanism in smoking induced disease (in particular chronic obstructive pulmonary disease (COPD)) and to gain insight in the mechanisms involved in airway epithelial dysfunction by smoking.

Cigarette smoke disturbs mitochondria and airway epithelial cells
Smoking cigarettes remains the major risk factor for the development of COPD. There is little knowledge of the pathophysiology of COPD. In this thesis we were able to introduce a new pathophysiological concept in the development of COPD and other cigarette smoke-induced diseases.

The lungs extract oxygen which is essential for mitochondria to generate ATP, necessary for life, by oxidative phosphorylation. The respiratory tract which is equipped with airway epithelial cells and epithelial lining fluid (ELF) is exposed to a higher level of oxygen tension than that of most tissues within the body (12; 17). Leakage of electrons during the oxidative phosphorylation and higher oxygen tissue levels, are favorable conditions to generate reactive oxygen species (ROS). Because oxygen is a strong oxidizer, electrons can be easily accepted by this molecule, converting it into $O_2^{\cdot -}$, a very potent free radical. Nevertheless, during normal respiration, airway epithelial cells contain enough antioxidants to protect the cells from oxidative injury. However, the oxidant burden in the lungs is enhanced in smokers. ROS either inhaled by cigarette smoke (CS) or released by the activated neutrophiles, alveolar macrophages and eosinophiles are not capable of diffusing through the plasma membranes of the epithelial barrier of the lung (1; 4; 11). These extra-cellular ROS will act on the external environment by depletion of extracellular reduced thiols and by direct attack on vulnerable lipids and proteins of the cellular surface (19; 24). Other substances, like lipophilic compounds easily pass the membrane of cells, disturb mitochondrial function and enhance ROS generation. The mitochondrial electron transfer chain (ETC) is essential in this ROS generation. Furthermore, lipophilic compounds inhaled by smoking, contribute to an imbalance between ROS and antioxidant defenses (3). In this thesis we showed that GSH in epithelial cells, which plays a key role in the maintenance of the cellular redox balance, is irreversibly lost when exposed to gaseous-phase CS. Identification by mass spectrometry shows that the decrease of GSH is attributable to the formation of glutathione-aldehydes derivatives. Persistent smokers may in that case inhale more ROS than can be scavenged by the residual anti-oxidants, resulting in increased vulnerability for oxidative stress. This makes the re-synthesis of GSH essential for cellular survival and protection of the lung.

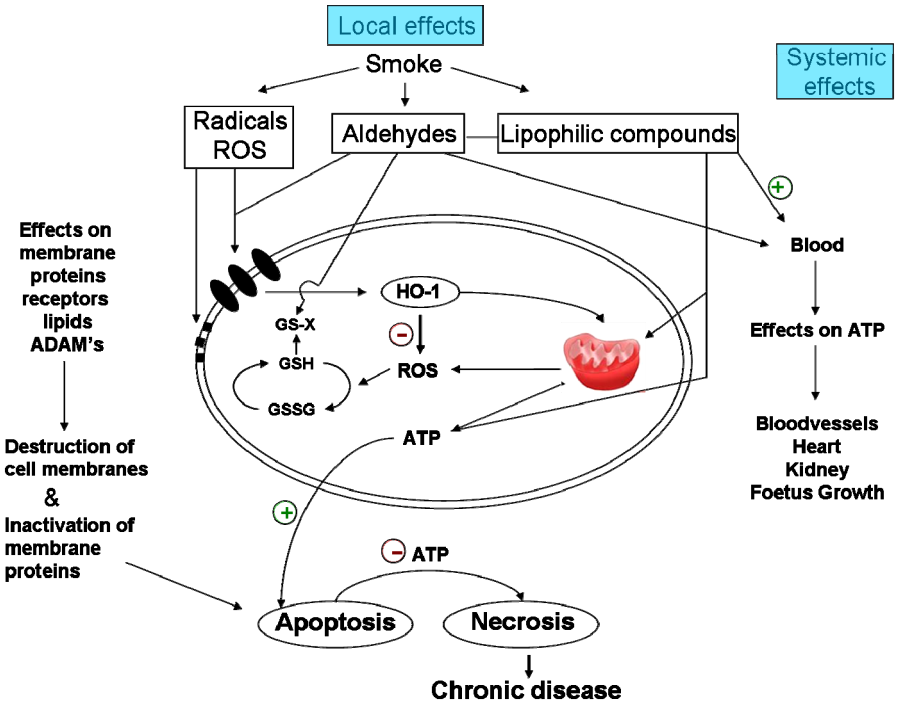

Figure 1. Effects of different compounds inside smoke on lung tissue cells

Aldehydes like acrolein and crotonaldehyde are one of the most prominent lipophilic compounds in gaseous-phase CS. Interestingly, it has recently been shown that acrolein acts as a mitochondrial toxin, with has comparable effects on mitochondrial function as we have observed in chapter 1 (22). Our *in vitro* experiments with airway epithelial cells and isolated mitochondria show that CS extract (CSE) is able to block complex I and II of the ETC. As a consequence of that, the consumption of oxygen and production of ATP is diminished. Removal of the lipophilic compounds from the CSE by hexane extraction significantly attenuate the effects on mitochondria, by restoring the mitochondrial membrane potential ($\Delta\psi_m$) and intracellular ATP synthesis. This may indicate that lipophilic compounds (aldehydes, nicotine, polycyclic aromatics, phenols etc.) inside CSE easily enters the cells and disturb mitochondrial function (9). Mitochondria are the main producers of cellular energy, but are also considered a key regulatory center of apoptosis. ATP depletion can result in necrosis or apoptosis. Apoptosis is an energy dependent process and, therefore, if the energy depletion is above a critical level necrosis will ensue (8; 10). A switch to necrotic cell death and release of their cellular contents, will result in an inflammatory response in the environment of these dying cells. Necrotic cell death may play an important role in the development of lung and airway inflammation and modulation of this pathway might reveal new

treatment modalities. The effects of smoke at the lung tissue cells are summarized in figure 1.

In this thesis we describe that heme oxygenase-1 (HO-1) may have a potential important protective role in CS-induced inflammation and cell death. HO-1 expression is induced by pro-inflammatory stimulants such as cytokines, heavy metals or CS. HO-1 is the rate-limiting enzyme in heme degradation, catalyzing the cleavage of the heme ring to form ferrous iron, carbon monoxide (CO), biliverdin and bilirubin, all of which have antioxidant and anti-inflammatory activities (Fig. 2) (16; 20).

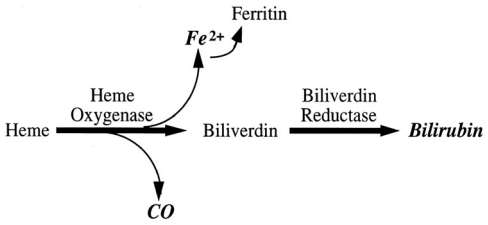

Figure 2. Enzymatic cleavage of heme by heme oxygenase-1.

We demonstrate that active HO-1 was present in higher concentrations in mitochondria than in the cytosol after stimulation with CSE. Overexpression of HO-1 in airway epithelial cells clearly preserves mitochondrial ATP production and prevent cell death, in the presence of CSE. HO-derived end products such as CO, biliverdin and bilirubin may contribute to this metabolic protection. Further studies are needed to elucidate the precise contribution of these end products inside the matrix of mitochondria.

FUTURE PERSPECTIVES

CS is the major risk factor for the development of COPD but also extends to systemic disease manifestations. In these patients, increased levels of oxidative stress parameters were found. We describe that lipophilic compounds inside the smoke of cigarettes induce a profound generation of ROS in alveolar epithelial cells with mitochondria, but not in alveolar epithelial cells that are devoid of mitochondria. We obtain similar results with CS devoid of ROS and water-soluble compounds, but still containing the lipophilic fraction. Our suggestion is that the lipophilic compounds are the major effectors of oxidative stress and systemic toxic effects after smoking cigarettes (see figure 1; right side). Based on our proposals two studies were awarded by grants provided by the Graduate School for Drug Exploration (GUIDE) for two Post-graduate students as a follow up of the study presented in this thesis.

First study: About local effects

To extend our results of chapter 2, we will try to identify which lipophilic compounds present in CS are the main compounds that disturb the mitochondrial function and thereby induce the intracellular ROS production. Furthermore we will investigate the effects of both gaseous-phase ROS and intracellular generation of ROS on release of inflammatory mediators by airway epithelial cells *in vitro*. To expand the *in vitro* results and to study the hypothesized acute affects of CS-induced intracellular generated ROS on airway inflammation, oxidant and anti-oxidant responses *in vivo* in mice and humans will be studied.

In chapter 1 we demonstrate that lung epithelial cells exposed to CS-extract (CSE) decrease there mitochondrial functions [4]. To investigate if also the structure of the mitochondria changed after CS exposure we recently exposed Beas-2b bronchial epithelial cells to CSE and observed a marked mitochondrial autophagy (Fig. 3A,B).

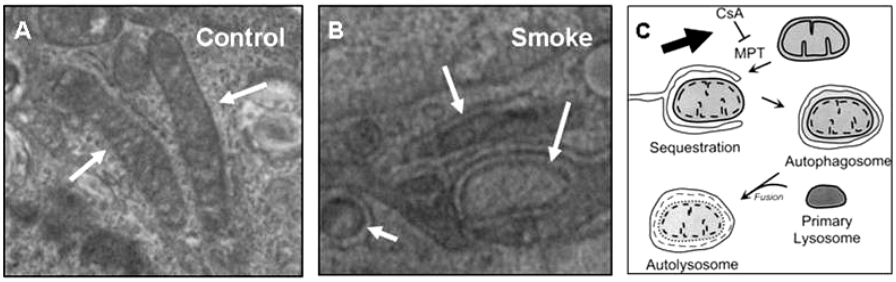

Figure 3. Beas-2b bronchial epithelial cells under normal culture circumstances showing normal mitochondria (A) and exposed to cigarette smoke extract showing marked mitochondrial autophagy (B) on electron microscopy (25.000x magnification, white arrows: mitochondria). (C): Cartoon showing the process of mitochondrial autophagy that can be inhibited by cyclosporine-A (CsA, black arrow).

Mitochondrial autophagy ('mitochondrial apoptosis') precedes cell death, possibly as a consequence of mitochondrial Ca^{2+} overload and increased oxidative stress, resulting in opening of the mitochondrial permeability transition pore (MPTP) and disruption of the mitochondrial matrix (2; 6). Furthermore, preliminary data with isolated mitochondria show that Ca^{2+} leads to mitochondrial swelling. Mitochondria exposed to increased levels of CSE and Ca^{2+} had left-shifted curves indicating that CSE strengthen mitochondrial swelling (Fig. 4). This process leads to the release of cytochrome c and other apoptotic factors such as apoptosis-inducing factor. Besides the well-known anti-inflammatory effects of cyclosporine-A (CsA), therapeutic intervention with CsA prevents opening of the MPTP (see chapter 6) thereby protecting mitochondria from autophagy (Fig. 3C). Therefore, we will investigate whether treatment with CsA under CS-induced toxic circumstances may provide protection against CS-injury (7).

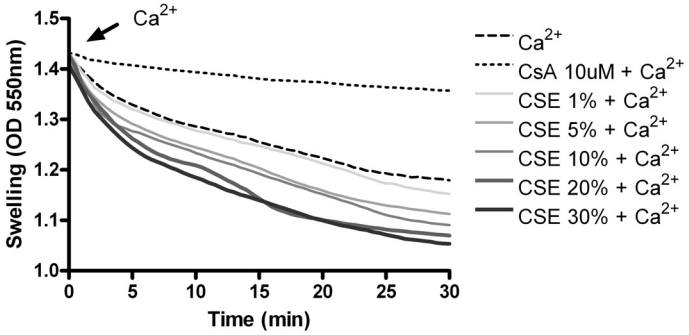

Figure 4. Mitochondrial permeability transition pore opening in isolated mitochondria.

Second study: About systemic effects

Smoking is a risk factor for development of COPD, cardiovascular disease and cancer. Evidence is now accumulating that smoking is also an important risk factor for development and progression of renal disease (13). In a cross-sectional study in the general population, it has been demonstrated that smoking is associated with microalbuminuria and low glomerular filtration rate in non-diabetic subjects (18). Similar associations in cross-sectional studies in patients with diabetes suggest that smoking increases susceptibility for development of diabetic nephropathy. Prospective studies in patients with diabetes have also documented a more rapid decline of renal function in association with smoking (14), even despite angiotensin-converting enzyme inhibition (5). Smoking has also been documented to be associated with a more rapid decline of renal function in patients with lupus nephritis, polycystic kidney disease, and other primary renal diseases (15; 21; 23).

To explore the effects of smoking, and to gain insight in the mechanisms involved in the induction of renal damage by smoking we will investigate in cultured tubular epithelial cells and endothelial cells the effects of the different lipophilic compounds of CS for their potential profibrotic and proinflammatory effects. Furthermore we will perform studies with Rho null cells from tubular epithelial cells and endothelial cells that are devoid of mitochondria. This will allow us to investigate whether different compounds of CS may induce ROS from other cell components than mitochondria. Animal studies will be performed to address the question whether the association between CS and development and progression of proteinuric nephropathies is indeed a causal relationship.

Smoking cessation is important for all smokers. It prevents development of smoke-related diseases. We will try to motivate currently smoking patients with either diabetic nephropathy and/or a status after renal transplantation to be admitted to the outpatient stop smoking clinic, were we will follow them through their follow-up. In the outpatient clinic, patients are supported in gradually decreasing uptake of nicotine supplementation and buproprion. Finally, they will be free of support. Follow-up of these patients, including repeated collection of 24h urine samples will allow us to investigate effects of smoking, nicotine, stopping of smoking, and (in

some cases) restart of smoking on creatinine clearance, albuminuria, markers of oxidative stress (e.g. F2-isoprostanes), and markers of tubulointerstitial involvement (e.g. β2-microglobulin, KIM-1, MCP-1, neopterin, and collagen fragments). Furthermore we will investigate if assessment of 24h urinary cotinine excretion in renal transplant recipients is valuable for detection of underreporting of current smoking. We will also assess whether there is a dose-effect relationship between smoking and future occurrence of graft loss.

Further remarks on systemic effects of smoking

It is known that smoking has deleterious effects on many organs increasing the risk for heart and brain diseases and blood vessel abnormalities. It maybe suggested that lipophilic compounds found in smoke are responsible for these adverse effects. Vulnerability of patients may vary according to the balance between destructive actions of these lipophilic compounds on intracellular ROS production and the anti-oxidative capacities of different tissues under attack. Further research on these anti-oxidative capacities of the different tissues and the genetic make-up of individuals are worthwhile to be studied for all manifestations of disease that are associated with smoking.

REFERENECES

1. Afri M, Gottlieb HE and Frimer AA. Superoxide organic chemistry within the liposomal bilayer, part II: a correlation between location and chemistry. Free Radic Biol Med 32: 605-618, 2002.

2. Basset O, Boittin FX, Cognard C, Constantin B and Ruegg UT. Bcl-2 overexpression prevents calcium overload and subsequent apoptosis in dystrophic myotubes. Biochem J 395: 267-276, 2006.

3. Bowler RP, Barnes PJ and Crapo JD. The role of oxidative stress in chronic obstructive pulmonary disease. COPD 1: 255-277, 2004.

4. Brzezinska AK, Lohr N and Chilian WM. Electrophysiological effects of O2*- on the plasma membrane in vascular endothelial cells. Am J Physiol Heart Circ Physiol 289: H2379-H2386, 2005.

5. Chuahirun T and Wesson DE. Cigarette smoking predicts faster progression of type 2 established diabetic nephropathy despite ACE inhibition. Am J Kidney Dis 39: 376-382, 2002.

6. Elmore SP, Qian T, Grissom SF and Lemasters JJ. The mitochondrial permeability transition initiates autophagy in rat hepatocytes. FASEB J 15: 2286-2287, 2001.

7. Elmore SP, Qian T, Grissom SF and Lemasters JJ. The mitochondrial permeability transition initiates autophagy in rat hepatocytes. FASEB J 15: 2286-2287, 2001.

8. Gabai VL, Meriin AB, Yaglom JA, Wei JY, Mosser DD and Sherman MY. Suppression of stress kinase JNK is involved in HSP72-mediated protection of myogenic cells from transient energy deprivation. HSP72 alleviates the stewss-induced inhibition of JNK dephosphorylation. J Biol Chem 275: 38088-38094, 2000.

9. Hellstrom-Lindahl E and Nordberg A. Smoking during pregnancy: a way to transfer the addiction to the next generation? Respiration 69: 289-293, 2002.
10. Izyumov DS, Avetisyan AV, Pletjushkina OY, Sakharov DV, Wirtz KW, Chernyak BV and Skulachev VP. "Wages of fear": transient threefold decrease in intracellular ATP level imposes apoptosis. Biochim Biophys Acta 1658: 141-147, 2004.
11. Mao GD and Poznansky MJ. Electron spin resonance study on the permeability of superoxide radicals in lipid bilayers and biological membranes. FEBS Lett 305: 233-236, 1992.
12. Massaro GD, Gail DB and Massaro D. Lung oxygen consumption and mitochondria of alveolar epithelial and endothelial cells. J Appl Physiol 38: 588-592, 1975.
13. Orth SR. Smoking and the kidney. J Am Soc Nephrol 13: 1663-1672, 2002.
14. Orth SR, Schroeder T, Ritz E and Ferrari P. Effects of smoking on renal function in patients with type 1 and type 2 diabetes mellitus. Nephrol Dial Transplant 20: 2414-2419, 2005.
15. Orth SR, Stockmann A, Conradt C, Ritz E, Ferro M, Kreusser W, Piccoli G, Rambausek M, Roccatello D, Schafer K, Sieberth HG, Wanner C, Watschinger B and Zucchelli P. Smoking as a risk factor for end-stage renal failure in men with primary renal disease. Kidney Int 54: 926-931, 1998.
16. Otterbein LE and Choi AM. Heme oxygenase: colors of defense against cellular stress. Am J Physiol Lung Cell Mol Physiol 279: L1029-L1037, 2000.
17. Parent R.A. Comparative Biology of the Normal Lung. 1992.
18. Pinto-Sietsma SJ, Mulder J, Janssen WM, Hillege HL, de Zeeuw D and de Jong PE. Smoking is related to albuminuria and abnormal renal function in nondiabetic persons. Ann Intern Med 133: 585-591, 2000.
19. Rahman I. The role of oxidative stress in the pathogenesis of COPD: implications for therapy. Treat Respir Med 4: 175-200, 2005.
20. Schwartz SM. A protective player in the vascular response to injury. Nat Med 7: 656-657, 2001.
21. Stengel B, Couchoud C, Cenee S and Hemon D. Age, blood pressure and smoking effects on chronic renal failure in primary glomerular nephropathies. Kidney Int 57: 2519-2526, 2000.
22. Sun L, Luo C, Long J, Wei D and Liu J. Acrolein is a mitochondrial toxin: effects on respiratory function and enzyme activities in isolated rat liver mitochondria. Mitochondrion 6: 136-142, 2006.
23. Ward MM and Studenski S. Clinical prognostic factors in lupus nephritis. The importance of hypertension and smoking. Arch Intern Med 152: 2082-2088, 1992.
24. Wright DT, Cohn LA, Li H, Fischer B, Li CM and Adler KB. Interactions of oxygen radicals with airway epithelium. Environ Health Perspect 102 Suppl 10: 85-90, 1994.

SAMENVATTING IN HET NEDERLANDS

Inleiding
Het beschreven onderzoek gaat over de mechanismen van sigarettenrook gerelateerde aandoeningen waaronder Chronic Obstructive Pulmonary Disease (COPD), ook bekend als longemfyseem en chronische bronchitis. Bij longemfyseem is sprake van rek uit de longen en verlies van longweefsel. Chronische bronchitis is een chronische ontsteking van het slijmvlies door langdurige blootstelling aan prikkelende deeltjes en/of gassen. Geschat wordt dat bij 75% van de patiënten met COPD de klachten zijn veroorzaakt door sigarettenrook. Uiteraard spelen huishoudelijke en stedelijke verontreiniging ook een rol. In de beginfase is er vooral sprake van een toename van slijmvorming en hoesten. In de loop van de tijd neemt de luchtwegvernauwing langzaam toe. De structuur van de longen raakt beschadigd en de inhoud van de longen neemt af. Het aantal patiënten met COPD is de afgelopen jaren sterk toegenomen en deze stijging gaat nog door. In Nederland is deze longziekte doodsoorzaak nummer 3. Helaas is COPD tot op heden nog niet te genezen.

Wat is de oorzaak van COPD
Veruit de belangrijkste oorzaak voor het ontstaan van COPD is het roken van sigaretten. Eén trekje van een sigaret bevat meer dan 4000 verschillende chemische stoffen en $1*10^{14}$ vrije radicalen. Naast de bekende componenten zoals teer, koolmonoxide, radicalen en nicotine zijn er vele andere componenten in sigarettenrook die schade kunnen toebrengen aan het lichaam. Tot nu toe is niet bekend welke componenten verantwoordelijk zijn voor het ontstaan van COPD. In het beschreven onderzoek zijn epitheelcellen van de luchtwegen bestudeerd. Uit recent onderzoek is gebleken dat epitheelcellen die de luchtwegwand bekleden en zo het longweefsel afschermen van het externe milieu, bijzonder gevoelig reageren op sigarettenrook. Net als bij de huid en de darmen spelen de epitheelcellen ook in de luchtwegen een belangrijke rol in de afweer. Bij patiënten met COPD zijn de luchtwegen chronisch ontstoken. In gezonde luchtwegen is een ontsteking in principe een snelle en kortdurende reactie om gevaarlijke, lichaamsvreemde deeltjes die het lichaam binnendringen onschadelijk te maken. Zodra het gevaar is bezworen zal de ontstekingsreactie stoppen. Bij patiënten met COPD is deze afweerreactie verstoord. Waarom epitheelcellen van COPD patiënten anders reageren dan die van gezonde personen is niet bekend. Uit recente studies is gebleken dat genetische factoren mogelijk hierin een rol spelen. Naast genetische factoren blijkt COPD een multifactoriële aandoening te zijn waarbij vele (nog onbekende) factoren een rol spelen.

Belangrijke factoren in de pathogenese van COPD zijn:

1) onbalans tussen reactieve zuurstofradicalen en anti-oxidanten

Zuurstofradicalen of vrije radicalen zijn kortlevende, reactieve deeltjes in de gasfase van sigarettenrook. Ook kunnen deze zuurstofradicalen gevormd worden tijdens het metabolisme van de cel. Tevens is bekend dat ontstekingscellen (macrofagen, neutrofielen) zuurstofradicalen uitscheiden om ziekteverwekkers te doden tijdens

ontstekingsreacties. Zuurstofradicalen zijn erg reactief en kunnen schade aanrichten aan eiwitten, membraanlipiden en DNA, wat kan leiden tot celdood. Epitheelcellen zijn beschermt tegen de schadelijke effecten van zuurstofradicalen met behulp van anti-oxidanten. Deze anti-oxidanten reageren met zuurstofradicalen en zetten deze om in niet-reactieve stoffen. Bij gezonde personen beschikken de epitheelcellen over voldoende bescherming. Echter wanneer een onbalans ontstaat tussen de hoeveelheid zuurstofradicalen en anti-oxidanten, bijvoorbeeld door het roken van sigaretten of wanneer de productie van zuurstofradicalen sterk toeneemt tijdens ontstekingsreacties, ontstaat oxidatieve stress. Onderzoek heeft aangetoond dat oxidatieve stress een rol speelt bij COPD.

2) onbalans tussen proteases en anti-proteases

Proteasen zoals elastine, proteïnase 3, cathepsines en metalloproteïnases zijn enzymen die worden geproduceerd door ontstekingscellen. Sommige proteases zijn in staat om chemotactische peptides te genereren die ontstekingscellen naar de long doen aantrekken. Andere proteases kunnen bindweefsel van het longparenchym afbreken, met name elastine, waardoor uiteindelijk emfyseem ontstaat. Bij gezonde personen worden bovengenoemde proteolytische enzymen tegengewerkt door anti-proteases. Sigarettenrook kan een ontsteking en een toename van proteases induceren. Gezonde mensen hebben voldoende hoge concentraties anti-proteases om de schadelijke effecten van de proteases op het longparenchym te voorkomen. Bij patiënten met COPD echter kan de productie van anti-proteases ontoereikend zijn om al de schadelijke effecten van proteases te neutraliseren.

3) verhoogde weefselschade en celdood

Hoewel bij gezonde personen weefselschade en celdood in de luchtwegen niet of nauwelijks wordt waargenomen, is dit wel het geval bij patiënten met COPD. Weefselschade als gevolg van bovengenoemde factoren gaat altijd gepaard met celdood, wat ontsteking tot gevolg heeft. Bij gezonde personen is de long prima in staat om zich te herstellen. Bij patiënten met COPD worden waarschijnlijk wel de normale herstelprocessen in gang gezet maar raken deze vervolgens verstoord. Tot op heden is er onvoldoende kennis waarom deze herstelprocessen zijn verstoord.

4) verstoring van mitochondriale functies in luchtweg epitheelcellen

In dit proefschrift beschrijven we dat verstoring van mitochondriale functies in luchtweg epitheelcellen door sigarettenrook mogelijk een geheel nieuw mechanisme is dat een belangrijke rol speelt in het ontstaan van longschade en luchtwegontsteking.

De rol van het mitochondrium in de pathogenese van COPD

Een mitochondrion of mitochondrium (meervoud mitochondriën of mitochondria) is een celorganel dat een dubbel membraan bevat en in het cytoplasma van de cel ligt. Mitochondriën zijn de energiecentrales van elke cel in ons lichaam. Het aantal mitochondriën per cel staat dan ook in relatie tot de energiebehoefte van de cel. Deze energie wordt beschikbaar in de chemische energievorm adenosine-tri-fosfaat (ATP) die aangemaakt wordt bij het omzetten van suikers en vetzuren in water en CO_2. Dit proces kan enkel plaatsvinden in aanwezigheid van zuurstof (dit is de enige

reden waarom wij inademen) en gebeurt in een proces dat citroenzuurcyclus (of Krebs cyclus) wordt genoemd. Het mitochondrion is de enige plaats in de cel waar oxidatie met zuurstof (aerobe stofwisseling) kan plaatsvinden. Bij de ademhaling wordt zuurstof opgenomen dat via de longen en de bloedbaan getransporteerd wordt naar de mitochondriën in de cel. Een beperking van zuurstofopname als gevolg van een luchtwegaandoening zal directe gevolgen hebben op het functioneren van de energiecentrales. Uit het beschreven onderzoek blijkt dat sigarettenrook de functies van mitochondriën kan beïnvloeden. Mitochondriën komen in al onze cellen voor. Wanneer in deze cellen een energiecrisis ontstaat zal dit directe gevolgen hebben op het functioneren van deze cellen en dus van de weefsels. Klachten zullen voornamelijk plaatsvinden in weefsels waarin veel mitochondriën in de cellen voorkomen. Ook zullen luchtweg epitheelcellen, door gebrek aan energie, niet goed in staat zijn de long te beschermen tegen het externe milieu.

Mitochondriën zijn in staat om energie te genereren uit suikers en vetzuren. Hierbij is zuurstof nodig en ontstaat er water en CO_2. Dit proces wordt de mitochondriale ademhalingsketen genoemd. Om te begrijpen hoe deze mitochondriale ademhalingsketen werkt volgt hier een korte beschrijving. In de cel wordt suiker eerst in een aantal stappen omgezet in een andere stof, pyruvaat, waarbij een klein beetje energie in de vorm van ATP vrijkomt. Maar om echt alle energie heel efficiënt vrij te maken, moet het pyruvaat eerst via een transportsysteem het mitochondrion ingebracht worden. Daarna wordt het pyruvaat omgezet in Acetyl-CoA. De citroenzuurcyclus is een opeenvolging van enzymreacties waarbij het Acetyl-CoA wordt omgezet in de volgende scheikundige stoffen: NADH, $FADH_2$ en CO_2. In dit stofwisselingsproces wordt de rest van de energie dat opgeslagen zat in suiker en vet omgezet in de stoffen NADH en $FADH_2$, waarbij CO_2 vrijkomt als afvalstof. Dit koolzuurgas ademen wij uit (dit is de enige reden waarom wij uitademen). Het NADH en $FADH_2$ wordt vervolgens verder verwerkt in de ademhalingsketen.

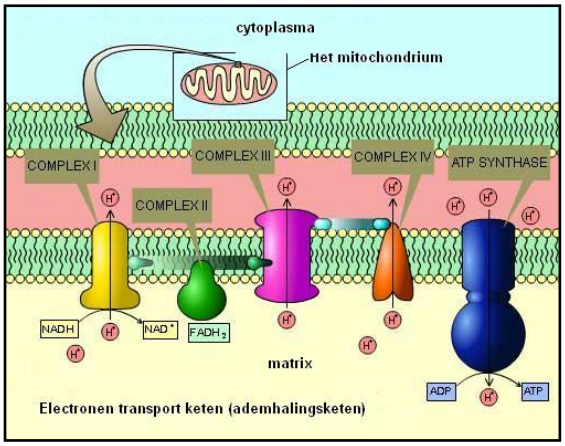

Figuur 1. De elektronen transport keten (ademhalingsketen).

De ademhalingsketen bestaat uit 5 verschillende enzymcomplexen. Het feit dat er over complexen gesproken wordt wil zeggen dat deze enzymcomplexen bestaan uit meerdere enzymen. De complexen 1, 2, 3 en 4 vormen de eigenlijke ademhalingsketen (zie figuur 1). Complex 5 (aangegeven als ATP synthase) is het enzymcomplex waar ATP wordt gevormd. De mitochondriale ademhalingsketen zit vast in de binnenmembraan van het mitochondrion. Het NADH wordt bij complex 1 omgezet tot NAD+, het $FADH_2$ wordt bij complex 2 omgezet in FADH. Hierna vindt een ingewikkelde serie van reacties plaats, waarbij elektronen door de verschillende complexen stromen, waarna uiteindelijk bij complex 4 zuurstof wordt omgezet in water. Bij het stromen van de elektronen door de verschillende complexen worden waterstofprotonen (H^+) vanuit de mitochondriale matrix naar de tussenmembraanruimte gepompt. Deze waterstofprotonen kunnen via complex 5 vanuit de tussenmembraanruimte terugstromen naar de mitochondriale matrix. Dit terugstromen is de drijvende kracht achter de ATP synthese. In hoofdstuk 1 en 2 van dit proefschrift hebben wij de invloed van sigarettenrook op de ademhalingsketen bestudeerd. Het blijkt dat sigarettenrook de elektronen die door de keten heen stromen kan beïnvloeden. Elektronen die normaal door de keten heen stromen en worden geneutraliseerd door zuurstof in water, bereiken complex 4 niet maar lekken eerder uit de ademhalingsketen. Deze vrije elektronen kunnen zich dan direct aan zuurstof binden, waardoor er zuurstofradicalen worden gevormd. Zoals eerder besproken zijn deze zuurstofradicalen zeer reactief en slecht voor de cel. Tevens ontstaat er een onbalans tussen reactieve zuurstofradicalen en anti-oxidanten wat leidt tot oxidatieve stress.

Mitochondriën spelen een belangrijke rol in de regulatie van celdood. Ze kunnen cellen aanzetten tot een apoptotische en necrotische celdood. Apoptose is een georganiseerde en geprogrammeerde manier van doodgaan. Vervolgens treedt er een gecontroleerde reeks van activiteiten in de cel op die er voor zorgt dat alle celonderdelen gerecycled worden. Necrose daarentegen is een proces waarbij een cel op een abrupte manier doodgaat. Hierbij wordt de inhoud van de cel in het omringende weefsel vrijgelaten. Dit zorgt meestal voor een ontstekingsreactie. Mitochondriën spelen een unieke rol in de controle van geprogrammeerde celdood. Dit doen ze door het cytochroom c vanuit de ademhalingsketen via een speciale mitochondriale poort het cytoplasma in te pompen. Het in het plasma vrijgekomen cytochroom c zal de inactieve vorm van het pro-apoptotische eiwit Apaf-1 omzetten in de actieve vorm. Dit heeft tot gevolg dat er een energie afhankelijke cascade in gang wordt gezet die cellulaire bestanddelen doen afbreken. Wanneer bij deze cascade geen energie voorhanden is zal de cel een switch maken van een apoptotische naar een necrotische celdood.

Deze drie functies; 1) energieproductie, 2) productie van zuurstofradicalen, 3) regulering van celdood, maken mitochondriën het theoretische middelpunt van deze studie.

SAMENVATTING VAN DE HOOFDSTUKKEN

Hoofdstuk 1: Sigarettenrook geïnduceerde blokkade van de mitochondriale ademhalingsketen switcht luchtweg epitheelcellen van een apoptotische naar een necrotische celdood.
In **hoofdstuk 1** van dit proefschrift staat beschreven dat componenten uit sigarettenrook mitochondriale verstoringen kunnen veroorzaken in luchtweg epitheelcellen. Sigarettenrook blijkt een dosisafhankelijke afname te geven van de mitochondriale membraanpotentiaal en de ATP productie in deze cellen *in vitro*. Verder onderzoek aan geïsoleerde mitochondriën leert dat sigarettenrookextract aanleiding geeft tot een dosisafhankelijke remming van complex 1 en complex 2 van de mitochondriale ademhalingsketen. Deze veranderingen leiden ertoe dat epitheelcellen een switch maken van een apoptotische naar een necrotische celdood. In tegenstelling tot apoptotische cellen stimuleren necrotische cellen ontstekingsreacties. Hiermee hebben wij een nieuw mechanisme geïdentificeerd dat mogelijk een belangrijke rol speelt in het ontstaan van longschade en luchtwegontsteking door het roken van sigaretten.

Hoofdstuk 2: Mitochondriën zijn essentieel in sigarettenrook geïnduceerde zuurstofradicaal producties.
In de literatuur staat beschreven dat zuurstofradicalen aanwezig in sigarettenrook, bijdragen aan de ontwikkeling van COPD. Hoewel deze reactieve deeltjes niet of nauwelijks de luchtweg epitheelcellen kunnen passeren en zeker niet in de circulatie terecht kunnen komen, worden er toch verhoogde systemische niveaus van deze reactieve deeltjes gevonden in patiënten met COPD. In **hoofdstuk 2** beschrijven we dat lipofiele componenten in tegenstelling tot zuurstofradicalen aanwezig in sigarettenrook wel gemakkelijk de epitheelcelmembranen kunnen passeren. Deze componenten blijken een dosisafhankelijke afname te geven van de mitochondriale membraanpotentiaal en de ATP synthese. Verstoring van de mitochondriale electronentransportketen leidt tot generatie van intracellulaire zuurstofradicalen. Echter wanneer dezelfde experimenten worden uitgevoerd met epitheelcellen zonder functionele mitochondriën blijken de negatieve effecten te zijn verdwenen. Samenvattend, lipofiele componenten die aanwezig zijn in sigarettenrook verstoren mitochondriale functies. Deze verstoringen leiden tot afname van ATP synthese en toename van intracellulaire zuurstofradicalen. Deze resultaten zijn van belang voor het begrijpen van de systemische effecten van roken die worden waargenomen bij patiënten met COPD.

Hoofdstuk 3: Mitochondriale lokalisatie en functie van heem oxygenase-1 in sigarettenrook geïnduceerde celdood.
In **hoofdstuk 3** beschrijven we hoe heem oxygenase-1 (HO-1) bijdraagt tot de bescherming van luchtweg epitheelcellen tegen schadelijke componenten uit sigarettenrook. Eerder onderzoek heeft aangetoond dat ex-rokers met COPD een lagere expressie van HO-1 hebben in vergelijking met ex-rokers zonder COPD. We hebben daarom onderzocht of HO-1 mogelijk een regulerende en beschermende functie biedt bij patiënten met COPD door het behoud van de mitochondriale functie

en remming van celdood na sigarettenrook blootstelling. De belangrijkste uitkomsten van dit onderzoek zijn:

- sigarettenrook induceert de expressie van HO-1 zowel *in vitro* als *in vivo,*
- sigarettenrook geïnduceerde expressie van HO-1 veroorzaakt verhoogde eiwit spiegels van actief HO-1 in het cytosol en in de mitochondriën van epitheelcellen,
- overexpressie van HO-1 remt sigarettenrook geïnduceerde celdood mogelijk door preservatie van intracellulaire ATP.

De resultaten van dit onderzoek suggereren dat HO-1 een beschermende rol kan bieden in het voorkomen van COPD. Om een beter begrip te krijgen van de beschermende rol van HO-1 op mitochondriaal niveau moet uiteraard meer basaal onderzoek worden verricht. Vervolgonderzoek zal moeten aantonen of opregulatie van HO-1 een gunstig effect heeft op het ziektebeloop van COPD patiënten.

Hoofdstuk 4: Sigarettenrook geïnduceerde modificatie van glutathion in luchtweg epitheelcellen

Zoals al eerder genoemd lijden COPD patiënten aan verhoogde oxidatieve stress. Hierbij wordt gesuggereerd dat deze patiënten een verstoring van de anti-oxidante capaciteit hebben. Om te zorgen voor een adequate verdediging tegen longschade, zijn de luchtwegen bekleed met epitheelcellen. Tevens zijn deze cellen afgesloten van de buitenlucht door een epitheliale vloeistof. Zowel de epitheelcellen als de epitheliale vloeistof bevatten hoge concentraties glutathion. Dit molecuul speelt een sleutelrol in het cellulaire redox evenwicht en wordt geacht één van de meest belangrijke anti-oxidante verdedigingen te zijn in de luchtwegen. Uit recente patiëntenstudies blijkt dat sigarettenrook glutathion in de luchtwegen depleteert. In **hoofdstuk 4** beschrijven we dat zeer reactieve verbindingen in de gasfase van sigarettenrook onomkeerbaar kunnen reageren met glutathion. Enzymatische bepalingen in combinatie met massa-spectrometrie worden gebruikt voor het kwantificeren en identificeren van glutathion. Sigarettenrook blijkt ook *in vivo* glutathion te depleteren. Identificatie met massa-spectrometrie toont aan dat de vrije thiolgroep (-SH) van GSH irreversibel reageert met zeer reactieve aldehyde groepen in de gasfase van sigarettenrook. Hierbij ontstaan onomkeerbare GS-aldehyde moleculen. Deze resultaten verklaren mogelijk het chronisch gebrek aan bescherming tegen oxidatieve stress dat wordt gevonden bij patiënten met COPD.

Hoofdstuk 5: Schade en herstel van luchtweg epitheelcellen na waterstofperoxide expositie.

Zuurstofradicalen kunnen schade aanrichten aan onze luchtwegen. Rokers worden door het inhaleren van sigarettenrook blootgesteld aan zeer hoge concentraties zuurstofradicalen. De gangbare hypothese, die het ontstaan van longemfyseem verklaart gaat uit van een disbalans tussen oxidanten (zuurstofradicalen) en anti-oxidanten. In **hoofdstuk 5** hebben we prolifererende (delende) en niet-prolifererende (rustende) luchtweg epitheelcellen *in vitro* bestudeerd na blootstelling aan waterstofperoxide (oxidant aanwezig in sigarettenrook en ontstekingscellen). Vervolgens zijn vrije thiolgroepen (anti-oxidanten) in deze cellen gemeten als schade marker voor oxidatieve stress. Tevens is met behulp van flowcytometrie de

individuele epitheelcel geanalyseerd. De belangrijkste uitkomsten van dit onderzoek zijn:

- waterstofperoxide oxideert vrije thiolgroepen,
- oxidatieve stress lijdt tot een necrotische celdood,
- niet-prolifererende cellen zijn gevoeliger voor waterstofperoxide dan prolifererende cellen.

De resultaten van dit onderzoek suggereren dat vrije thiolgroepen een belangrijke rol spelen in de bescherming tegen oxidatieve stress. Niet-prolifererende cellen zijn gevoeliger voor oxidatieve stress dan prolifererende cellen. Hierbij spelen intracellulaire vrije thiol concentraties een belangrijke rol. Vervolgonderzoek zal moeten aantonen of inter-individuele verschillen en gevoeligheid voor oxidatieve stess een mogelijke rol speelt in het ontstaan van COPD en longemfyseem.

Hoofdstuk 6: Cyclosporine A geïnduceerde oxidatieve stress wordt niet veroorzaakt door een verhoogde mitochondriale membraan potentiaal

Er bestaan in toenemende mate sterke aanwijzingen over de rol die vrije radicalen spelen in de pathogenese van ziekte en veroudering. Vrije radicalen kunnen in het systeem worden geïntroduceerd door middel van blootstelling aan sigarettenrook. Daarnaast kunnen deze ook worden gegenereerd door het gebruik van medicijnen. Een voorbeeld hiervan is cyclosporine A (CsA). Dit geneesmiddel is ondanks duidelijke nefrotoxische en pro-atherogene effecten een veelgebruikt immunosuppressivum. Het feit dat CsA bindt aan cyclophiline A ligt ten grondslag aan de calcineurineremming en het immunosuppressieve effect van CsA. Deze verbinding verhindert opening van de zogenaamde ‘permeability transition pore’ (PTP) van het mitochondrion. Het doel van deze studie was de hypothese te toetsen dat blokkering van de mitochondriale PTP leidt tot mitochondriale dysfunctie en een chronisch verhoogde mitochondriale membraan potentiaal. Dit zou kunnen leiden tot oxidatieve stress en metabole veranderingen. Uit de resultaten beschreven in **hoofdstuk 6** blijkt dat expositie van tubulus epitheelcellen aan CsA weliswaar gepaard gaat met oxidatieve stress, maar dat het zeer onwaarschijnlijk is dat dit het gevolg is van het ontstaan van een hoge mitochondriale membraan potentiaal onder invloed van CsA. In geïsoleerde mitochondriën vonden wij onder bepaalde omstandigheden zelfs het tegenovergestelde: stimulatie van de productie van zuurstofradicalen door mitochondriën onder invloed van calcium kon worden tegengegaan door toevoeging van CsA. Calcium induceert onder die omstandigheden zwelling van mitochondriën door inductie van opening van de PTP. Mitochondriale zwelling leidt tot zuurstofradicaal productie, wat door CsA wordt tegengegaan. Naast dat wij onwaarschijnlijk hebben gemaakt dat mitochondriën de bron zijn van verhoogde zuurstofradicaal producties in cellen onder invloed van CsA, hebben wij het onwaarschijnlijk gemaakt dat andere bekende eigenschappen van CsA, zoals remming van calcineurine en blokkering van P-glycoproteïne pompen, hierbij een rol spelen. Hierdoor worden andere potentiële bronnen, zoals cytochroom P450, veel waarschijnlijker, en kan toekomstig onderzoek zich meer hierop richten.

CONCLUSIES

Uit het in dit proefschrift beschreven onderzoek blijkt dat sigarettenrook dodelijk is voor epitheelcellen van de luchtwegen. Deze schadelijke werking van sigarettenrook blijkt veroorzaakt te worden door: 1) toxische zuurstof- en stikstofradicalen; 2) agressieve aldehyden die essentiële functies van peptiden blokkeren; 3) lipofiele componenten die in celmembranen kunnen oplossen en vooral de functies van mitochondriën, de energiecentrales van de cel, blokkeren. Deze derde groep van stoffen blijkt vooral remmend te werken op de ademhalingsketen in geïsoleerde mitochondriën. Hierdoor worden de zuurstofconsumptie en energievoorziening van de cel geremd. In gekweekte longepitheelcellen leiden deze veranderingen tot een sterke toename van zuurstofradicalen en een verstoring van de anti-oxidante capaciteit. De epitheelcellen switchen hierdoor van een apoptotische naar een necrotische celdood. In tegenstelling tot apoptotische cellen veroorzaken necrotische cellen ontstekingsreacties die de schadelijke werking van roken door een chronische ontstekingsreactie gaan versterken. Hiermee hebben wij een nieuw mechanisme geïdentificeerd dat mogelijk een belangrijke rol speelt in het ontstaan van longschade en luchtwegontsteking door het roken van sigaretten.

Ziekten op afstand

Bij het roken worden veel verschijnselen/ziekten waargenomen die niet direct in de longen plaatsvinden maar schadelijk werken elders in het lichaam zoals; het ontstaan van hart en vaatziekten, invloed op foetale ontwikkelingen die zich later uiten in een verhoogde kans op bijvoorbeeld allergieën en astma, invloed op hersenfuncties, afstotingsreacties na orgaantransplantaties etc. Om dit te verklaren moeten we denken aan stoffen die vanuit de longen, waar de rook binnenkomt, door het lichaam getransporteerd kunnen worden. Veel van deze stoffen worden reeds door de longen weggevangen. Hierbij horen o.a. de radicalen (zuurstof-, stikstofradicalen) en agressieve aldehyden. Om in de bloedbaan te kunnen komen moeten rookdeeltjes de barrière van de longepitheelcellen en andere weefselcellen van de long kunnen passeren. Deze stoffen moeten tevens membranen kunnen passeren, dus zgn. vetoplosbare (lipofiele) eigenschappen hebben. Er zijn honderden stoffen in rook die membranen kunnen passeren en op cellen kunnen inwerken. De studies in dit proefschrift hebben aangetoond dat deze stoffen een belangrijke remmende werking hebben op de mitochondriën van de cel en aanleiding zijn tot de vorming van schadelijke radicalen. Door gebrek aan energie is de cel niet in staat om deze aanval van radicalen op te vangen. Het resultaat is dat overal in het lichaam waar veel energie gevraagd/vereist is (bij infecties, herstel van beschadigde cellen, hersenfuncties in het algemeen, etc.), cellen zullen zijn die aan deze eisen van hoge ATP aanmaak niet meer kunnen voldoen en dood gaan.

Dat er functies van belangrijke weefsels verminderd of beschadigd zullen raken is niet verwonderlijk. De recente onderzoeksresultaten in dit proefschrift geven nieuwe mechanismen en verklaringen voor de effecten van roken op weefsel op grote afstand van de longen. In het onderzoek naar de effecten van roken op het lichaam is het van groot belang ons te realiseren dat er een totaal nieuw veld van onderzoek is ontstaan dat vele kansen biedt voor het begrijpen van deze “ziekten op afstand”. Veel moet er in dit nieuwe gebied nog aan onderzoek gebeuren. Er ligt een

lange lijst van nieuwe stoffen te wachten op onderzoek die, in samenwerking met elkaar, verklaringen kunnen bieden voor veel ziektebeelden die door roken op andere plaatsen veroorzaakt worden. Ook kan het verklaringen bieden voor de schadelijke werking van roken op andere mensen die deze rook inhaleren.

DANKWOORD

Na een paar jaar hard werken is het zover, het boekje is af. Uiteraard gaat onderzoek gepaard met pieken en dalen, maar met een fantastisch team van mensen om je heen kom je heel ver. Daarbij moet ik wel vermelden dat de dalen vaak gepaard gingen met het drinken van een biertje en de pieken met het eten van Limburgse vlaai. Kortom, een geweldige periode om nooit te vergeten. Een aantal mensen wil ik graag persoonlijk bedanken.

Mijn promotor, Prof. dr. H.F. Kauffman.
Beste Henk, waar jij ooit mee begonnen bent, ben ik dertig jaar later mee verder gegaan, namelijk het isoleren van mitochondriën. Ik heb enorm veel van je geleerd. Je bent niet alleen een geweldige wetenschapper, maar ook een goede diplomaat. Ik ben blij dat je mijn promotor bent en dat alles tot een goed einde is volbracht.

Mijn promotoren, Prof. dr. R.O.B. Gans en Prof. dr. G.H. Koëter.
Beste Rijk, graag wil ik je bedanken voor de mogelijkheid die ik heb gekregen om onderzoek te doen.
Beste Gerard, ik vind het jammer dat we niet wat meer hebben kunnen samenwerken. Geniet van je vrije tijd.

Mijn co-promotor dr. D-J. Slebos.
Beste wetensjapper, wat had ik zonder jouw hulp gemoeten. Je hebt een belangrijke bijdrage geleverd aan dit proefschrift zoniet de belangrijkste. Tevens is het ons gelukt een bursaal binnen te halen. Het zou fantastisch zijn als we dat zouden kunnen uitbreiden met een postdoc positie. Ik hoop in ieder geval dat we nog een paar jaartjes blijven samenwerken.

Mijn co-promotor dr. S.J.L. Bakker.
Beste Stephan, het verbaast mij altijd weer hoeveel kennis jij hebt van fundamenteel onderzoek. Bedankt dat jij deze kennis met ons hebt willen delen.

Ik heb het geluk gehad dat ik met twee fantastische research analisten op dit project heb mogen samenwerken. Allereerst wil ik Inge bedanken waarmee ik het project ben begonnen. Jij bracht zo nu en dan wat orde en netheid in mijn zooi. Toen jij een andere baan kreeg in Hoogeveen heeft Harold het stokje overgenomen.
Beste Harold, uiteraard kan ik heel wat anekdotes over jou schrijven, maar ik zal je sparen. Ik denk dat we een gouden team waren. Naar mijn mening heb je nergens zo relaxed kunnen werken (ik heb je regelmatig om 11:00 ’s ochtends uit je bed moeten halen) en toch zo veel resultaten behaald als op dit project. Daarnaast vind ik het fantastisch dat je mijn paranimf wilt zijn, al heb ik hiervoor wel tweemaal de promotie datum moeten verzetten. Kortom, bedankt voor deze geweldige en vooral gezellige tijd.

Beste Raymond, ik vind het geweldig dat jij mij wilt bijstaan als paranimf. We hebben in het verleden al eens eerder bewezen dat we enorm goed kunnen samenwerken; de schutting staat nog als een huis.

Op dit project heb ik twee studenten mogen begeleiden.
Klaas, je was mijn eerste student. Helaas ben jij er niet meer. Ter nagedachtenis aan jou wil ik het volgende zeggen; Klaas je zou een zeer talentvolle research analist zijn geworden. Ik hoop dat je in vrede rust.
Esther, jij was mijn tweede student. Jouw zuurstofmetingen aan geïsoleerde mitochondriën zijn de basis geweest voor hoofdstuk 1 van dit proefschrift. Ik wil je bedanken voor je inzet en succes wensen met je verdere carrière.

In de periode dat ik werkzaam ben geweest als promovendus is er veel veranderd op het lab. Henk ging met pensioen en Antoon werd het nieuwe hoofd van het laboratorium. Antoon, ik ben blij dat wij het goed met elkaar kunnen vinden en ik hoop nog vele jaren onderzoek met je te kunnen doen. Uiteraard wil ik alle (ex)medewerkers van ons lab, Door (met jou ben ik gestart op dit lab), Marian (weet altijd alle nieuwtjes), Andre (was altijd lachen), Janneke (wacht maar tot je moeder bent ☺), Hessel (de beste taart komt uit Friesland), Sicco (je nieuwe speeltje piept wel heel vaak), Ibolya (is niet op haar mondje gevallen), Hein (is fijn met pensioen), Brigitte (Groningen wordt geen kampioen), Ineke (staat nog steeds op het antwoordapparaat), Renee (zit gezellig naast mij), Alex (A bientôt), Irene en Martijn (25 publicaties, klaar voor de start….af), Jacobien (is streng maar rechtvaardig), Simone (klaagt nooit over bestellingen), Judith (is een gelukkige jonge moeder), Wim (is geen labmedewerker maar onze labmanager), Johan, Lisette en Uilke (welkom als nieuwkomers), bedanken voor de gezellige werksfeer met name de lab uitjes, kroegen tochten, feest avonden, etentjes enz. Tevens wil ik onze aanstormende talenten, Hadi, Soheila, Benoit, Dries, Henk, Roland, Dennie, Sijranke, en Delaram, succes wensen met jullie eigen promotietraject. Speciaal tegen Delaram wil ik zeggen dat ik het erg leuk vind dat jij op ons project bent begonnen.

Naast de werkzaamheden in ons eigen laboratorium heb ik veel metingen verricht in andere laboratoria waaronder het chirurgisch onderzoekslaboratorium, het MDL-laboratorium, het laboratorium kindergeneeskunde, het laboratorium pathologie en de analytische biochemie groep van de faculteit wiskunde en natuurwetenschappen. De volgende personen wil ik hiervoor bedanken, dr. H. Leuvenink, Prof. dr. H. Moshage, Prof. dr. F. Kuipers, Prof. dr. R. Bischoff, Prof. dr. W. Timens en dr. M. Hylkema.

De leden van de beoordelingscommissie Prof. dr. A.M.W.J. Schols, Prof. dr. R.P.H. Bischoff, Prof. dr. H.A.M. Kerstjens, wil ik bedanken voor de snelle beoordeling van mijn manuscript.

Tot slot wil ik mijn gezin, Lottie (mijn grote liefde), Yaël (mijn boksbal), Lior (zal nog eens wat voorlezen uit mijn proefschrift als je niet kunt slapen) en mijn kleine Jairo (je kunt al lopen) bedanken voor het warme nest. Jullie zijn in deze periode altijd mijn steun en toeverlaat geweest. Laten we eerst maar eens lekker gaan genieten van een vakantie in Azië om te zien of dit wat voor ons is.

PS: Uiteraard is het mogelijk dat ik iemand ben vergeten te bedanken; mocht dit het geval zijn vul je naam dan in op de stippellijn……

PUBLICATIONS

Rezayat D**, van der Toorn M**, Gras R, de Bruin HG, Slebos DJ, van Oosterhout AJ. Acute cigarette smoke induced airway neutrophilia in a Mouse model is ROS dependent. Submitted 2009

van der Toorn M, Rezayat D, Kauffman HF, Bakker SJ, Gans RO, Koeter GH, Choi AM, van Oosterhout AJ, Slebos DJ. Mitochondria are essential in cigarette smoke induced ROS generation. Submitted 2008

Abello N, Geurink PP, **van der Toorn M**, van Oosterhout AJ, Lugtenburg J, van der Marel GA, Kerstjens HA, Postma DS, Overkleeft HS, Bischoff R. Poly(ethylene glycol)-based stable isotope labeling reagents for the quantitative analysis of low molecular weight metabolites by LC-MS. Anal. Biochem. 2008**,** 80 (23), pp 9171–9180

Slebos DJ, **van der Toorn M**, Bakker SJ, Kauffman HF. Mitochondrial dysfunction in COPD patients with low body mass index. Eur Respir J. 2007 Sep;30(3):600.

van der Toorn M, Smit-de Vries MP, Slebos DJ, de Bruin HG, Abello NJ, van Oosterhout AJ, Bischoff R, Kauffman HF. Cigarette smoke irreversibly modifies glutathione in airway epithelial cells. Am J Physiol Lung Cell Mol Physiol. 2007 Nov;293(5):L1156-62.

Bathoorn E, Slebos DJ, Postma DS, Koeter GH, van Oosterhout AJ, **van der Toorn M**, Marike Boezen H, Kerstjens HA. Anti-inflammatory effects of inhaled carbon monoxide in patients with COPD: a pilot study. Eur Respir J. 2007 Dec;30(6):1131-7.

van der Toorn M, Kauffman HF, van der Deen M, Slebos DJ, Koeter GH, Gans RO, Bakker SJ. Cyclosporin A-induced oxidative stress is not the consequence of an increase in mitochondrial membrane potential. FEBS J. 2007 Jun;274(12):3003-12.

Smit-de Vries MP, **van der Toorn M**, Bischoff R, Kauffman HF. Resistance of quiescent and proliferating airway epithelial cells to H2O2 challenge. Eur Respir J. 2007 Apr;29(4):633-42.

van der Toorn M, Slebos DJ, de Bruin HG, Leuvenink HG, Bakker SJ, Gans RO, Koeter GH, van Oosterhout AJ, Kauffman HF. Cigarette smoke-induced blockade of the mitochondrial respiratory chain switches lung epithelial cell apoptosis into necrosis. Am J Physiol Lung Cell Mol Physiol. 2007 May;292(5):L1211-8.

Slebos DJ, Ryter SW, **van der Toorn M**, Liu F, Guo F, Baty CJ, Karlsson JM, Watkins SC, Kim HP, Wang X, Lee JS, Postma DS, Kauffman HF, Choi AM. Mitochondrial localization and function of heme oxygenase-1 in cigarette smoke-induced cell death. Am J Respir Cell Mol Biol. 2007 Apr;36(4):409-17.

Schepers H, Geugien M, **van der Toorn M**, Bryantsev AL, Kampinga HH, Eggen BJ, Vellenga E. HSP27 protects AML cells against VP-16-induced apoptosis through modulation of p38 and c-Jun. Exp Hematol. 2005 Jun;33(6):660-70.